MSc THESIS DISSERTATION

CHARACTERISATION OF THE EFFECT OF ALTERATION ON THE PPM PLATINUM ORE AND EVALUATION OF SELECTED STRATEGIES TO IMPROVE METALLURGICAL PERFORMANCE

Mpho Ramonotsi

Thesis Presented in Partial Fulfilment of the Degree of Masters of Science

In the Department of Chemical Engineering

University of Cape Town

February 2011

ABSTRACT

The flotation process is used to produce the Platinum Group Metals (PGM) bearing concentrates, which subsequently undergo a combination of pyrometallurgical and hydrometallurgical enrichment. Concentrators can comfortably upgrade run-of-mine ore by over 60 times. However, there are challenges associated with the geology of the ore body, and most plants sacrifice recovery to achieve the required concentrate specifications. The metallurgical performance at Pilanesberg Platinum Mines (PPM) is currently seen as erratic, dominated by low recoveries. This is largely due to the predominance of weathered/oxidised mineral phases present in the ore. It is suspected that this scenario will persist while the mine is extracting ore primarily near the surface. Better recoveries are anticipated as material is extracted from deeper levels in the future.

The aim of this study is in two parts; the first part focuses on mineralogical quantification of the extent of weathering at PPM by profiling the flotation behaviour and host rock density with spatial depth. The second part of the study is to evaluate selected strategies that could improve the flotation recoveries of weathered ores.

The body of work presented in this thesis shows strong evidence that the PPM PGM ore deposit is increasingly weathered and/or oxidised toward the surface. The flotation recoveries of PGMs from ore mined near the surface were found to be significantly reduced. This supports claims in the literature that altered PGM minerals tend to report mostly to the tailings during flotation. There was a strong correlation between metallurgical performance and the spatial depth at which the ore was mined. The flotation performance was poor for ore from near the surface and improved to over 80% recovery for ore from below 40 m. The density profile although with less convincing trend due to the changes occurring within the data variance, also indicated that the host rock density increased towards the density of fresh rock below 40 m, implying the country rock might have undergone some transformation which lowered its density nearer to the surface.

The mineralogical study done on the PPM material showed oxidation and weathering as the plausible causes of low metallurgical performance of the ore. The study included Q-XRD, SEM and MLA analyses, where Q-XRD was able to quantify the abundance of host mineral showing secondary silicates to be abundant. The observations made through SEM were not quantifiable, but signs of alteration and weathering on the material were observable. The work done with the MLA was able to show quantitatively the PGM mineral

liberation, the PGM association and the PGM occurrence. Significant quantities of liberated PGM minerals, mostly associated with base metals sulphides (22%), were found in the tailings.

The second part of the thesis evaluates selected strategies in an effort to try to improve metallurgical performance of the weathered ore. These were acid pre-leaching and the use of co-collectors. Acid pre-leaching showed significant improvement on recoveries (20% increase), but selectivity was low. It is not clear from the work done what other minerals were activated by acid etching. However, operations in the platinum mining industry may not be inclined to adopt sulphuric acid pre-treatment since it requires additional reagents, such as alkali to raise the pH, and infrastructural adjustments to cater for a corrosive environment. However, there is some evidence in the literature that carbon dioxide may provide some milder form of acid pre-treatment, which also assists in creating non-oxidative environment by inhibiting oxygen absorption into the slurry media.

Using co-collectors to improve metallurgical performance, it is shown that hydroxamate-based reagents offer significant improvement in terms of both recovery (10% increase) and selectivity. Hydroxamates are believed to have strong affinity towards copper and iron minerals, both of which are known to host PGMs. The advantage of hydroxamate also lies in the fact that these reagents do not affect the effectiveness of traditional xanthate collectors. However, there is some indication in both the literature and in this work that hydroxamates are sensitive to residence time and dosage.

Thionocarbamates as co-collector did not show significant improvement in recovery, and the selectivity was marginally improved, especially with the thionocarbamate that contained xanthogen formate as well. Fatty acids, on the other hand, have shown to result in high recoveries (30% improvement), but the mass pull was substantial (~50%) with very low selectivity. Fatty acids, especially unsaturated fatty acids, are known to be effective collectors for oxide minerals. Their selectivity has always been an issue, and they work well where the gangue mineral contingent is not significant. It was not clear whether the fatty acids acted largely as frother or whether their collecting power for oxide mineral was substantive. Combining fatty with thionocarbamates seems to improve the recovery and selectivity to some degree.

Mineralogical investigation did not positively identify the passivation layer on the sulphide mineral surfaces, perhaps due to higher resolution required to observe oxide layers, it is

therefore recommended to conduct further investigations at higher resolutions to characterise passivation on the PGM bearing mineral surface. Further work will also be required to study both mechanism and optimisation of hydroxamate collecting power on oxidised PPM ore. Other techniques, which were not considered in this study, but have been reported to have exhibited significant metallurgical improvements, such as sulphidisation, may also be recommended for investigation.

Declaration

This thesis has not been submitted in part, or in whole for another degree at any other institution.

Signed Signed by candidate Signature Removed

List of Publications

Becker, M., Ramonotsi, M. Petersen, J. Effect of alteration on the mineralogy and flotation performance of PPM platinum ore. Paper submitted for presentation at the 10th International Congress of Applied Mineralogy (ICAM), Norway, August 2011.

Acknowledgements

First and foremost I would like to thank my advisors, Dr J Petersen and Dr M Becker, for their guidance, suggestions, criticism and the lessons I obtained through hydrometallurgical course where Prof. Mike Nicol came as a guest lecturer and imparted rich insight on process operations and experiences. The support afforded by everyone at Boynton/PPM was indispensible particularly Colin Campbell, John Derbyshire, and Terry Holohan who gave support for this work. Acknowledgements also go to Keith Liddell for the initial concept of the work and guidance on using flotation bench work to assess metallurgical performance.

I would also like to express my sincere appreciation to my family; my wife Hloni, my daughter Katleho and my son Mabitso for the patience they have afforded me during the course of my MSc study. Without such patience and support from them, this work would not have been feasible.

TABLE OF CONTENTS

LIST OF FIGURES

LIST OF TABLES

List of Abbreviations

BIC	Bushveld Igneous Complex
BMS	Base Metal Sulphides
Ccp	Chalcopyrite
LPR	Lower Pseudo Reef (Pegmatoidal Olivine Pyroxenite)
MLA	Mineral Liberation Analyser
MRHW1	Merensky Reef Hanging Wall One
MRFW1	Merensky Reef Footwall One
Pent	Pentlandite
PGE	Platinum Group Element
PGM	Platinum Group Minerals
Po	Pyrrhotite
PRHZB	Pseudo Reef Harzburgite
PPM	Pilanesburg Platinum Mine
Py	Pyrite
QEMSCAN	Quantitative Evaluation of Minerals by Scanning Electron Microscopy
Q-XRD	Quantitative Powder x-ray diffraction
SEM	Scanning Electron Microscopy
SIBX	Sodium Isobutyl Xanthate
UPR	Upper Pseudo Reef (Pegmatoidal Pyroxenite)
XPS	X-ray Photoelectron Spectroscopy
XRD	X-ray Diffraction
ToF-SIMS	Time of flight Secondary ion mass spectroscopy

1. CHAPTER ONE: INTRODUCTION

1.1. BACKGROUND

Precious metals have superb physicochemical properties such as high conductivity, catalytic activity, corrosion resistance and appealing lustre. Furthermore, precious minerals have earned their place in both financial and investment markets owing to their value.

The six platinum group metals: platinum, palladium, rhodium, osmium, ruthenium, iridium, gold and sometimes silver occur together in the Bushveld Igneous Complex (BIC). Platinum, palladium and rhodium, the most economically significant of the PGMs, are found in the largest quantities. The remaining PGMs are produced as co-products. South Africa is currently the World's leading platinum and rhodium producer and the second largest palladium producer after Russia. South Africa's PGM production is sourced entirely from the Bushveld Complex (Reuters, 2010).

There are three main reefs found in the Bushveld, namely Merensky Reef, Platreef and UG2 reef. All of these reef types contain some form of base metal sulphides which mostly host platinum group elements (PGE). The base metal sulphides in the Merensky reef primarily consist of chalcopyrite, pentlandite and pyrrhotite. Platreef consists of an increased content of base metal sulphides and oxides disseminated in coarse pegmatoidal pyroxenites, gabbros and phlogopite (Armitage et al., 2002). UG2 reef on the other hand, consists mainly of chromitite disseminated by finer grains of both base metal sulphides and PGM mineralisation (Penberthy and Merkle, 1999).

The beneficiation process of PGMs (see Figure 1) generally follows six major steps, designed to increase the grade of the valuable minerals relative to the original run-of-mine ore. This is systematically achieved by rejecting the bulk of the gangue material in waste streams such as flotation tailings, waste rocks, smelter slags and aqueous effluents. Figure 1 illustrates the relative operating costs for each unit operation in the beneficiation process as a percentage of the entire value chain. It also shows both the commonly achieved recoveries as well as the concentration factor at each unit operation. The highest upgrade is achieved at the base metal refinery (BMR). The BMR is

also one of the lowest cost drivers, making the BMR the highest value adding process in the PGM value chain.

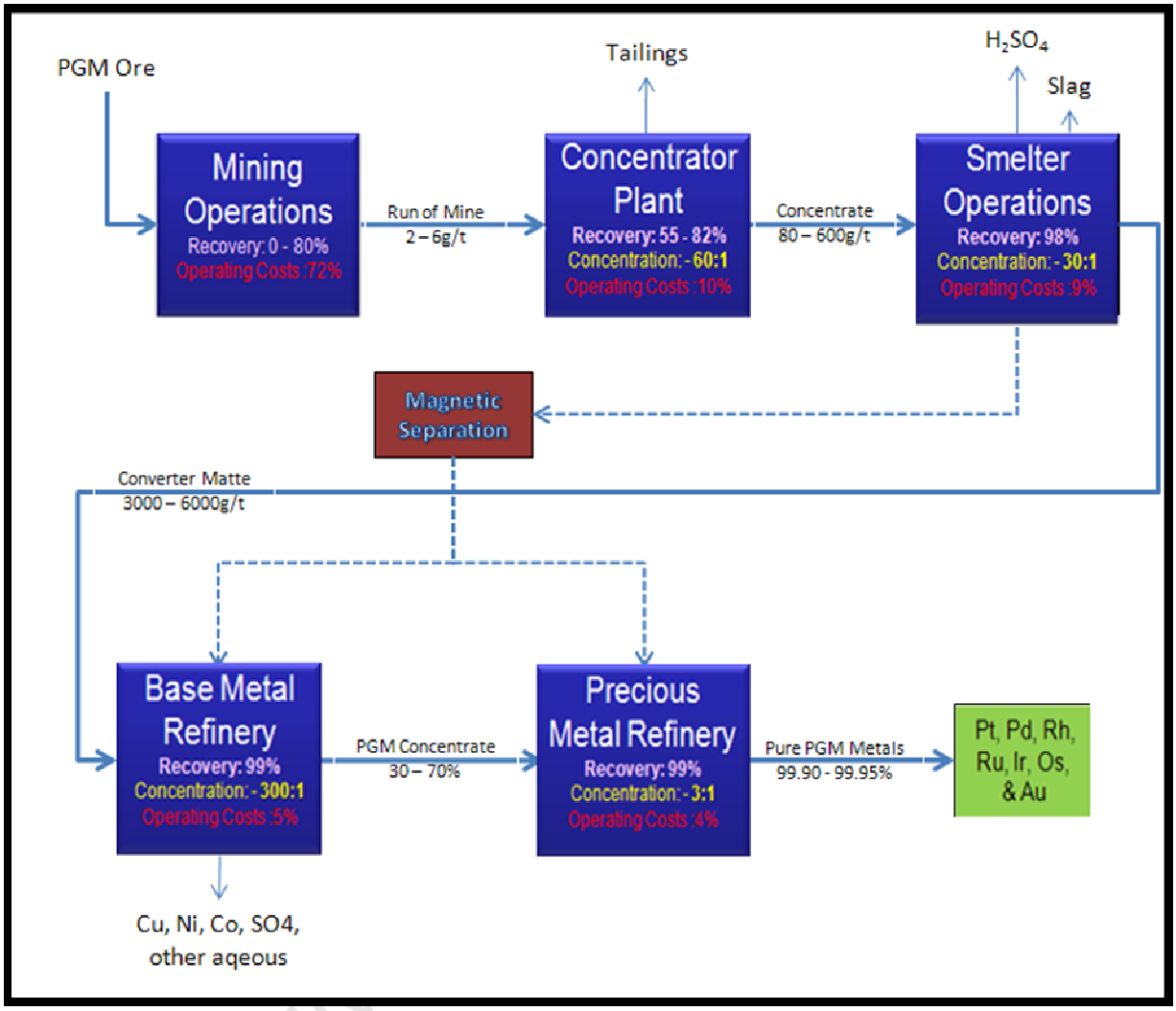

FIGURE 1: PGM BENEFICIATION ROUTE FOR SOME PGM PRODUCERS IN SOUTH AFRICA

Figure 1 illustrates the PGM beneficiation process flow and indicates typical grades obtained from each unit operation. It also indicates the relative upgrade or concentration ratio with relative costs. For instance, comminution and flotation upgrades the-run of-mine ore of about 2 - 6 g/t to about 80 - 600 g/t. The flotation concentrates are then smelted in the furnace and subsequently converted to produce a PGM-containing nickel-copper matte containing around 3000g/t - 6000g/t. The matte is treated hydrometallurgically to separate the base metals from the precious metals, thereby generating “Final PGM-Concentrate” at around 30% - 70% PGMs. Finally, the Final PGM Concentrate is refined to separate the individual precious metals into their

near pure forms, generally 99.90% purity for rhodium, ruthenium and osmium and 99.95% for platinum, palladium, and gold.

The lowest percentage recovery in the PGE value chain is at the concentrators (Figure 1). The concentrators separate the valuable PGM from the unwanted gangue minerals by froth flotation. Flotation is a physico-chemical separation process based on the surface properties of the minerals. The surfaces of the valuable minerals are rendered hydrophobic with the addition of suitable reagents and those of the gangue minerals hydrophilic. Under some circumstances the surfaces of the valuable minerals are not easily rendered hydrophobic using conventional flotation reagents, resulting in poor flotation recoveries (< 70%). This has commonly been attributed to some prior mineralogical alteration of the ore (Runge et al., 2003).

It has been reported in the literature that PGM mineralisation in PGM reefs vary relative to location (Cawthorn et al., 2002). The effects of such mineralogical variations are seen on metallurgical ore performance and have been related to potholes, discordant pipes as well as the nature of the footwall sequence and the reef thickness ((Kinloch and Peyerl, 1990), (Brough, 2008)). Penberthy and Merkle, (1999) further attest that mineralogical variation is mostly related to local disturbances such as potholing, local faulting, replacement pegmatoidal as well as the presence of hydrothermal activities. Prendergast, (1988) also noticed that PGM minerals of the main sulphide zone near the surface are largely oxidised, and attempts to extract the PGE from these ore type proved to be uneconomic due to low PGE recoveries achieved by conventional metallurgical methods.

Pilanesberg Platinum Mines (PPM) also began observing low recoveries with the ore that was tested during the feasibility study. This prompted the commissioning of a mineralogical study to investigate the possible cause of low recoveries. The study was designed to determine the PGM species in the tailings, their modes of occurrence and degree of liberation (Duarte et al., 2004). The study concluded that there were PGM values that reported to the tailings which were within floatable size range. This was attributed to mineral weathering, either in the form of surface coatings, mineral alteration or mineral oxidation.

The PPM operation treats open pit material and the recoveries are mostly low and erratic, particularly with near-surface ore. The average recovery is 35% but sometimes the PGM recovery can climb as high as 70%. The low PGM recovery is argued to be due to the weathering of the ore (Duarte et al., 2004). The PPM plant operation aims to recover PGM to such an extent that only 0.5g/t (or even lower) is left in the tailings. However, the average tailing grade was measured at 1.3g/t against the feed head grade of 1.89g/t.

Although froth flotation is a well researched mineral processing technique, it shows low mineral extraction efficiencies relative to the hydrometallurgical process. Moreover, the process is sometimes not necessarily suited to deal with more complex ores, such as weathered ores.

1.2. Objectives of the Study and Key Questions

The objective of this study is in two parts; the first part of the study is focussed on assessing the extent of weathering at the PPM mining pit. This is achieved by evaluating host rock density and flotation profiles. In the second part the study then evaluates selected strategies to improve flotation recovery. The use of co-collectors and the effect of acid pre-treatment form the main focus of the study.

The objective of this study is also to answer questions raised by the mineralogical study conducted during the project feasibility study.

Key Questions:

1. How does the PPM ore body change with depth?
2. Can the loss of recovery be correlated with depth and why?
3. How can flotation performance of weathered PPM ore body be improved?

1.3. Scope of Study

The project is divided into two phases, the first phase reviews and establishes the extent of ore weathering down the mining pit. The initial phase aims to answer the question as to how deep the mining pit has to go before “fresh” ore, that is ore responsive to metallurgical treatment, can be realised. The weathering profile of the ore body will be

established by studying the density profile of the host rock down the mining depth as well as flotation recovery from ore sampled down the mining depth.

The second phase of the project will investigate ways to improve the flotation recovery of weathered ore. As oxidation of ore is thought to result in mineral passivation, initially, the use of acid pre-treatment will be investigated together with the normal reagent suite of sodium isobutyl xanthate (SIBX) as collector. Then oxide co-collector based on hydroxamate paired with normal sodium iso-butyl xanthate collector will be studied. Furthermore, a cocktail of reagents that involves both fatty acids and thionocarbamates collectors will also be investigated.

1.4. Research Approach

The project is divided into two phases, the first phase reviews and establishes the extent of ore weathering down the mining pit. The initial phase aims to answer the question as to how deep the mining pit has to go before "fresh" ore that is responsive to metallurgical treatment can be realised. The weathering profile of the ore body will be established by studying the density profile of the host rock down the mining depth as well as flotation recovery down the mining depth.

The second phase of the project will investigate ways to improve the flotation recovery of weathered ore. The use of flotation activators such as copper sulphate will not be included in this study but the base case scenario will consists of normal reagent suite of sodium isobutyl xanthate (SIBX) as a collector. Then oxide co-collector based on hydroxamate paired with normal sodium iso-butyl xanthate collector will be studied. Furthermore, a cocktail of reagents that involves both fatty acids and thionocarbamates collectors will also be investigated. Finally, as oxidation of ore is thought to result in mineral passivation, an acid pre-treatment of the ore will be included in the investigation.

1.5. Thesis Outline

Chapter two will review the literature in more detail with a brief description of the mine site and its geology. A brief description of the flotation process will be presented followed by the review of mineralogy. Within the literature review in chapter two, the

mineral oxidation mechanisms will also be considered. Chapter two will culminate with the proposed hypothesis.

Chapter three discusses experimental work where experimental method, the sampling method, and data analysis will be discussed.

Consistent with the problem statement, chapter four will present the results with some comments on observations. The results will then be discussed in chapter 5 where recovery weathering profile relative to mining depth and discussion on some flotation strategies to improve the recovery will be presented. The flotation strategies that will be evaluated will include oxide co-collectors, the thionocarbamates based co-collectors, and fatty acid based co-collectors. The effect of pre-leaching on flotation performance will also be evaluated. Chapter six will conclude the thesis conclusions together with recommendations or proposals for further work. The detailed tables of results and the description of analysis method utilised will be appended in the appendix.

2. CHAPTER TWO: LITERATURE REVIEW

2.1. GEOLOGY AND MINERALOGY

2.1.1. BUSHVELD GENERAL GEOLOGY

Platinum bearing ores were discovered in South Africa in the lode deposits of the Waterburg District in 1923 by Adolf Erasmus and then on the farm Maandagshoek by Andries Lombaard in 1924. Hans Merensky identified the platinum-iron alloy from Lombaard's panning and this quickly led to the discovery of the Merensky reef within the broader Bushveld Igneous Complex (Viljoen and W., 1998).

The Bushveld Complex was intruded about 2,060 million years ago into rocks of the Transvaal Supergroup, between the Magaliesberg quartzite of the Pretoria Group and the overlying Rooiberg felsites ((Molengraaff, 1904), and (Viljoen and W., 1998)). It is a large igneous complex formed by injection into the earth's crust of multiple phases of magma pulses. The total extent of the Bushveld Complex is approximately 66,000km^2, just over half of which is covered by younger formations (Guilbert and Park, 1986). The mafic rocks of the Bushveld Complex host layers rich in PGEs, chromium and vanadium, and constitute the world's largest known resource of these metals.

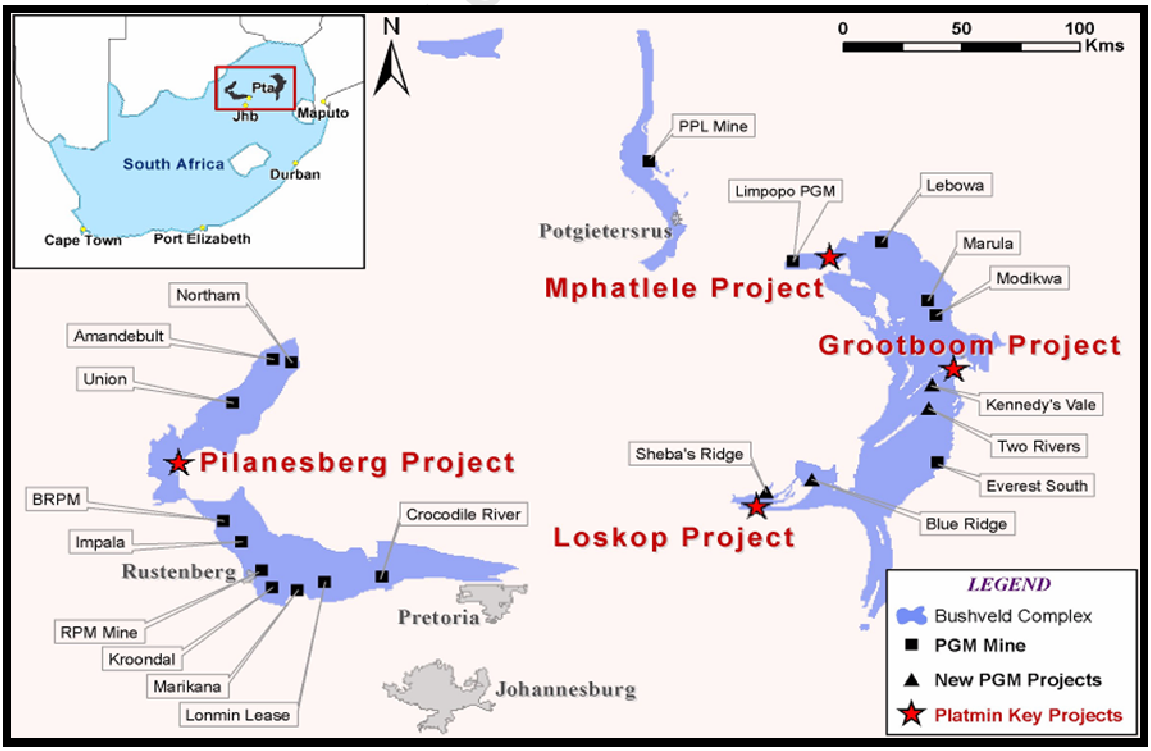

FIGURE 2: BUSHVELD GEOLOGICAL MAP SHOWING THE LOCATION OF PILANESBEG PLATINUM MINE (PPM) PROJECT (WALDECK, 2007)

The mafic rocks (collectively termed the Rustenburg Layered Suite or “RLS”) have been divided into five zones known as the Marginal, Lower, Critical, Main and Upper Zones from the base upwards

There are three main reefs with economic value found in the Bushveld Complex, namely Merensky Reef, Plat reef and UG2 reef (See Figure 3).

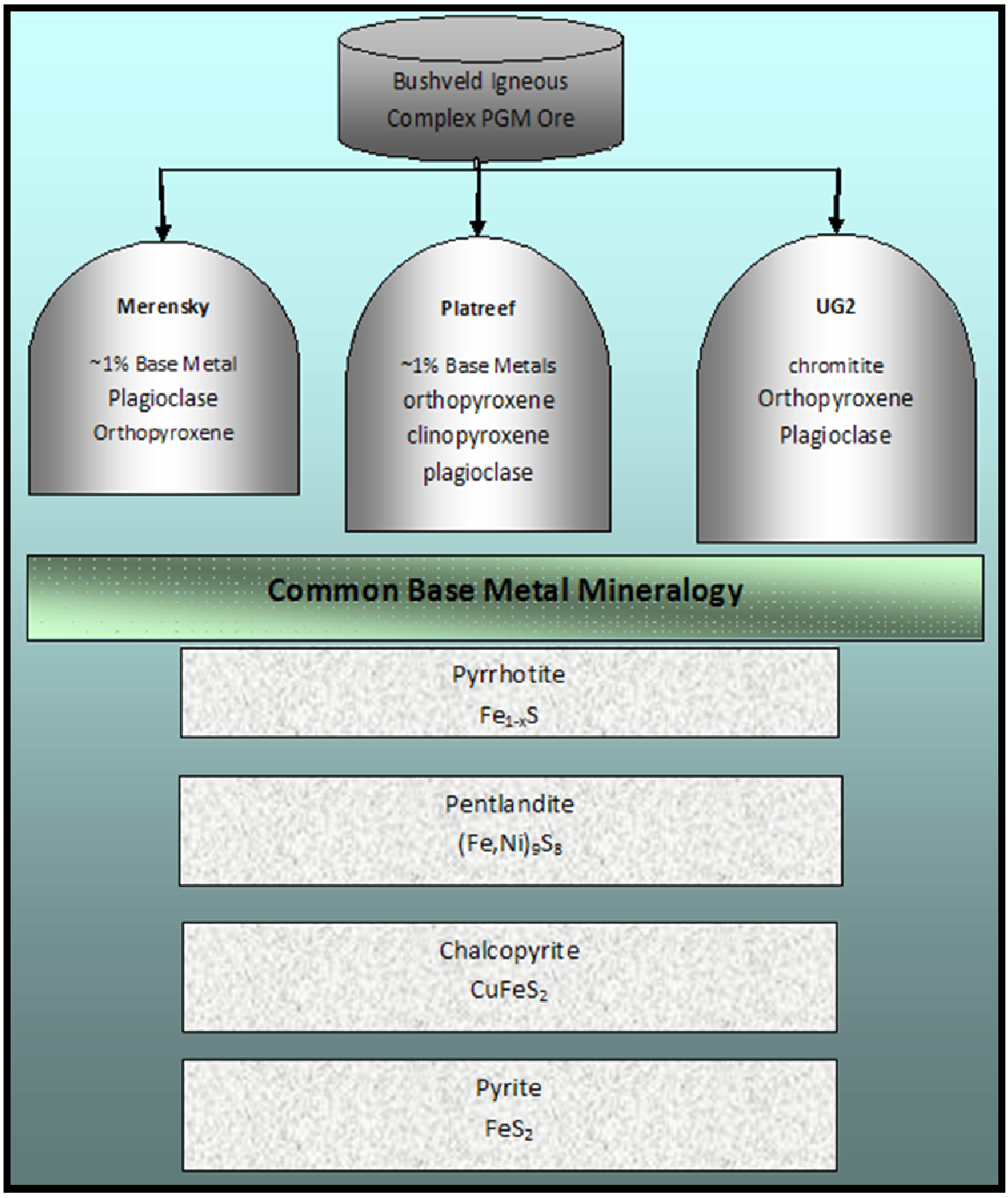

FIGURE 3: TYPICAL BUSHVELD IGNEOUS COMPLEX (BIC) MINERALOGY

In the normal stratification, the Merensky Reef consists of heterogeneous pegmatitic feldspathic pyroxenite bounded by narrow stringers of chromitite (Smith and Basson, 2003). The pegmatite varies and may comprise very coarse-grained feldspathic harzburgite or even medium-grained melanorite (Viljoen, 1999). The Merensky reef primarily consists of orthopyroxene and plagioclase. The base metal sulfide minerals, such as chalcopyrite, pentlandite and pyrrhotite which host platinum group elements (PGE) are minute (~1% contingent). Platreef is primarily orthopyroxene, clinopyroxene and plagioclase. The base-metal sulphides content in the Platreef is slightly higher than that of the Merensky reef (Armitage et al., 2002). However, the UG2 reef consists primarily of chromite, orthopyroxene and plagioclase, and even less base metals as opposed to the other reef types (Randolph, 1993).

PGM's may associate with base metals, oxide or silicate minerals in the ore. The mineralogy consists of PGM sulphides, arsenides, tellurides, and PGM alloys (see Table 1). This will vary across the reef types and over geographical regions. All major players in the platinum industry are mining Merensky and UG2 ores, the third type, Platreef, is currently mined only by Anglo Platinum. The value chain of PGM processing is essentially similar for all ore types, but each flow-sheet will have a slightly different processing route, dictated by the ore mineralogy.

TABLE 1: TYPICAL PGM MINEROLOGY FOUND IN BUSHVELD COMPLEX (RANDOLPH, 1993)

Pt-Cooperite	(Pt,Pd)S
Pd-Pt-Cooperite	(Pt,Pd)S
Pt-Rh-Cooperite	(Pt,Rh)S
Sperrylite	$PtAs_2$
Native Pt	Pt
Stillwaterite	Pd_8As_3
Hollingworthite	(Rh,Pt,Pd)AsS
Braggite	(PtPdNi)S
Moncheite	$(PtPdNi)(TeBiSb)_2$
Kotulskite	$(PtPdNi)(TeBiSb)_2$
Laurite	$(RuFeOsIrPt)S_2$
Pt-Fe alloy	Pt-Fe

2.1.2. GEOLOGY AT PPM

Pilanesberg Platinum Mine (PPM) project on the western limb of the Bushveld Complex is bounded within Tuschenkomst farm (Figure 4).

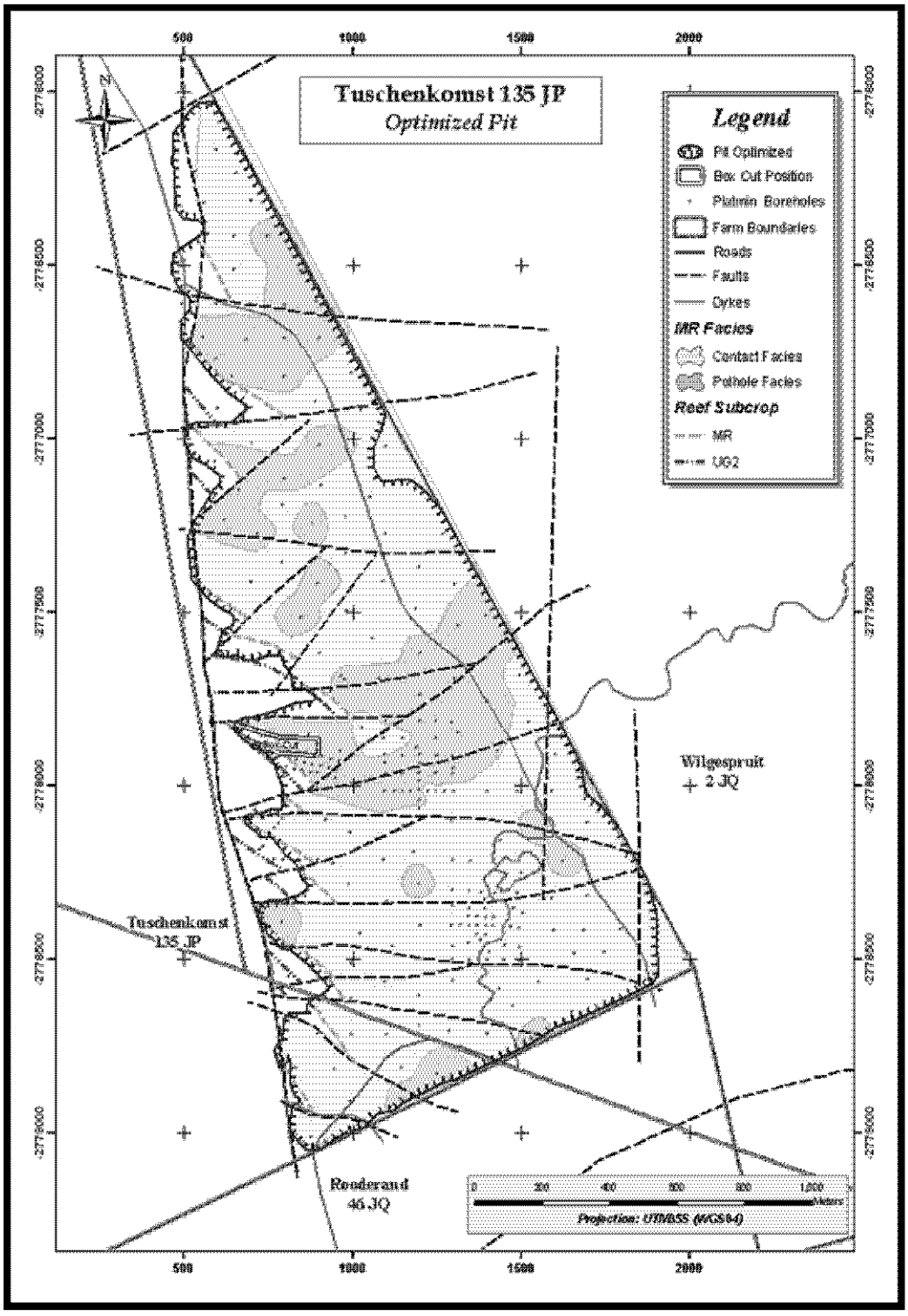

FIGURE 4: PPM GEOLOGICAL PLAN OF TUSCHENKKOMST FARM SHOWING PPM OPEN PIT OUTLINE (CROSSLING AND MUPAKATI, 2009B)

The farm neighbours the western and north-western boundary of the Pilanesberg Game Reserve. The topography within the project area is gently sloping towards the north, with steep sloping hills on the western side of the Pilanesberg Alkaline Complex. The project farm itself has rocks of the Critical Zone of the Bushveld Complex generally strike north-south and dip eastwards at between 5° and 40°.

The mineralised PGM horizons targeted at PPM stratigraphically descend in the following order: the Merensky Reef, the mineralised pods of the Merensky Footwall, the Upper Pseudo Reef, the Pseudo Harzburgite reef, and the Lower Pseudo Reefs. The whole package is collectively known as the "Silicate Reefs" (See Figure 5). The UG2 reef appears about 15m below the lower pseudo reef.

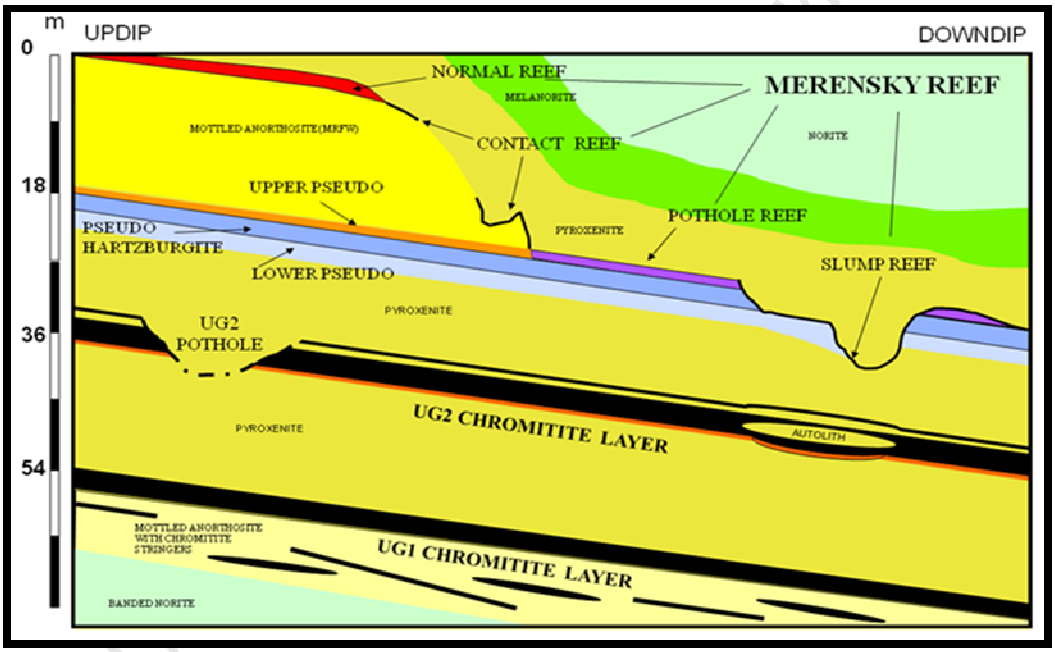

FIGURE 5: SIMPLYFIED STRATIFICATION MODEL FOR PPM PROJECT (CROSSLING AND MUPAKATI, 2009A)

The Merensky Reef is a feldspathic pegmatoidal pyroxenite, bounded top and bottom by thin chromitite layers. The PGMs present in this horizon are predominantly PGE–iron alloys and PGE-sulphides (Waldeck, 2007). The Merensky Reef is identified as a single chromitite stringer at the base of the Merensky hangingwall pyroxenite. The areas where Merensky reef is well developed are known as contact reef. Below the Merensky Reef is the Merensky footwall which consists of anorthosite bed rock. Some areas are found to have no chromitite stringer and Merensky hanging wall sit directly on the footwall. Such areas are known as potholed

reef. At Tuschenkomst both contact reef and pothole reef are well developed (See Figure 4).

The Pseudo Reef horizon is a distinctive feldspathic harzburgite layer, also bounded by thin chromitite layers, and normally situated some 15m below the Merensky Reef. The Pseudo Reef is generally split into an Upper Pseudo Reef with the average thickness of 67 cm, and a Lower Pseudo Reef with the average thickness of 1.2 m. There is also Pseudo Reef Harzburgite that occurs in between the lower and upper pseudo stringers.

The UG2 is the most consistently developed mineralised horizon at PPM project and accounts for 60 % of the PGE metal content on the farm ore reserves. There are also minor intrusions of Iron-Rich Ultramafic Pegmatites (IRUP) in the form of pipes, and dykes which generally replace the normal stratigraphic sequence.

Most of reefs mentioned above outcrops within the Tuschenkomst property. For mining and processing purposes, PPM classified both Merensky reef and Pseudo reefs as “Silicate reef”. This terminology will hence forth be used in this study. The open pit mining method was chosen as the most economically viable method to exploit the PGM mineral reserves. The pit is divided into three smaller sections developed as north, central and south pit (See Figure 4).

2.1.3. Mineralisation at PPM

In order to obtain more insight into the PPM ore body, Mintek Minerals Processing divisions were given two batches of samples. The first batch comprised of two Merensky borehole cores (Mineralised Footwall and Merensky Potholed Reef) which were derived from the mine site. The second batch comprised of two milled flotation feed samples also derived from the composite of borehole cores. The former samples were used to determine mineralogy while the latter samples were used to determine the PGM mode of occurrence and prediction of floatability. The samples were prepared using a rotary sample splitter to provide representative sub-samples (Duarte et al., 2004).

Mintek used optical microscopy and XRD to determine the major base-metal sulfide characteristics and major gangue minerals respectively. The optical microscopy

images of the sample studies are shown in Figure 6. The results indicate that PPM Sulfides occur mainly as discrete grains of up to 300 µm often locked in silicates. The most abundant base metal sulphide appears to be pyrrhotite (Duarte et al., 2004). At the same time pyrite seems to be a minor phase which sometimes constitutes sulphide mineral particles (see Figure 6).

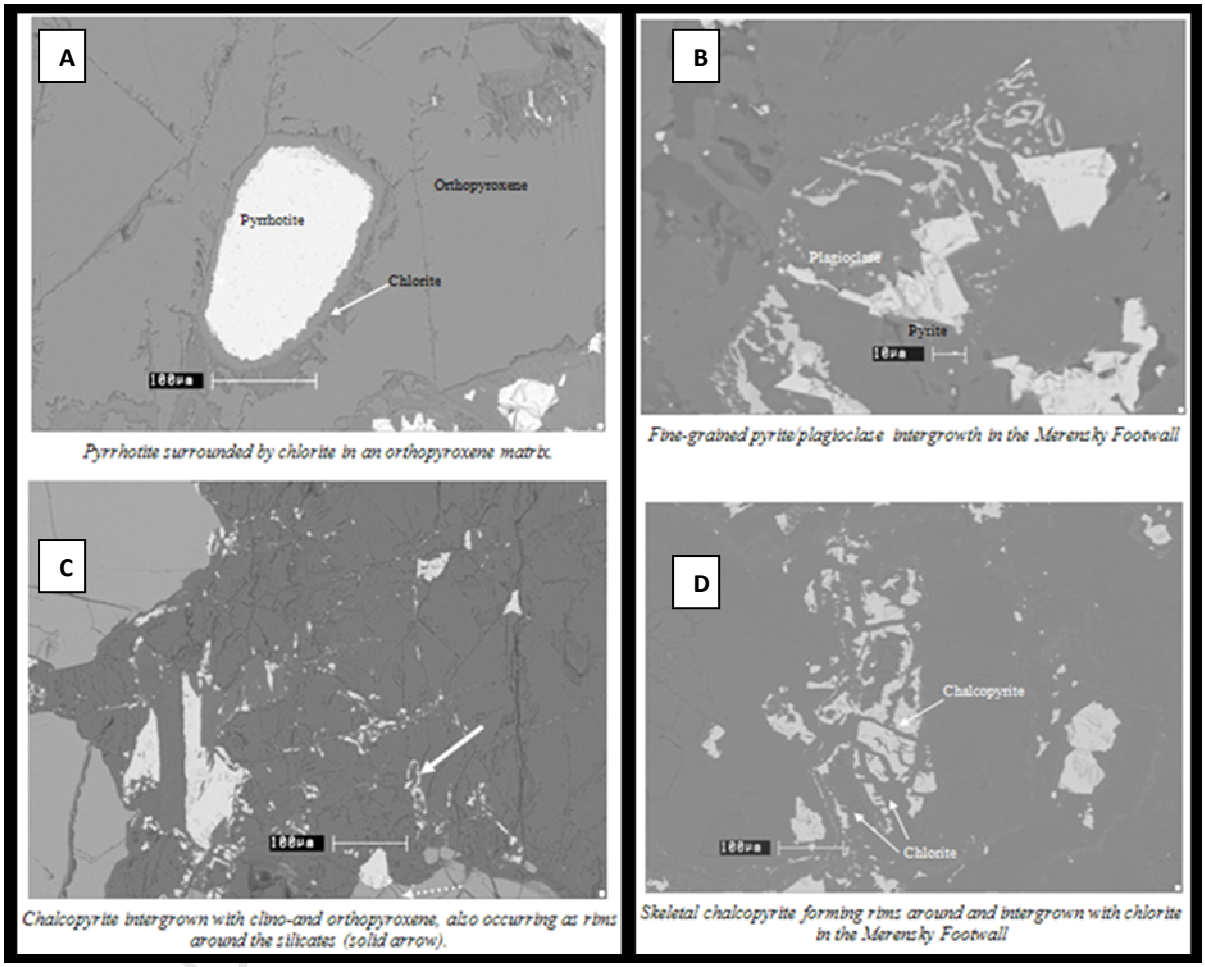

FIGURE 6: OPTICAL MICROSCOPY OF MERENSKY SAMPLES SHOWING SECONDARY BMS, RELATIVE SIZE, AND RELATIONSHIP TO THE GANGUE MINERAL (DUARTE ET AL., 2004)

The fine-grained intergrowth of sulfides and gangue as shown in Figure 6 (B) occurs sporadically. The optical microscopy images also show that the chalcopyrite with an average diameter of 10 µm, and pentlandite are often intergrown with the silicates. In some cases the sulfides have a skeletal appearance where sulphides have intergrown with chlorite Figure 6 (D). The optical microscopy images further showed that the sulfides were often associated with olivine.

The mineralogical findings indicated that the mode of occurrence of PGMs in the samples was attachment of particles to gangue minerals. The results showed significant amount of PGMs occurring in a form of PGM alloys (Mintek, 2004a). Platinum ferrite, Pt-Fe, was the most abundant of the alloys and it was associated mostly with silicates (see Figure 7). The PGMs associated mostly with secondary silicates in the normal Merensky, and mostly with secondary silicates in the potholed Merensky (Mintek, 2004a). In terms of Base Metal Sulphides (BMS), the potholed Merensky reef seemed to have higher quantities of pentlandite, chalcopyrite and pyrrhotite, while normal Merensky had more pyrite instead (see Figure 7). The presence of violarite on both normal Merensky reef and potholed reef indicated some degree of mineral alteration. Some PGM particles were found liberated within the milled composite sample, but their size appeared too small for optimal flotation (particle size less than 2 microns) (Mintek, 2004b).

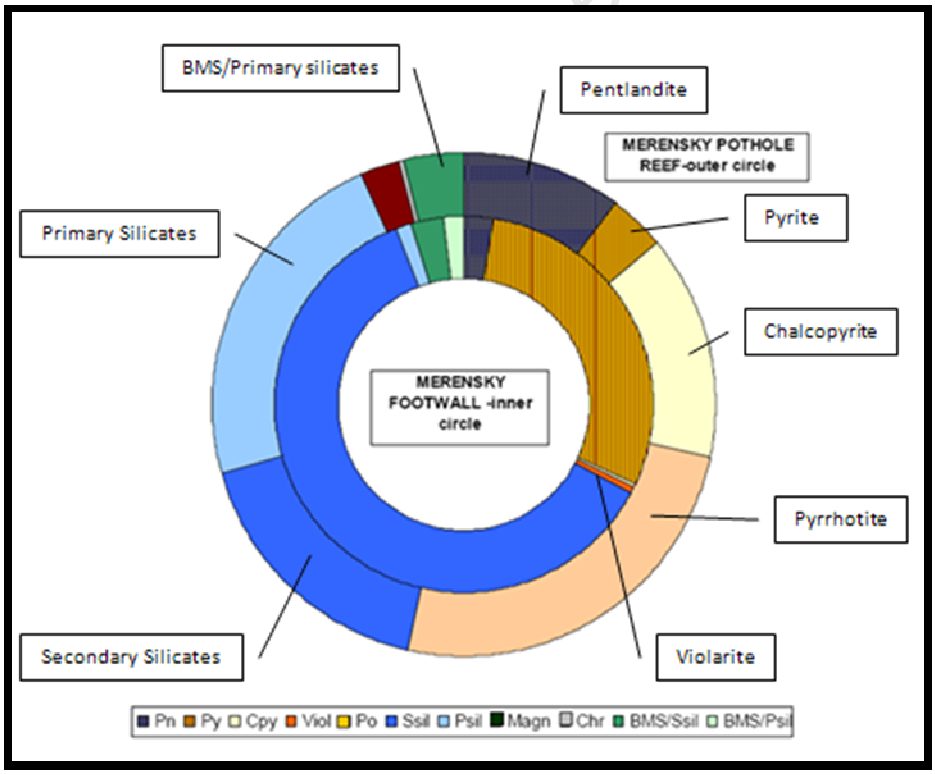

FIGURE 7: PGM HOSTS IN MERENSKY FEED SAMPLES (PGM VOLUME %) (DUARTE ET AL., 2004). THE INNER CONCENTRIC DOUGHNUT CHART SHOWS PGM DISTRIBUTION AND ASSOCIATION IN THE NORMAL MERENSKY AND THE OUTER DOUGHNUT CHART SHOWS PGM ASSOCIATION ON THE POTHOLE MERENSKY REEF.

Researchers such as Xiao et al. (2004) and Lamya (2007) have also observed that the base metal sulphides that associate with PGMs in the Merensky reef are pyrrhotite,

chalcopyrite, and pentlandite. However, Xiao et al. (2004) and Lamya (2007) did not distinguish between pothole and normal Merensky reef. They reported that base metal sulphides in Merensky reef appear in the following order of abundance: pyrrhotite at 41%, pentlandite at 37%, chalcopyrite at 18% and pyrite at 4%.

Other mineralogical studies done on the area have shown that the complexity of postcumulus growth, and a variety of complex intergrowths, pervade the occurrence and relationships of the PGM oxide minerals, thereby highlighting the need for experimental data on these phases ((Vermaak and Hendriks, 1976), (Ballhaus and Ryan, 1995), and (Stumpfl and Clark, 1965)). Vermaak et al. (1976) argued that the base metal sulfides occur as a temporal sequence typical of magmatic assemblages (pyrite, pyrrhotite, pentlandite, and chalcopyrite) with a host of rare minor PGM minerals. They also asserted that the PGM minerals are predominantly associated with the base metal sulphides, where idiomorphic braggite, cooperite, and laurite, with minor sperrylite, are the major discrete platinoid minerals. Another main platinoid that was observed by Vermaak et al. (1976) also constituted Pt-Fe alloy, which most commonly occurred as complex intergrowths with other PGM minerals, particularly the base metal sulfides. It was also contended that a significant "invisible" portion of the platinoids occurs within pyrrhotite, pentlandite, or pyrite, either as a true or as a "colloidal" solid solution (Vermaak and Hendriks, 1976). Studies of relationships of the PGM minerals with the silicate-oxide gangue indicate a clear preference for their occurrence at the contact of the base metal sulfides with the gangue. PGM mineral grains were found to be significantly smaller in chromite-rich ore compared with silicate-rich ore.

2.2. Mineral Processing Overview

2.2.1. Comminution and Liberation

In order to extract the PGM minerals from the mined ore, the run-of-mine is first taken through comminution and liberation before flotation. Comminution and liberation processes involve the reduction of rock size by way of crushing and milling. The run-of-mine ore is subjected to primary crushing, normally with a jaw crusher, and followed by secondary crushing, which mostly make use of cone crushers. The final stage of comminution and liberation involves milling and pulping of ore in a

semi-autogenous mill. The objective of the comminution process is to break complex particles, consisting of numerous minerals, into smaller particles (Gay, 2004). The aim is to break the host rock into individual particles consisting primarily of the desired mineral. This process, in which the mineral composition distribution in particles changes due to breakage and grinding, results in targeted mineral liberation. In order to increase liberation, particles need to be broken to as close as possible to the targeted mineral grain size. However, care must be taken to avoid over-grinding, which is associated with high energy costs, and it also becomes more difficult to subsequently separate particles (Tromans, 2008). Subsequent to comminution and liberation, the ore slurry is pumped to the flotation circuit for separation. Most operations subdivide flotation circuits into two sections: the primary and secondary flotation circuits. The primary flotation is used to recover fast floating PGM minerals, while the secondary flotation circuit provides the necessary residence time to recover slow floating PGM minerals. The flotation circuit use froth flotation technology to separate targeted PGM minerals from gangue minerals.

2.2.2. Froth Flotation

The flotation process is based on physiochemical principles, which use selective attachment of some particles to air bubbles in aqueous media, known as hydrophobicity, and on the other hand preferentially adhere other solids to water, a property known as hydrophilicity (Fuerstenau et al., 1985).

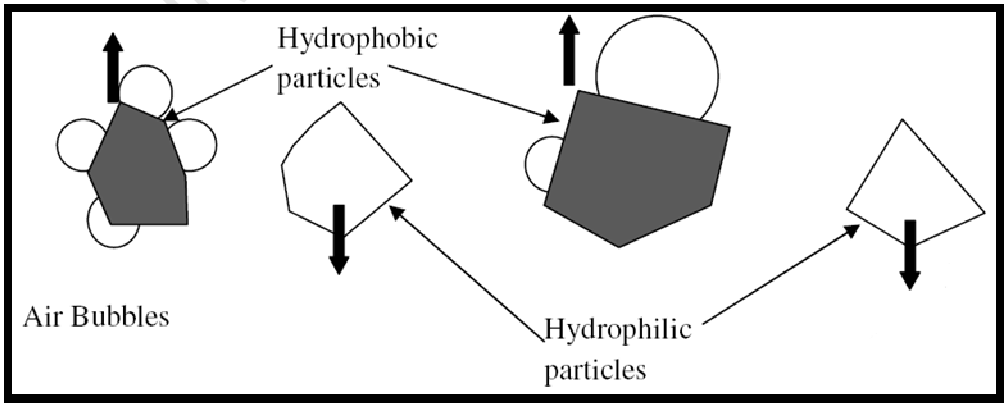

FIGURE 8: ILLUSTRATION OF SELECTIVE ATTACHMENT OF AIR BUBBLES TO HYDROPHOBIC PARTICLES

Many researchers such as Glembotskii et al. (1972), Klassen et al. (1963), and Metso (2006), have made contributions on the fundamentals of froth flotation. Froth

flotation is a highly versatile method for physically separating particles based on differences in the ability of air bubbles to selectively adhere to specific mineral surfaces in mineral/water slurry (see Figure 8).

The particles with attached air bubbles are then carried to the surface and removed, while particles that remain completely wetted stay in the liquid phase. Therefore flotation relies on the surface of the valuable mineral being hydrophobic while the surface of the gangue minerals remains hydrophilic (Whelan and Brown, 1956). The attachment of the bubbles to the surface is determined by the interfacial energies between the solid, liquid, and gas phases.

As noted by Gupta et al. (2006), the balance of forces can be altered by any factor, as illustrated in Figure 9, which changes any of the interfacial tensions. Hydrophobic mineral surfaces prefer to make contact with air over water due to a lower free energy (Kawatra and Eisele, 1992).

The nature of particle surface is very important to the chemistry required for froth flotation. It is important that the mineral particle surface is sufficiently hydrophobic to enable targeted mineral particles to attach to the rising bubbles thereby separating from the gangue minerals.

The flotation system has many interrelated components (Figure 9) that have significant bearing on the final separation outcome. Variables highlighted in Figure 9 are chosen for this study.

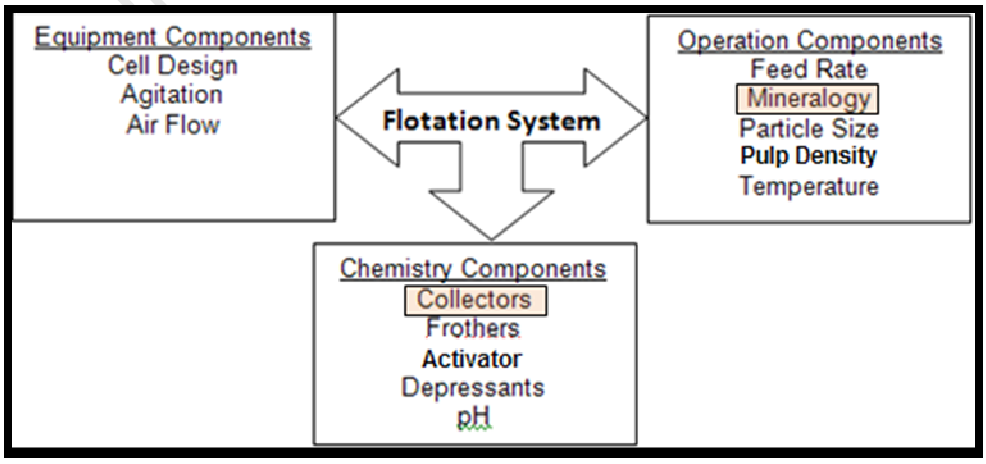

FIGURE 9: ILLUSTRATION OF FLOTATION SYSTEM THAT INCLUDES MANY INTERRELATED COMPONENTS

Changes in the settings of one component, say pulp density, will automatically cause or demand changes in other parts of the system such as flotation rate, particle size recovery, air flow, feed rate, etc. As a result, it is difficult to study the effects of any single factor in isolation, and compensation effects within the system can keep process changes from producing the expected effects (Klimpel, 1995).

In order to expose the hydrophobic surface of a mineral surface, it usually requires varying degrees of agitation. The air is introduced at the bottom of the cell in order to supply the necessary air required for bubble generation.

2.2.3. Flotation Reagents

Reagents are normally used in pre-treatment to enhance the hydrophobicity of desired mineral particles, and at the same time some reagents are added to increase hydrophilicity of gangue minerals. Other reagents are added to aid in creating sufficient bubbles within the slurry and maximise surface area for bubble particle attachment. The typical reagent suite for many operations consists of collectors, depressants, frother, and sometimes activators. Collectors are typically heteropolar organic substances - they contain both polar and non-polar chemical groups. The non-polar end is almost always a long chain or cyclic hydrocarbon group that is hydrophobic. The collector must be able to attach to the solid, and it does so through its polar end, which is typically an ionic group or sometime referred to in literature as solidophil group (Bulatovic, 2007). Depressants, on the other hand, induce more hydrophilic surfaces onto gangue minerals and discourage gangues material to attach to the rising bubbles.

Whilst it may be possible to initially obtain solid particle attachment to air bubbles in agitated slurry under aeration, the air bubbles unaided by a frother tend to be unstable and quickly break down due to collisions with other bubbles, solid particles and the vessel walls. In addition, the bubble size may not be sufficient to effectively carry a solid particle to the surface of the liquid. Consequently, frothers are added to promote the formation of stable air bubbles under aeration. Frothers also comprise of both polar and non-polar ends. The non polar hydrophobic end orients them into the air phase. Activators are sometimes added to chemically coat the solid surface and increase the interaction with collectors that are ineffective by themselves.

Dispersants are only used when mineral particles are agglomerated together, in order to break agglomeration of particles apart so that single particles interact with collector and air bubbles.

It is sometimes necessary to add a modifier or conditioner such as pH adjustment, where mineral surface change, or where precipitation of soluble salts, and reagent concentration change may be necessary. Powdered activated carbon can be used as modifier or conditioner because it can improve separation of metals by adsorbing excess depressants and other organic reagents, such as collectors, from the solution or mineral surface.

2.2.3.1. COLLECTORS

Collectors are reagents that are used to selectively adsorb onto the surfaces of particles. They form a monolayer on the particle surface that essentially makes a thin film of non-polar hydrophobic hydrocarbons. Selection of the correct collector is critical for an effective separation by froth flotation.

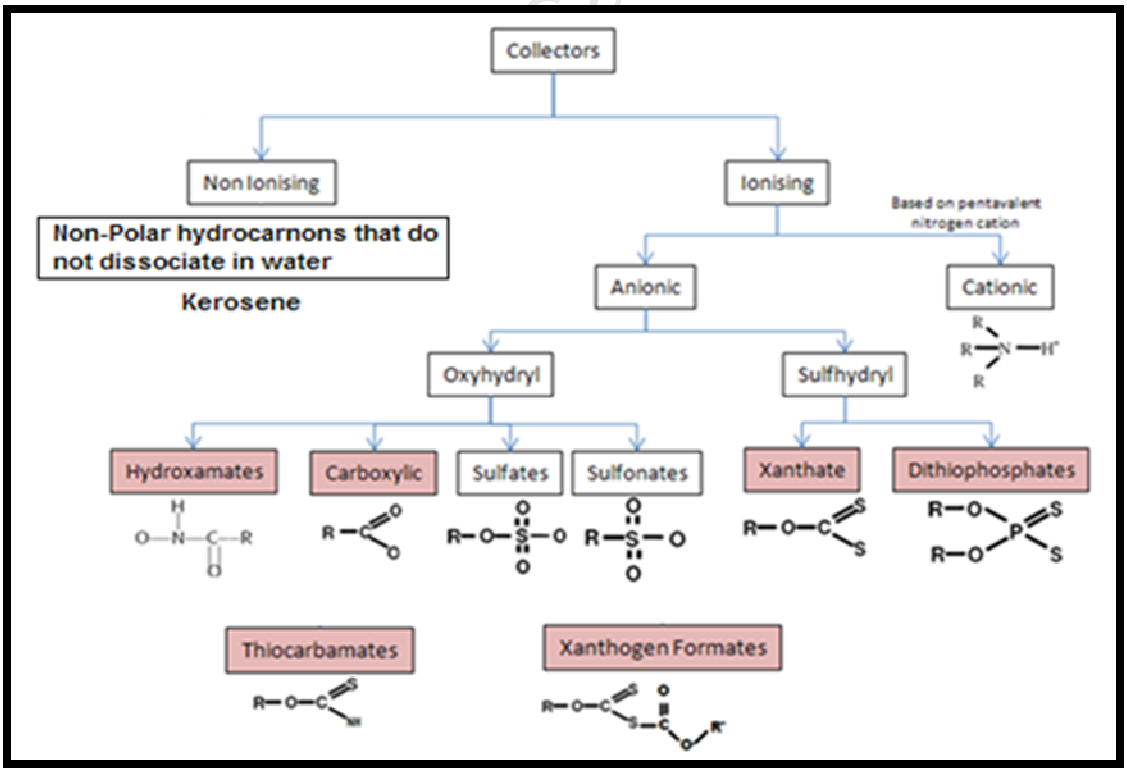

FIGURE 10: BASIC COLLECTOR TYPES (ADAPTED FROM BULATOVIC, 2007)

Collectors are classified according to their ability to dissociate in aqueous solution and with regard to the type of ions that produces the water repellent

effect (Mudd, 1992). Where collectors dissociate into an anion and cation, the ion that is the direct cause of the water repellent action is considered as the active ion and the other as non-active. The water-repellent ion structure always includes a hydrocarbon radical, the presence of which ensures that the mineral is water repellent. However, hydrocarbons do not exist in the free state and are unable to attach themselves directly to the mineral surface. Therefore, the repellent ion structure includes a second group of atoms (in addition to hydrocarbon) to form a link between the hydrocarbon and the mineral surface. This linking group is called the solidophil group (Bulatovic, 2007). Thus a water-repellent collector ion includes a hydrocarbon radical linked to a solidophil group. The water-repellent effect is directly associated with the length of the hydrocarbon group, while the solidophil controls both the strength and the selectivity of the ion attachment to the mineral surface.

As shown in Figure 10, collectors can be classified according to ionic dissociation, anionic and cationic activity in relation to the mineral surface, and the solidophil group structure. Anion collectors are, therefore, those in which anion (negatively charged) renders the mineral water repellent. Cation collectors are those where water repellence is secured by the cation (positively charged).

Most anion collectors such as xanthate are very selective and have strong attachment to the mineral surface. The solidophil group of xanthate is a bivalent sulphur.

The particles that are immersed in water develop a net charge due to exchanging ions with the liquid. The idea behind flotation reagents is to manipulate the chemistry of the solution so that one mineral has a strongly positive charge, while other minerals have a charge that is either only weakly positive, or negative. In these conditions, the anionic collector will preferentially adsorb onto the surface with the strongest positive charge and render them hydrophobic.

2.2.3.2. FROTHERS

Frothers are compounds that act to stabilize air bubbles so that they will remain well-dispersed in the slurry. They are surfactants which are usually heteropolar

organic compounds. The most commonly used frothers are alcohols, particularly MIBC (Methyl Isobutyl Carbinol, or 4-methyl-2-pentanol, a branched-chain aliphatic alcohol) or any of a number of water-soluble polymers based on propylene oxide (PO) such as polypropylene glycols. The polypropylene glycols in particular are very versatile, and can be tailored to give a wide range of froth properties. Due to heteropolar properties, a frother adsorbs at the water/air interface, resulting in reduced water surface tension. This has the effect of producing smaller bubbles and it stabilises the froth on top of the slurry level. It is important to ensure that the bubble is stable long enough to allow concentrate to be removed from the flotation cell.

2.2.3.3. ACTIVATORS

Activators are specific compounds that make it possible for collectors to adsorb onto surfaces that they could not normally attach to. A classic example of an activator is copper sulfate as an activator for sphalerite (ZnS) flotation with xanthate collectors (Fuerstenau, 1982). The reaction mechanism for copper activation on sphalerite as earlier proposed by Fuerstenau (1982) could be summed up by the following two Equations :

Equation 1: $$\mathbf{ZnS(s) + Xanthate^- \rightarrow S(s) + ZnXanthate\ (aq)}$$

Equation 2: $$\mathbf{ZnS(s) + CuSO_4(aq) \rightarrow CuS(s) + ZnSO_4(aq)}$$

The mechanism shown in Equation 1 and Equation 2 purport that the surface of the sphalerite is activated by reacting it with a metal ion which does not form a soluble xanthate, such as soluble copper from dissolved copper sulphate. In this case, a cation exchange takes place between the zinc from the sphalerite crystal lattice and copper from copper sulphate. The copper forms much stronger bond with xanthate than zinc would do. This effectively activates the mineral surface of sphalerite by forming a thin film of copper sulfide on the sphalerite surface, which allows for stable attachment of the xanthate, rendering the sphalerite particle hydrophobic and floatable.

However, more recent studies Gerson et. al. (1999) have proposed a different mechanism whereby the replacement of a bulk Zn cations by a Cu cations is

achieved, compared to the replacement of a surface Zn as proposed by Fuerstenau (1982). This new proposed mechanism offers a possible explanation for the two step activation kinetics observed through experiments. The replacement of zinc by copper atoms in accordance with mechanism advanced by Gerson et. al. (1999) requires no additional bond breakage. It was postulated that the three Zn–S bonds are replaced with three Cu–S bonds with different electron density, requiring low activation energy compared to the activation energy required for bulk replacement of Zn by Cu.

The ToF-SIMS analysis of the iron containing sulphide mineral surface subsequent to copper activation (Gerson and Jasieniak, 2008) suggested an increased surface oxidation on the samples that experienced increased conditioning time in water prior to copper activation compared to the samples that were treated with copper solution in the first place, provided the ore was fresh in the first place. This observation suggested the role of copper activation as stabilising the mineral surface thereby reducing the mineral propensity to oxidise. However, in the case of oxidised ore (ore that was conditioned in water for a long time), the study of the mineral surface revealed the presence of Cu(II) on the sulphide mineral surface indicating the formation of Cu(II)-containing precipitates. This inferred that the copper activation was non-specific as seen in the case of fresh ore were Cu(I) was still present, resulting in higher recovery but lower grades. This work showed that prolong oxidation prior to copper activation causes reduction of Cu(I) to Cu(II) on the mineral surface. But most importantly the ineffectiveness of copper activation on highly oxidised ore such as PPM oxidised ore.

2.2.3.4. DEPRESSANTS

Depressants have the opposite effect of activators; preventing collectors from adsorbing onto particular mineral surfaces. Their typical use is to increase selectivity by preventing one mineral from floating, while allowing another mineral to float unimpeded.

It is important to note that depressants are very sensitive to specific mineral/collector combinations. However, most operations floating sulphide minerals and PGMs generally use organic polysaccharide compounds as flotation

depressants. These tend to be soluble polymers (such as starch, cellulose and guar) that selectively coat mineral surfaces and prevent collectors from attaching.

2.2.4. Flotation of Oxidised Ores

The flotation of PGMs from the ore mined near surface is normally met with limited success. Due to atmospheric and weather realities around the ore body, the material near surface tends to be found much more altered and oxidised compared to the material found buried deep in the ground. The extent of oxidation on the ore body tends to diminish with increasing depth.

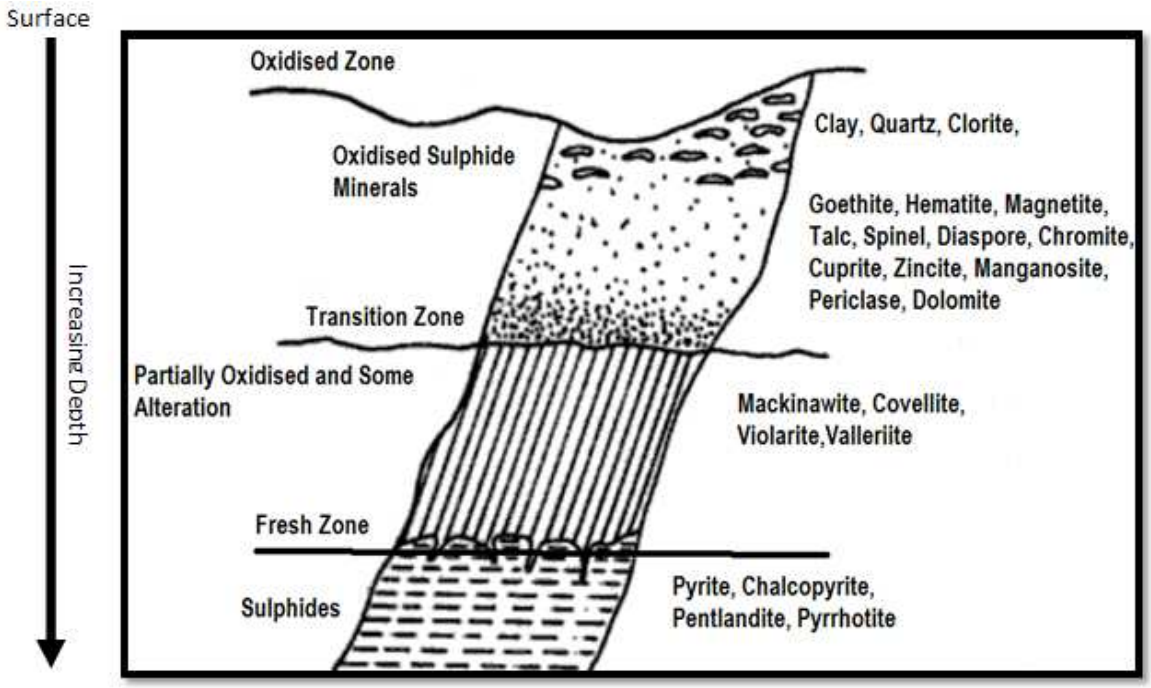

FIGURE 11: IDEALISED MODEL OF ORE DEPOSITE SHOWING OXIDATION NEAR SURFACE AND TRANSITIONING TO SECONDARY SULPHIDE AND FRESH SULPHIDES AT THE DEEP END, ADAPTED FROM (BARTLETT, 1998)

Figure 11 shows an idealised cross section of an ore body in terms of weathering and alteration. The primary sulphidic ore begins to be dominant at depth. Above this zone is a transition zone with a secondary enrichment zone and the oxidized zone, where naturally weathered material tend to reside towards the surface. Legrand et al. (2005a) studied the mode of occurrence of sulphide minerals within the oxidised zone. In particular, using X-ray photoelectron spectroscopy (XPS), it was shown that altered pentlandite [$(Fe,Ni)_9S$] and pyrrhotite ($Fe_{1-x}S$) co-existed within the oxidised zone.

With regard to silicate minerals, primary silicate minerals such as orthorpyroxene, olivine, and plagioclase also get affected by alteration near surface. The oxidation transforms these silicate minerals into various hydrated phyllosilicates such as talc, serpentine and chlorites. Becker et. al. (2006) observed naturally floating pyroxene within some Merensky ores. It was argued that the naturally floating pyroxene was really a function of the surface association of talc with pyroxene. Table 2 below shows that altered silicate minerals generally have lower density compared to parent silicate minerals.

TABLE 2: SPECIFIC GRAVITY OF SILICATE MINERALS FOUND AT PPM (KLEIN AND HURLBUT, 1993)

Silicate Minerals	Composition	Specific Gravity
Enstatite	$(Mg, Fe)SiO_3$	3.2- 3.5
Diopside	$CaMgSi_2O_6$	3.2
Plagioclase	$(Na, Ca)AlSi_3O_8$	2.6 - 2.8
Forsterite	Mg_2SiO_4	3.2
*Hornblende	$(Ca,Na)_{2-3}(Mg,Fe,Al)_5Si_6(Si,Al)_2O_{22}(OH)_2$	3 – 3.4
*Lizardite	$Mg_3Si_2O_5(OH)_4$	2.5 – 2.6
*Talc	$Mg_3Si_4O_{10}(OH)_2$	2.7 – 2.8
*Chlorite	$(Mg,Fe)_3(Si,Al)_4O_{10}(OH)_2$	2.6 – 3.3
*Quartz	SiO_2	2.65

*Altered Silicate Minerals

Hydrated silicate minerals such as talc, chlorite and serpentine are generally soft with density ranging from 2.5 g/cm^3 to 2.96 g/cm^3 (Scott, 1921). However, plagioclase minerals such as anorthosite tend to be relatively resilient to alteration. Therefore, the structure and texture of plagioclase minerals tends to preserve them from oxidation ((Cawthorn and Lewis, 2009) and (Lundgaard et al., 2006)). Anorthosite density of about 2.8 g/cm^3; remains unchanged, whether it lies near surface or at depth. In contrast, mafic minerals like pyroxenes readily exchange Mg-Fe, making then easily susceptible to alteration (Cawthorn and Lewis, 2009).

Alteration of both the primary sulphides and primary silicates has profound impact on flotation characteristics. As mentioned in the preceding paragraph, normal

flotation reagents suites in the PGM industry are based on sulphide collectors and are not particularly suited for altered or oxidised ores. Lindsay (1988) in his work made similar observations and reported that altered minerals, both silicate and base metal sulphide, tend to report mostly to the tailings during flotation. The study by Becker (2009) also showed that the amenability of pyrrhotite towards oxidation has a detrimental effect on flotation response because of hydrophilic iron hydroxide that forms on the sulphide mineral surface and renders the pyrrhotite less responsive to flotation.

The impact of oxidation could not only be confined to pyrrhotite but other sulphide minerals which tend to suffer the same fate. Legrand et al. (2005a) managed to obtain the Fe 2p, Ni 2p, S 2p, and O1s spectra for sulphide minerals from polished surfaces, and reacted the surfaces with aqueous solutions at pH 9.3 for up to 180 minutes. They observed that sulphide minerals oxidize rapidly to give mostly a relatively thin layer of Fe(III) oxyhydroxide, perhaps in the form of FeOOH. The study further observed the presence of violarite ($FeNi_2S_4$), $Ni(OH)_2$, and $NiSO_4$ around the pentlandite oxidized overlayer. Traces of Fe(III)-S and polysulphide species were also found in the overlayers.

The ore body that is dominated by pyrrhotite such as the PPM ore body creates added challenges in the flotation circuit. The study by Legrand et al. (2005b) has shown that a pyrrhotite surface oxidizes more rapidly than other sulphide minerals, such as pentlandite. However, even though pentlandite was less responsive to oxidation, it still had small amounts of nickel hydroxide ($Ni(OH)_2$) and nickel sulphate ($NiSO_4$) in the Fe(III) oxyhydroxide (FeOOH) - dominated overlayer.

The observations of the oxidation and alteration on the mineral sulphide surface are entirely consistent with thermodynamic calculations made on the relative stabilities of pentlandite, violarite, nickel hydroxide, Nickel sulphate, and iron oxyhydroxide. It was postulated by Legrand et al. (2005a) that the initial stage of oxidation or alteration of sulphidic minerals like pentlandite is characterized first by the formation of violarite together with iron oxyhydroxide. A further oxidation yields nickel sulphate, also accompanied by iron oxyhydroxide and violarite. The

pentlandite, if further exposed to more oxidising conditions, ends up converting to nickel hydroxide, violarite and iron oxyhydroxide. However, Legrand et al. (2005b) observed that violarite ultimately gets consumed and only $NiSO_4$ and FeOOH remain as thermodynamically stable oxidation products on the mineral surface. Perhaps, geologically the presence of violarite as opposed to nickel sulphate could be used to determine transition zone where ore body changes from oxidised zone to the fresh/un-weathered zone (see Figure 11). Furthermore, nickel sulphate has a solubility of 75.6g/100mL while ferric oxyhydroxide has very low solubility. This allows nickel sulphate to migrate from the mineral surface and leaves iron (III) oxyhydroxide behind.

Becker (2009) also suggested other oxidisation mechanism, whereby sulphide minerals undergo anodic oxidation when exposed to dissolved oxygen or atmospheric air. With regard to pyrrhotite, Becker (2009) argued the susceptibility of pyrrhotite to oxidation compared to other sulphide minerals such as pentlandite, pyrite and chalcopyrite by comparing relative conductivity of these minerals. Pyrrhotite as a complete metallic conductor, Becker (2009) concluded was more amenable to oxidation than other sulphide minerals which were more like semi-conductors. Hence the ease of sulphide mineral oxidation as a function of mineral rest potential is more favoured with pyrrhotite compared to other sulphide minerals. The mineral rest potential is defined as an equilibrium potential of the mineral at zero electric current.

Smart (1991) studied the surface of sulphide minerals and contended that there exists evidence of relatively thick carbonaceous, hydrophobic layers on some specific ores which gives minerals such as pyrite and chalcopyrite their natural floatability. Smart (1991) found that sulphide mineral surfaces may have substantial hydroxide content in three forms; namely as thin (5–80 nm) layers, oxidised fine particles (0.1–5 µm) attached to larger sulphide particles or colloidal such spheroidal iron hydroxide that precipitated from solution. This study effectively concluded that the flotation of sulphide minerals is dependent on the exposure of clean surface that can complex with collectors and attach to the rising bubble.

The surface oxidation of sulfide minerals as observed by Newell et al. (2006) can have a significant impact on flotation. Newell et al. (2006) studied Merensky ore type sulfides where an ore containing pyrrhotite, pentlandite and chalcopyrite was thermally oxidised. They presented back-scattered scanning electron microscope images, showing the oxidation layer which formed on the sulphide mineral surfaces.

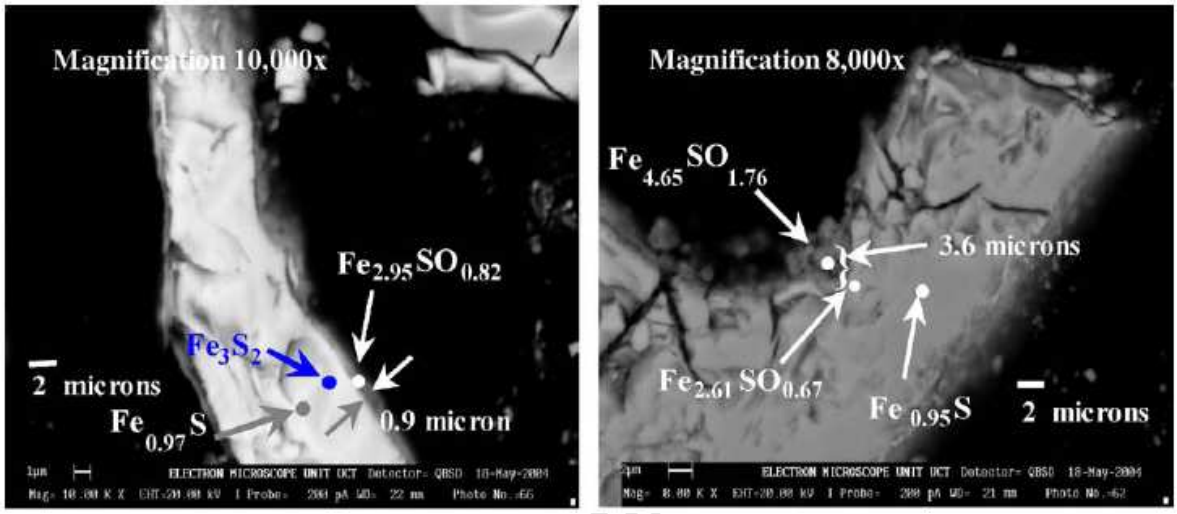

FIGURE 12: SEM BACK-SCATTERED ELECTRON IMAGES OF CROSS-SECTIONS OF HEAVILY OXIDISED PYRRHOTITE PARTICLES: (A) 50 DAYS AND (B) 60 DAYS (20 KV ACCELERATION (NEWELL ET AL., 2006)

The technique Newell et al. (2006) used to analyse the oxidation on the sulphide mineral surface was based on the fact that the oxidation layers were depleted in both sulfur and iron with incorporated oxygen. Particles with hydrophilic oxidation coatings are observed to float more slowly than particles with clean surfaces (Smart, 1991). The studies by Smart et al. (1998) and Rumball et al. (1996) found that the degree of oxidation on the particle surfaces is invariably greater in tailings than in concentrate. Newell et al. (2006) have also shown that the flotation recoveries decreased rapidly with increasing oxidation. And they found that oxidation had more impact upon the finer size fractions, particularly for pyrrhotite, therefore it will be common in operating plants treating oxidised ores to experience greater loss of PGE in the finer size fractions.

Vaughan et al. (1997) illustrated sulphide mineral surface oxidation mechanism using chalcopyrite, as it provides a good example of a relatively reactive metal sulphide surface and of the influence of stoichiometry on reaction rates.

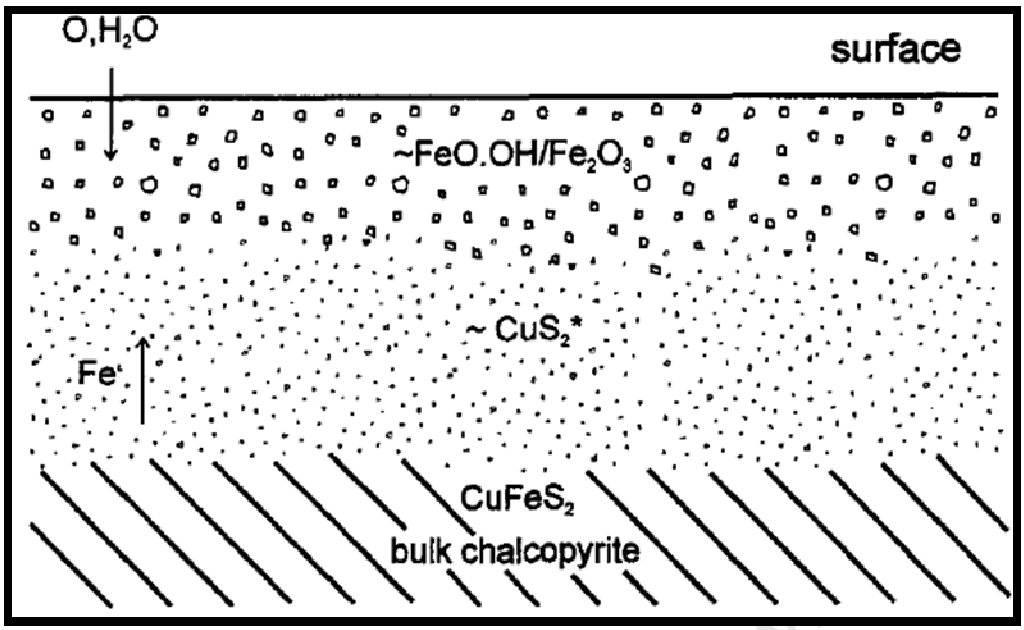

FIGURE 13: ILLUSTRATION OF THE DEVELOPMENT OF OXIDATION ON CHALCOPYRITE SURFACE (VAUGHAN ET AL., 1997)

Figure 13 shows an illustration of oxidation of chalcopyrite sulphide mineral. In this work Vaughan et al. (1997) considered a cyclic voltammogram for a chalcopyrite electrode in a solution at pH 9.2. In conjunction with XPS and XAS data, they proposed the sequence of oxidation reactions as shown below:

Equation 3: $$2CuFeS_2 + 3xOH^- \rightarrow 2CuFe_{1-x}S_2 + xFe_2O_3 + 3xH^+ + 6xe^-$$

Equation 4: $$2CuFeS_2 + 6OH^- \rightarrow 2CuS_2 + Fe_2O_3 + 3H_2O + 6e^-$$

Equation 5: $$2CuFeS_2 + 3OH^- \rightarrow 2CuS_2 + Fe(OH)_3 + 3e^-$$

Equation 6: $$2CuS_2 + 2OH^- \rightarrow 2CuO + 2S + H_2O + 2e^-$$

Equation 7: $$2CuS_2 + 2OH^- \rightarrow 2Cu(O)_2 + 2S + 2e^-$$

Vaughan et al. (1997) proposed that whenever the bulk solution potential exceeds the rest potentials, a monolayer of $Fe_2O_3/Fe(OH)_3$ is formed on sulphide mineral. The migrations of iron from the bulk sulphide mineral to the surface, say in chalcopyrite (Figure 13); leaves Cu and S within the bulk sulphide mineral un-oxidised in a metastable phase of CuS_2 stoichiometry. Both the oxide layer and metastable phase layer underneath causes the passivation of the sulphide mineral from the flotation process.

Exposing the sulphide mineral for longer periods and/or increasing potential sustains the oxidation reaction, thereby removing iron from deeper within the chalcopyrite. The rate controlling step in this mechanism is likely to be the solid state diffusion of ions to the sulphide mineral surface. It was further argued by Vaughan et al. (1997) that the above mechanism is dependent on Eh-pH. The passivation of the CuS_2 phase decomposes further according to EQUATION 6 and EQUATION 7. In the case where the control of the oxidation reaction rate is governed by diffusion from the bulk to the surface, it might be expected that variations in metal-sulphur ratio influence oxidation rate.

The oxidation mechanism proposed by Vaughan et al. (1997), shown in Figure 13, is not only exclusive to chalcopyrite. Most sulphide minerals emanate from the basic crystal structure, such as PbS, ZnS and FeS_2 that get modified to give rise to ordered substitution such as chalcopyrite, $CuFeS_2$, pentlandite, $(Ni,Fe)_9S_8$ and pyrrhotite, $Fe_{1-x}S$. It is therefore anticipated that other sulphide minerals are likely to follow the same oxidation mechanism.

2.2.5. Refractory PPM Ore Deposit

The PPM PGM ore deposit has proven rather difficult to process due to the specific characteristics of mineralogical weathering and oxidation, especially on the ore body closer to the surface. The presence of over ten different lithological layers and fine size of sulphide minerals adds to the complexity in terms of ore treatment. Most of the PGEs are found present in mottled anothosite, pegmatoidal pyroxinite, harzburgite, pegmatoidal olivine pyroxinite and UG2 chromitite layer. However, the biggest challenge with regard to this ore body is poor metallurgical response due to weathering. The weathering and/or alteration is believed to have followed the shrinking core model, whereby the sulphide mineral suffers either oxidation or alteration from the particle surface inwards ((England et al., 1999), (Cai et al., 2005) and (Mphela, 2010)). The oxidation, or alteration, changes the surface chemistry of the sulphide mineral particle, which weakens the particle ability to interact with flotation reagents.

In his thesis Lamya (2007) has also contended that alteration of base metal sulphides can cause changes to the surface chemistry that result in partial loss of

hydrophobicity and therefore affect the ability of sulphide minerals to float. In the western Bushveld, as reported by Lamya (2007), the most common altered sulphides includes but not limited to mackinawite (FeS_{1-x}), covellite (CuS), violarite ($FeNi_2S_4$) and valleriite ($4(Fe,Cu)S{\cdot}3(Mg,Al)(OH)_2$). As mentioned earlier, oxidation or partial oxidation of targeted minerals particles also have adverse effects on the flotation process. It is believed that, oxidation can occur in-situ or even during the milling process due to suspected galvanic interactions to form iron oxide, hydroxide and sulphate rim on the iron sulphide mineral surface (Adam et al., 1984). The oxidation layer on the sulphide mineral surface also interferes with surface hydrophobicity and causes such oxidised sulphide minerals to report to tailings.

The problem is also compounded by the fact that altered silicate minerals such as talc, serpentine, and chlorites becomes hydrophobic and begin to compete with targeted PGM minerals for reagents. Altered gangue minerals such as talc are known to float even without assistance of collectors (Martinovic et al., 2005). The positive flotation of these gangue minerals, also result in poor concentrates grades; that becomes difficult to sell to the smelter.

It has been established in literature that all sulphide minerals exhibit oxide and hydroxide species on their surfaces when exposed to air and aqueous medium for an extended period of time ((Buckley and Woods, 1985) (Buckley, 1987) (Buckley et al., 1985), (Smart, 1991), (Fornasiero et al., 1994), (Pratt et al., 1994), (Zachwieja et al., 1989), (Richardson and Vaughan, 1989), and (Jones et al., 1992)). Pilanesburg Platinum mine is running open cast mining operations, which invariably deal with the portion of the ore bodies that are close to the surface. Surface ore bodies are subject to varying degree of weathering and PPM ore body is no exception (Figure 14).

As mentioned earlier, the recovery of PGEs at PPM operations are somewhat depressed and mostly erratic. There seems to be a significant portion of material that is somehow refractory to the current flotation process as seen in the recovery profile in Figure 14. It is hypothesised that the low and erratic recoveries experienced are due to both geological oxidation and galvanic passivation during milling. It was found that the PGE reefs at PPM were generally oxidised down to a

depth of 40 m below surface, particularly where the reefs are affected by faulting (Waldeck, 2007). Although the level of oxidation did not seem significant, the effect on the flotation characteristics was much more pronounced as seen on the recoveries (See Figure 14).

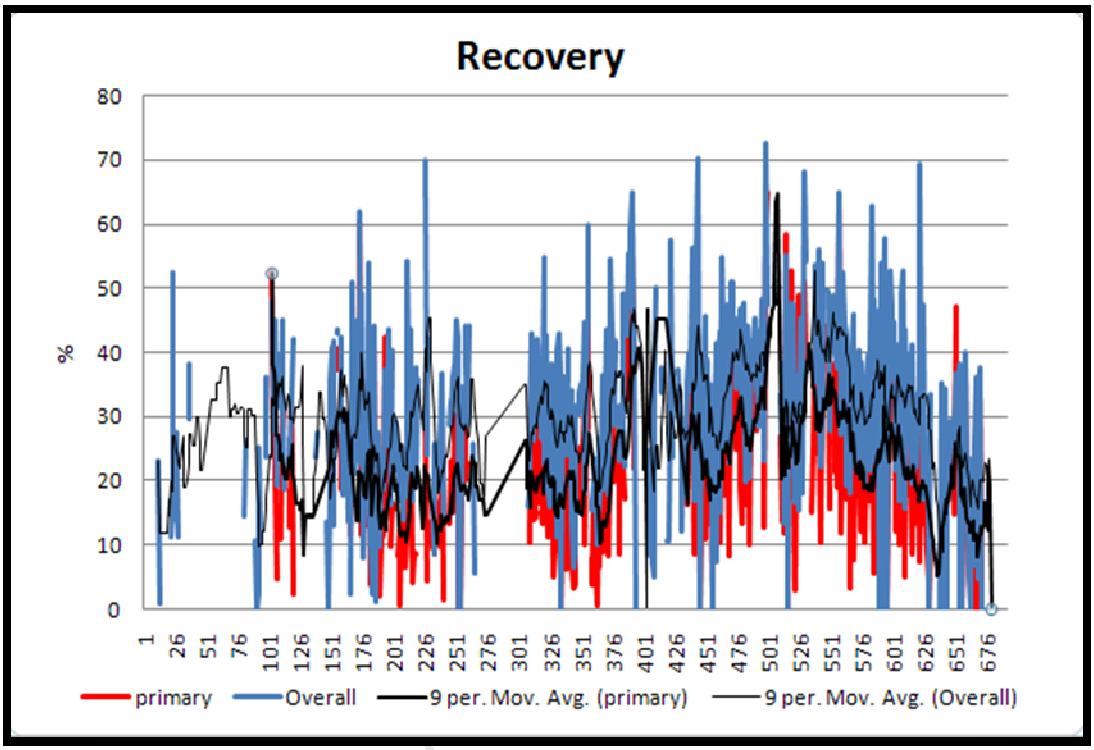

FIGURE 14: CURRENT PPM PLANT RECOVERIES (DERBYSHIRE, 2009)

The material from all reefs mined above 40 metres deep was treated as oxidised with lower metallurgical recoveries, which progressively improve as mining gets deeper towards 40 metres depth where material is expected to be un-oxidised or "fresh" ore. It has also been noted in literature (Davidson, 2009) that the oxidized zone cannot progress below the water table because flooding water prevents air and hence impedes oxidation.

2.3. Potential Remedies for Treatment of Oxidised Ores

Oxidisation of PGM bearing mineral particles impairs metallurgical recovery of these minerals, causing most of valuable mineral to report to the tailings (Newell et al., 2006). Xanthate type collectors make use of oxidation by dissolved oxygen to interact with sulphide minerals (Rao, 2004). However, oxidation that affects the sulphide mineral surface tends to diminish that mineral floatability (Mphela, 2010). The impaired floatability of oxidised sulphide minerals is largely driven by the failure of the collector to

adsorb on the sulphide mineral surface and the failure to make the mineral surface hydrophobic (Mphela, 2010). Various method have been employed in the past to either remove the oxide layer on the sulphide mineral surface or use other reagents that can make oxidised layer on the sulphide mineral surface adsorbent or hydrophobic.

2.3.1. Acid Pre-Treatment

As reported in literature (Belzile et al., 2004), the iron and sulphur depth profile for oxidised pyrrhotite can be modelled as shown in Figure 15.

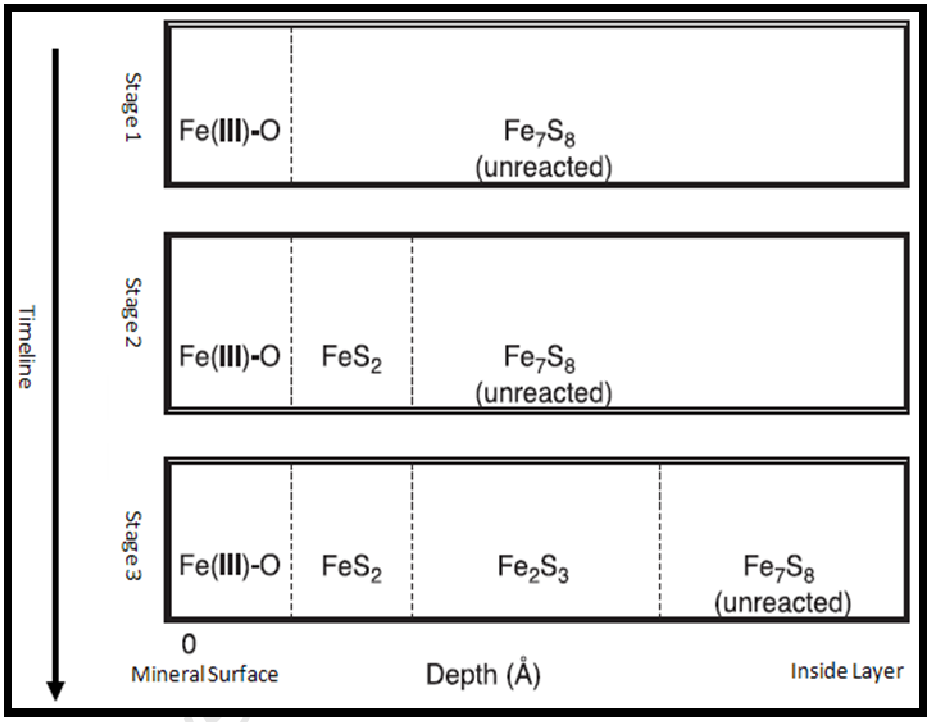

FIGURE 15: DEMOSTRATION OF THE SEQUENCE OF OXIDATION PRODUCTS AT THE SURFACE OF PYRRHOTITE (BELZILE ET AL., 2004)

Considering the ore body is dominated by the presence of pyrrhotite, the researchers in the field of sulphide mineral oxidation have come to recognise the presence of ferric oxyhydroxides on the surface of pyrrhotite, and depending on the level of oxidation, there would be an underlying layer that is iron depleted (Becker, 2009).

The surface oxidation mechanism was first proposed by Pratt et al. (1994) but later refined by Mycroft et al. (1995), who confirmed with the angle-resolved XPS, that ferric oxyhydroxides requiring the presence of water are the only species to form during the initial stages of air oxidation of pyrrhotite. Some earlier research (Buckley

et al., 1985) indicated that oxidation of pyrrhotite by air occurs by diffusion of iron from the outermost layers of the solid lattice to form iron(III) hydroxyl-oxide or hydrated oxide at the air-solid interface through iron(II) oxide mechanism. The model shown in Figure 15 can also be extended to other sulphide mineral such as pentlandite. Other researchers, (Chanturiya et al., 2004) also contended that the rate of oxidation of individual sulphide minerals like pentlandite and pyrrhotite crystalline grains, as well as the composition of products newly formed on them; depends on the crystallochemical peculiarities and the type of mineral aggregations. The study by Legrand et al. (2005b) also showed that both pentlandite and pyrrhotite form a thin layer of oxyhydroxide, which again was overlying a metal deficient sublayer. One way of improving oxidised sulphide mineral flotation, is to remove the oxyhydroxide layer to expose the sulphide rich surface underneath.

The technique of pre-leaching aims to target the oxide coating and selectively digest it using sulphuric acid. It has been reported in copper deposits that non-oxidative leaching of copper ore in an oxygen-free atmosphere seems to be a very efficient process for enhancement of the metal recovery via flotation process (Luszczkiewicz and Chmielewski, 2008).

It has been accepted that oxygen is the ultimate oxidant of sulphide minerals in natural surface waters, and oxygen acts as a direct oxidant at pH greater than 4 (Belzile et al., 2004). However, at pH below 4, sulphides are oxidized by ferric iron. When oxygen is the primary oxidant, Nicholson et al. (1994) proposed that the oxidation reaction proceed as shown below in Equation 8:

Equation 8: $$Fe_{1-x}S + \left(2 - \frac{1}{2}x\right)O_2 + xH_2O \rightarrow (1-x)Fe^{2+} + SO_4^{2-} + 2xH^+$$

The proposal further stated that the oxidation of ferrous ions (see Equation 8) produces ferric oxyhydroxides at relatively higher pH (see Equation 9 and Equation 10):

Equation 9: $$Fe^{2+} + {}^1/_4 O_2 + 2H^+ \rightarrow Fe^{3+} + {}^1/_2 H_2O$$

Equation 10: $$Fe^{3+} + 3H_2O \rightarrow Fe(OH)_{3(s)} + 3H^+$$

Selective leaching of the ore is based on chemical reactions between sulphuric acid and oxide layer. One assumption is that the gangue mineral is hardly amenable to mild sulphuric acid attack in the slurry while the acid is able to attack the oxidised layer on the sulphide mineral surface. The other assumption is that sulphur in the sulphide mineral has been completely replaced by oxygen to form an oxide layer in accordance with the shrinking core model. This process, which is called either acid pre-leaching or non-oxidative, leaching, relies on treatment of the ore with a less-than stoichiometric amount of H_2SO_4 required for decomposition of oxide layer. It is further assumed that the atmospheric leach of the sulphide mineral itself is limited by the reaction kinetics involved Luszczkiewicz and Chmielewski, 2008). The amount of sulfuric acid applied in the leaching corresponds to the content of oxidised sulphides in the ore and must be controlled to maintain the final pH of the slurry to an appropriate level.

Because the reaction can not necessarily be maintained in a non-oxidizing atmosphere, it is possible that further reaction will reverse the reaction by passivating the sulphide mineral again with an oxide layer. The exposing or polishing of sulphide minerals from the oxide layer, when applying sulfuric acid, is fairly rapid, once the acid arrives at the particle surface (Luszczkiewicz and Chmielewski, 2008), (Arlauckas et al., 2004). It can be performed at ambient temperature in a standard reactor equipped with mechanical stirring. This suggests the reaction kinetics are controlled by boundary layer diffusion, implying mass transport limitations.

The products of the decomposition of oxidised sulphide mineral are mobilised base metal sulphate (e.g. $FeSO_4$) and water. The following chemical reactions (Equation 14 to EQUATION 17) describe the non-oxidative leaching assumed to occur at the oxidised sulphide mineral surface. However, it possible for mobilised iron to react again with oxygen and precipitate iron again on the sulphide mineral surface (EQUATION 13):

Equation 11: $2Fe(OH)_3 + 3H_2SO_4 \rightarrow Fe_2(SO_4)_3 + 6H_2O$

Equation 12: $Fe_2O_3 + 3H_2SO_4 \rightarrow Fe_2(SO_4)_3 + 3H_2O$

Equation 13: $FeSO_4 + 3H_2O + O_2 \rightarrow 2FeOOH + 2H_2SO_4 \rightarrow \alpha\text{-}Fe_2O_3$

Equation 14: $FeO + H_2SO_4 \rightarrow FeSO_4 + H_2O$

Equation 15: $CuFeO_2 + 2H_2SO_4 \rightarrow FeSO_4 + CuSO_4 + 2H_2O$

Equation 16: $CuO + H_2SO_4 \rightarrow CuSO_4 + H_2O$

Equation 17: $NiO*Fe_2O_3 + H_2SO_4 \rightarrow NiSO_4 + Fe_2O_3 + H_2O$

The success of these reactions is also dependent on the solubility of the metal oxide. The solubility products of ferric oxides are usually high, making them somewhat slow to dissolve (see Table 3). However, dissolution of iron oxide is a well know phenomenon and is extensively described in the literature (Cornell and Schwertmann, 2003), (Diakonov et al., 1999), (Chesworth, 2008) and (Jang et al., 2007)). Palmer et al. (2004) also studied the solubility of copper oxide as well as nickel oxide.

TABLE 3: SOLUBILITY PRODUCT OF SELECTED METAL OXIDES FOUND ON SULPHIDE MINERAL SURFACE

Metal Oxide	Solubility Product	Solubility Constant (Feitknecht and Schindler, 1963)
$Fe(OH)_3$	$Fe(OH)_3 + H_2O \rightarrow Fe(OH)^{2+} + 2OH^-$	$K_{so} = [Fe(OH)^{2+}][OH^-]^2 = -38$
Fe_2O_3	$0.5\ \alpha\text{-}Fe_2O_3 + 2.5\ H_2O \rightarrow Fe^{3+} + 3OH^-$	$K_{so} = [Fe^{3+}][OH^-]^3 = -42.7$
FeO	$FeO_{(s)} + H_2O \rightarrow Fe^{2+} + 2OH^-$	$K_{so} = [Fe^{2+}][OH^-]^2 = -14$
CuO	$CuO_{(s)} + H_2O \rightarrow Cu^{2+} + 2OH^-$	$K_{so} = [Cu^{2+}][OH^-]^2 = -17.1$
NiO	$NiO_{(s)} + H_2O \rightarrow Ni^{2+} + 2OH^-$	$K_{so} = [Ni^{2+}][OH^-]^2 = -14.7$

The reaction is appreciated when it produces effervescences of gas especially at the beginning of the reaction, this can be attributed to the presence of tiny amount of dolomite type mineral. The reactions (Equation 18 and Equation 19) listed below mimic the evolution of carbon dioxide that may be responsible for effervesces liberation.

Equation 18: $MgCO_3 + H_2SO_4 \rightarrow MgSO_4 + CO_2 \uparrow + H_2O$

Equation 19: $3CaCO_3 + 3H_2SO_4 \rightarrow 3CaSO_4*2H_2O + 3CO_2 \uparrow + H_2O$

The advantage of carbon dioxide evolution during the reaction assists in inhibiting further oxygen absorption in the liquid phase. The retarding of oxygen dissolution

creates a superficial non-oxidizing atmosphere in the slurry during the leaching, and therefore also helps prevents the leaching of metals from the sulphide minerals.

Carbon dioxide may also participate in the leaching process as contended by Baltrusaitis et al. (2010) and Baltrusaitis et al. (2007). It has also been argued that iron oxide adsorbs a thin layer of water which provides a medium for reaction with dissolved CO_2 (Baltrusaitis and Grassian, 2005). The brief review of carbon dioxide pre-leaching is given in section 2.3.2 below.

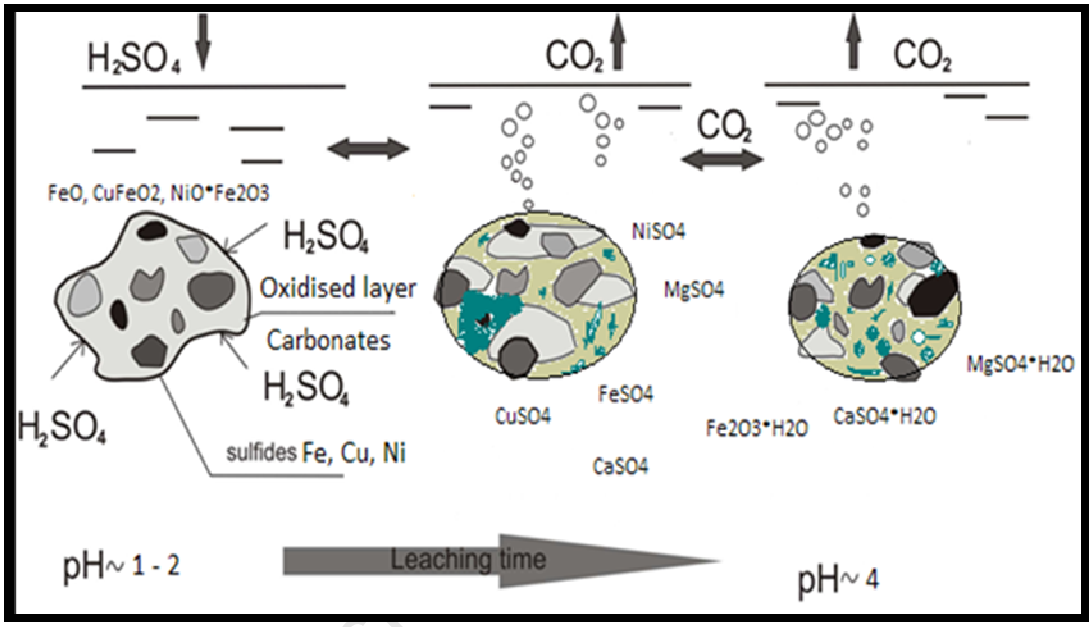

FIGURE 16: SELECTIVE CHEMICAL DECOMPOSITION OF OXIDE LAYERED-SULFIDE MINERAL WITH SULPHURIC ACID (LUSZCZKIEWICZ AND CHMIELEWSKI, 2008)

A selective chemical digestion of oxide layer together with small amounts of dolomite is shown schematically in Figure 16.

It can also be seen that at ambient conditions it is possible to solubilise base metals from their oxide form by simply lowering the pH to below 4 (See Figure 17). The evolution of carbon dioxide retards the dissolution of oxygen into the liquid and consequently decreases the redox potential. The Eh-pH diagram (Figure 17) shows that it is much easier to solubilise iron compared to other base metals (copper and nickel), but is possible to solubilise copper and nickel oxidised sulphide minerals if carbon dioxide can drop the redox potential low enough. Pyrrhotite has been identified as the most common sulphide mineral within the Tuschenkomst PPM ore

body (Duarte et al., 2004) and it is expected that acid reaction at the sulphide mineral to involve mostly the iron mobilisation.

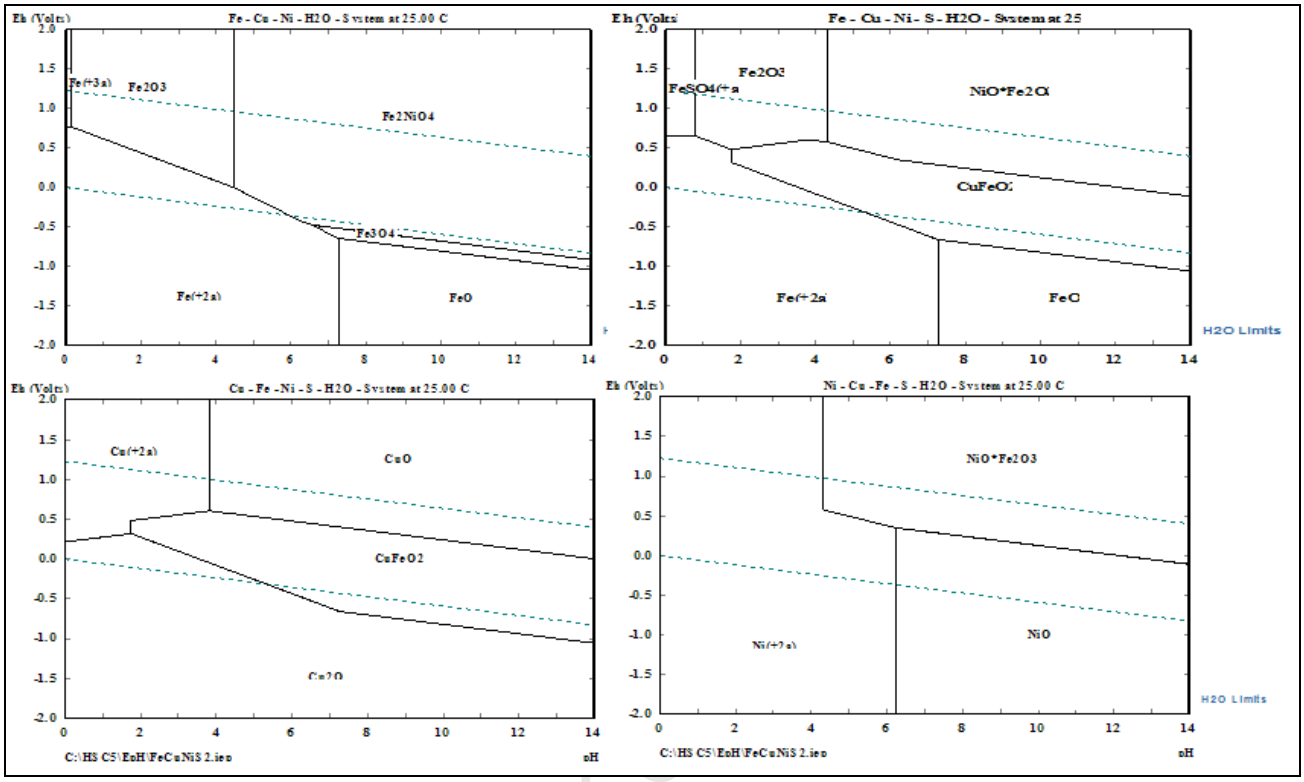

FIGURE 17: Eh-pH DIAGRAMS FOR *Fe-Cu-Ni*-H_2O-SYSTEM AT AMBIENT CONDITIONS

The Eh-pH diagrams shown in Figure 17 suggest that the dominant reaction occurring during pre-leaching with sulphuric acid would be the solubilisation of iron oxide as this reaction covers a wide range of redox Potential. Nickel ions also show a wide range of stability below the pH of 7, but the amount of pentlandite in the ore body has been found to be scarce.

2.3.2. Other Treatments for Oxidised Ores

Ultrasonic

One alternative technique intended to deal with oxidised ore is the method explored by Newell et al. (2006) to use ultrasonic treatment prior to collector conditioning and observed improve flotation recoveries. The ultrasonic treatment was found to have the greatest effect on chalcopyrite particles. This method effectively aims to shake off the oxide layer on the sulphide mineral surface, thereby exposing fresh surface. It is not clear how this method can be applied in large scale operations though.

FATTY ACIDS

The other method that has traditionally been used to target superficially oxidised sulphide minerals is the use of fatty acids as oxide collector. They include organic complexing agents, fatty acids and fatty amines. The limitation of most of fatty acids collectors is the lack of their selectivity over gangue minerals, particularly carbonate minerals such as dolomites and calcites. Therefore flotation with fatty acids is hardly favoured in oxidised sulphide minerals since; it only works on ores that had relatively insoluble valuable minerals (Ramachandra, 2004). Traditional fatty acid collectors tend to release metallic ions into solution and create undesirable activation of gangue minerals. However, studies have shown (Ramachandra, 2004) that fatty acids readily float iron minerals such as pyrite and pyrrhotite.

Several studies have been recorded in the literature alleging the collecting power of unsaturated fatty acids towards oxide minerals such as ilmenite, rutile, hematite, and magnetite ((Hukki and Vartiainen, 1953) and (Buckenham and Mackenzie, 1962)). The hydrocarbon chain of fatty acids extends outward on the mineral surface and induces hydrophobicity. The mineral should be able to attract the polar hydrophilic carboxyl group onto its surface. The carboxyl group of fatty acids are weak acids and therefore they remain undissociated in acidic pH, but dissociate in alkaline media, to the carboxylate anion as shown in Equation 20 below (Pearse, 2005):

Equation 20: $RCOOH + OH^- = RCOO^- + H_2O$

In most cases, fatty acid collectors are found to be self-frothing and therefore save the frothing agent costs. Although the main application of fatty acids as flotation reagents is found in phosphate and fluorite recovery, there are studies that have shown the relevance of fatty acids in metal oxides such as iron oxide((Quast, 2000) and (Ramachandra, 2004)).

The chain length of fatty acid in flotation plays a significant role. It was shown that homologous series of saturated fatty acids show a steady gradation of properties with chain length (Quast, 2006). This work showed that shorter chain fatty acids make use of undissociated acid to induce hydrophobicity on the oxide mineral surface. The hydrophobicity is supplemented by the physical adsorption of acid

anions as the chain length increased (Quast, 2000). However, the reduced solubility of the longer fatty acid carbon chains makes them ineffective as flotation agents.

One fatty acid that has shown considerable success with hematite (iron oxide) was decanoic acid. Decanoic acid showed flotation reactivity throughout a wide range of pH between pH = 3 and pH = 8 (see Figure 18) (Quast, 2006).

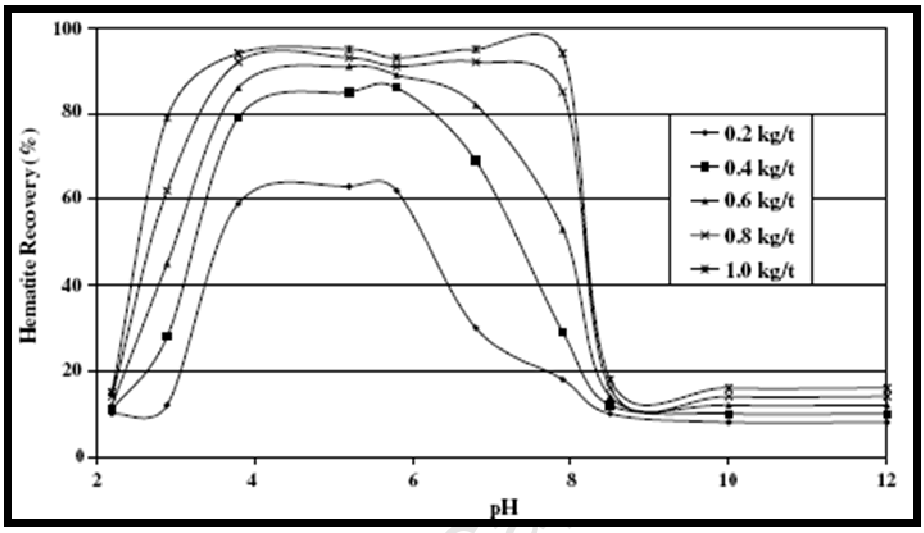

FIGURE 18: HEMATITE RECOVERY WITH DECANOIC ACID AS A FUNCTION OF PH (QUAST, 2006)

Research is continuing to find suitable fatty acids with sufficient selectivity to recover oxidised sulphide minerals (Grobler, 2010). It is because of this renewed interest that this work will also assess the flotation efficacy of one of the newly developed fatty acid collector branded Betacol 364/316 (BC364).

THIONOCARBAMATES AND THIOCARBAMATES

Thionocarbamates (TC) are a new family of sulphide collectors that are having reasonable success with copper activated zinc minerals and other sulphide minerals (Huang, 2010). However, there is a modest amount of research on these collectors that has been published. Some studies published recently have shown that thionocarbamates exhibit improved selectivity particularly towards valuable copper sulphide minerals against gangue sulfides such as pyrite (Sheridan et al., 2002). Early developmental work had indicated that these collectors influence froth characteristics and the extent of impact depends on the chain length. The work done by Liu et al. (2008) indicated that the interaction of thionocabarmates with copper cations on the sulphide mineral surface involves the formation of a six-membered

chelate ring, which is responsible for their collecting power and their selectivity against iron sulphide. In many collector systems, an increase in collector chain length (within reasonable limits) generally increases flotation recovery at the expense of grade, but thionocarbamates seem to respond otherwise (Sheridan et al., 2002).

Thiocarbamates reagents have also been found to be effective in most sulphide mineral flotation applications (Bradshaw et al., 1995). The work of Bradshaw et al. (1995) indicated that thiocarbamate adsorbs preferentially on sulphide mineral surface, attributable to its faster adsorption kinetics and the more stable nature of the surface complex. The study by Yoon and Basilio (1993) indicated that thiocarbamate tends to prevent the oxidation reaction on the mineral surface. However, Bradshaw et al. (1995) observed that thiocarbamates undergo similar initial reaction at the mineral surface as xanthates in acid conditions, but the adsorption of thiocarbamates onto mineral surface is dependent on the pH, and above pH of 7 the reaction of thiocarbamates stops.

SULFIDISATION

This process is largely used to float copper oxide ores since it offers selective advantages over fatty acids (Phetla and Muzenda, 2010). The method makes use of reducing agents like sodium sulphide or sodium hydrosulphide to activate oxidised sulphide mineral surfaces. Recently Newell et al. (2006) had reasonable success with the sulfidisation technique and reported to have restored floatable surfaces of passivated sulphide minerals and improved the recovery of the heavily oxidised sulphide minerals. However, they observed that longer conditioning times with sulfidisation were not conducive to good flotation recoveries of sulphide minerals due to re-oxidation of freshly induced sulfide surfaces. Some oxidised minerals require excessive addition of xanthate before they can get activated without having to employ strategies such as sulfidisation.

CHELATING REAGENTS

Chelating reagents make use of two metal co-ordinating atoms such as oxygen, nitrogen, sulphur or phosphorus (Phetla and Muzenda, 2010). The chelate structure is formed when more than one atom of a single ligand molecule or ion interacts with a metal ion by bending around the central atom to form a complex ring structure

(Phetla and Muzenda, 2010). The chelate-forming reagents have been found to be highly selective to certain metals (Hughes, 2005). In order to effect flotation, the chelating functional group is coupled with a long hydrocarbon chain in order to induce hydrophobicity for the targeted mineral. Hydroxamates have been found to exhibit sufficient chelating mechanism for flotation reagents (Hughes, 2005).

The success of hydroxamate as collectors is embedded in their structure which makes them to be selective collectors of oxidised metal minerals (Phetla and Muzenda, 2010). The hydrophobic tail promotes bubble attachment while the hydroxamate moiety selectively attaches to the oxidised metal surface by chelating. The alkyl hydroxamates have been found to be the most effective. Alkyl hydroxamates were also considered for use as oxide collector reagents that can be used in tandem with normal PGM flotation reagents. It has been reported (Hughes, 2005) that of the range of alkyl hydroxamate introduced, the most effective reagent was potassium n-octyl hydroxamate, termed AM2 by the manufacturer.

According to Hughes (2005), AM2 has a stabilised hydroxamate structure which results in strong and selective surface chelating during its application as a flotation reagent. They have found that when used as a 20% solution in dilute potassium hydroxide, AM2 acts as a flotation collector for oxidised base metal sulphides, precious metals (Ag, Au, and PGMs) plus copper metal and lithophile metal oxides. It has also been reported that a trial with AM2 is synergistic with sulphide collectors and is seen to upgrade oxidised sulphide minerals and lower mine tailings grade. The flotation chemicals based on hydroxamates are anionic collectors, which have been around and known in the industry for many years. They exhibit weak acid properties with a pKa lying between 9 and 10. These reagents are known to be most effective at high pH, but they have also been shown to improve metal recovery in slurries with pH ranging between 7 and 10.

This work will also consider the use of alkyl hydroxamate to improve flotation of valuable minerals at PPM.

CARBON DIOXIDE TREATMENT

There has been some reports in literature which show carbon dioxide successfully enhancing floatability of coal particles (Jin et al., 1988). Miller and Misra (1987) developed a hydrophilicity index from FTIR spectroscopy and used it to describe the surface state of coal and hence its flotation behaviour under carbon dioxide pre-treatment. They found that hydrophobicity for the fine coal, as characterized by in-situ FTIR spectroscopy, increased significantly after a 50-minute treatment of dry powdered coal at a carbon dioxide pressure of 20 psi. As a result, Miller et al. (1987) developed a method that made use of carbon dioxide to enhance floatability of coal. The enhanced hydrophobicity of carbon dioxide-treated coal was attributed to the high specific affinity of coal for carbon dioxide, which results in the formation of nano-bubbles on the coal surface in aqueous suspension (Jin et al., 1988).

However, other researchers (Linter and Burstein, 1999) recognised the surface cleaning action of carbon dioxide in steel pipes. It was noticed that dissolved carbon dioxide accelerates the dissolution of low alloy steels in aqueous solutions by destabilising the oxide layer that usually protects the steel pipes from corrosion. The destabilisation was thought to occur by the reaction of oxide film to produce ferrous carbonate (see Figure 19). The resulting complex of Fe designated as bicarbonato-Fe(II), $FeCO_2^{2-}$, dissolves away from the metal surface, leaving the steel vulnerable to corrosion.

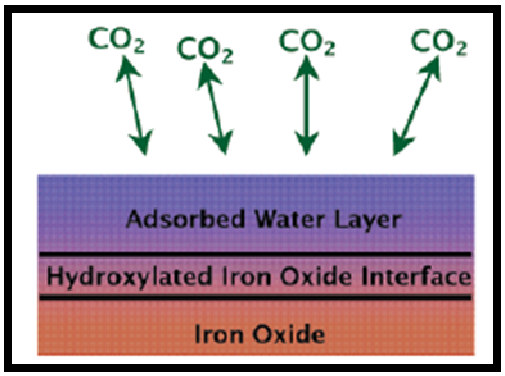

FIGURE 19: SCHEMATIC ILLUSTRATION OF CARBON DIOXIDE REACTIVITY WITH MINERAL SURFACE IN AQUEOUS MEDIA (BALTRUSAITIS AND GRASSIAN, 2005)

Equation 21 through to Equation 24 shows possible reactions of carbon dioxide with water on the oxidised iron mineral surface.

Equation 21: $H_2O_{(a)} + CO_{2(g)} \leftrightarrow H_2CO_{3(a)}$

Equation 22: $H_2O_{(a)} + H_2CO^{3(a)} \leftrightarrow H_3O^{+}_{(a)} + HCO_3^{-}{}_{(a)}$

Equation 23: $Fe\text{-}OH + HCO_3^{-}{}_{(a)} \leftrightarrow Fe\text{-}OCO_2H + OH^{-}_{(a)}$

Equation 24: $Fe\text{-}OCO_2H + OH^{-}_{(a)} \leftrightarrow Fe\text{-}OCO_2^{-}\ H_2O_{(a)}$

The studies published by Baltrusaitis et al. (2005), Baltrusaitis et al. (2010), and Baltrusaitis et al. (2007), using FTIR spectroscopy, have shown that carbon dioxide at the adsorbed water-iron oxide interface forms a thin acidic water film which perhaps corrodes the oxide layer on the metal or mineral surface.

More recently, the work of Mphela (2010) has shown that carbon dioxide can be used to clean oxidised sulphide minerals in order to enhance their floatability. In this work, Mphela (2010) was able to show that carbon dioxide had a depassivation impact on oxidised pyrrhotite surface, by restoring the polarity resistance to values similar to those of a polished pyrrhotite surface. It was also shown, using both the electrochemical measurements and ToF-SIMS; that carbon dioxide manages to de-oxidise the metal mineral surface and enhance anodic reactivity, with or without the presence of xanthate. The microfloation test work performed by Mphela (2010) further confirmed the positive impact carbon dioxide has on the floatability of pyrrhotite, and there is no reason why this should be any different with other sulphide minerals.

2.4. PPM FLOWSHEET

Several metallurgical test works were done at Mintek to determine both the plant configuration and flotation kinetics for plant design. It was found that both ore types were amenable to a mill-float-mill-float circuit (MF2 circuit). As expected, weathered ores returned worse flotation kinetics than the fresh ores. Figure 20 shows the simplified PPM Merensky plant flowsheet.

The process flow-sheet begins with the run-of-mine ore undergoing comminution followed by liberation milling. The milled pulp is then pumped to the primary rougher flotation bank for initial separation. The primary rougher separates the pulp feed into flotation froth overflowing the primary rougher cells and the primary rougher tailings

slurry as rougher bank underflow. The primary rougher flotation froth is then transferred to the primary cleaner flotation bank. The primary cleaner bank removes as much gangue mineral as possible to provide high quality concentrate grade. At the same time the primary rougher tailings go through the secondary milling stage and are then fed to the secondary rougher bank. Once again, the secondary rougher bank pulls the concentrate froth and transfers it to the secondary cleaner bank for concentrate cleaning. The secondary rougher tailings report as final tailings and get transferred to the tailings dam. The final concentrate is dried and sold as concentrate to smelters. The simplified PPM flowsheet, illustrated in Figure 20, represent an "MF2" (Mill-Float-Mill-Float) configuration. The chrome recovery and PGM scavenging are left for future consideration.

Blending of the weathered and fresh UG2 ores showed no deleterious effects on overall recovery at the pilot plant scale. However, blending of the Merensky ores resulted in more unstable plant operation compared to using the fresh Merensky.

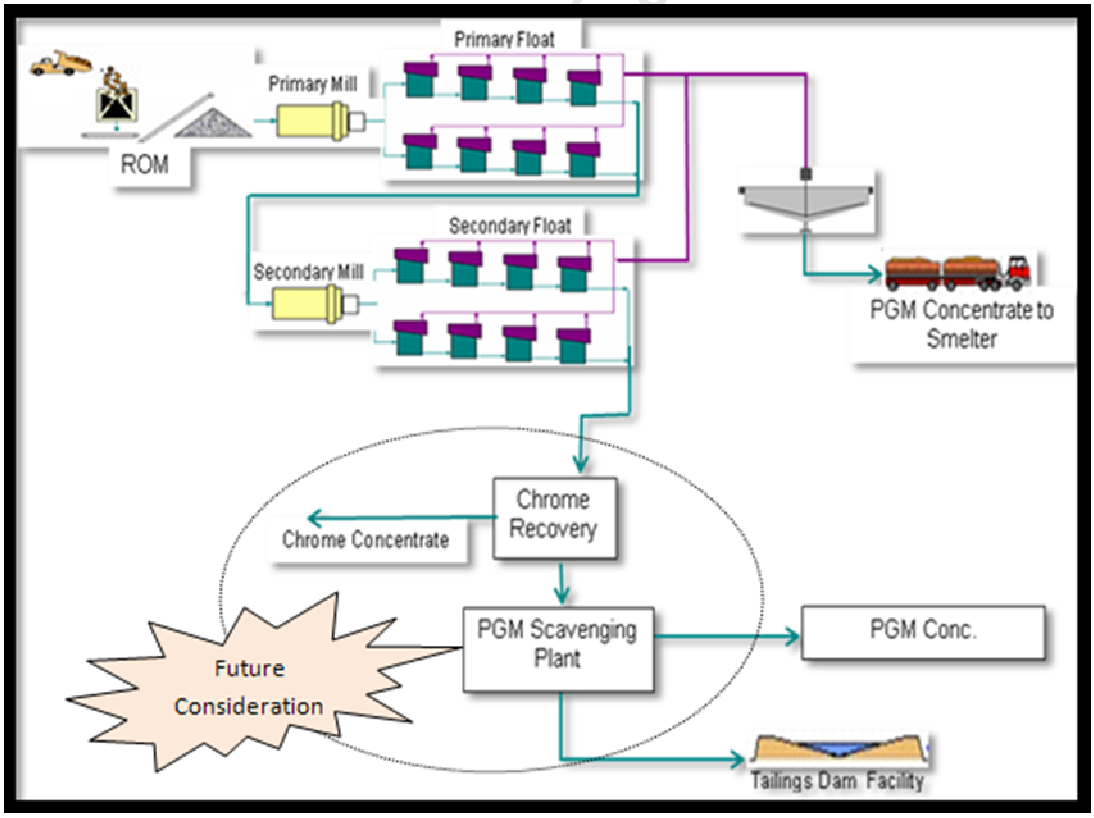

FIGURE 20: CONCENTRATOR BLOCK FLOW DIAGRAM AT PPM

Treating all the ores by standard flotation methods revealed that the PGM values were difficult to liberate effectively, and achieving high concentrate grades at high recoveries was going to be problematic. However, fine grinding appeared beneficial in most cases.

One of the recommendations from the bankable feasibility report (Waldeck, 2007) was that further work should be undertaken to investigate whether the PGM grade-recovery relationship can be enhanced through one or a combination of the following procedures:

- Coarse grind-float-mill-float, varying secondary grind from 60% passing -75µm to 90% passing -25ìm, with the objective to determine whether the increased rougher recovery from fine milling can be supported.
- The use of alloy collectors in the secondary rougher to increase PGM recovery.
- The use of varying amount of CMC depressants in high grade cleaner to improve the grade.
- Evaluate the use of secondary cleaner including the use of acid, or attritioning fine milling.

As the PPM metallurgical plant is currently treating material mined closer to the surface, the recoveries are found to be erratic, with the average recovery of 35% but sometimes as high as 70% (Figure 14). The low average recovery is attributed to the nature of the ore where weathering is believed to play a major role.

The PPM plant operation aims to recover PGM to an extent that only 0.5 g/t is left in the tailings of the Merensky reef. However, as can be seen from Figure 21, the tailings grade remained well above the target grade. The average tailing grade was measured at 1.3 g/t against the feed head grade of 1.89 g/t.

Since the mine will continue to receive near surface material for the next three years, any attempt to improve recoveries of this weathered ore will improve the mine prospects.

The metallurgical plant performance depicted in Figure 14 and Figure 21 shows that the flotation process is less well suited to deal with weathered ores. Furthermore, smelters are increasingly pressured to reject or financially penalize concentrates with low grades.

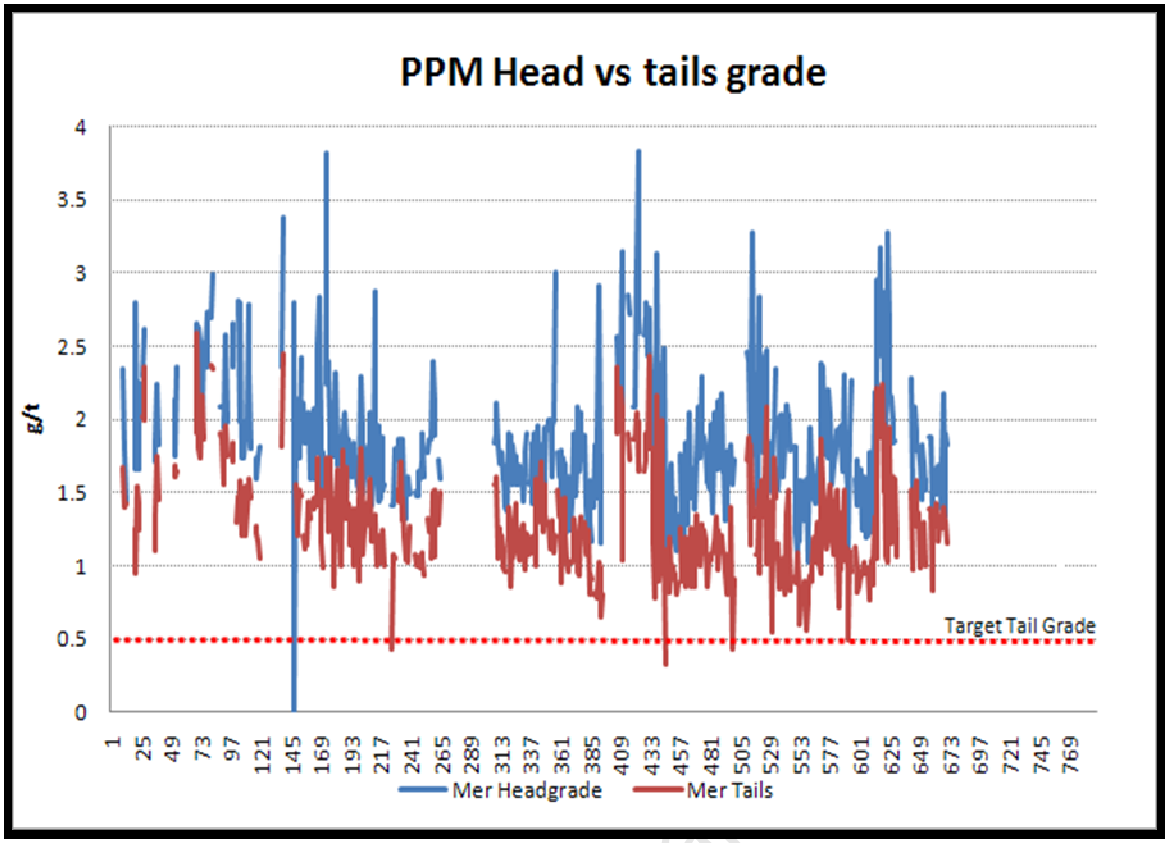

FIGURE 21: A GRAPH SHOWING HEADGRADE AND TAIL GRADE OF MATERIAL MINED NEAR SURFACE AT PPM

2.5. THE KEY QUESTIONS:

1. Because of vertical oxidation profile suggested in some ore bodies (Bartlett, 1998); it is possible that the PPM ore body will exhibit similar profile. The material mined near surface will be expected to be mostly altered and oxidised, transitioning into secondary sulphides at the intermediate depth. The fresh sulphides will be expected to be at deeper levels. The material near surface can also be expected to have lower density due to alterations of the parent rocks. The first key question would determine the characteristics of the PPM ore body relative to increasing depth.

   That is: How does PPM ore body change with depth?

2. Because PPM is currently treating material from near surface, the metallurgical performance is very poor and erratic (Figure 14). The metallurgical profiling the ore body can assist the operations to plan the operations cash flows relative to mining advances. The material from surface is expected to show poor flotation

performance. The metallurgical performance of the ore body should improve as material mined from deeper levels is extracted. Then the second key question examines the possibility of profiling the metallurgical performance of the ore with increasing depth.

That is: Can the loss of recovery be correlated with depth and why?

3. Although the metallurgical performance of oxidised ore near surface is known to have poor metallurgical recovery, it is still important to ask if the metallurgical performance of such ore can be improved.

That is: How can flotation performance of weathered PPM ore body be improved?

The third key question give rise to a hypothesis that a suitably adapted reagent suite or pre-treatment with acid can account for increased recovery of weathered ores, either by activating passivated sulphide mineral surface or polishing the mineral surface to expose clean sulphide surface respectively.

3. CHAPTER THREE: EXPERIMENTAL AND ANALYTICAL METHOD

3.1. SAMPLING AND MEASUREMENTS

3.1.1. SAMPLING: DENSITY PROFILING

The bulk rock density measurements in this study were obtained either using the Archimedes principle, or through geophysical surveying depending upon the state of the ore samples (in terms of fresh versus altered ore).

The density measurements of "fresh" ore were done on exploration diamond drill core, sampled on a 100 x 100 m grid of the PPM ore body. The measurements were based on the Archimedes principle (weight in air/weight in water) and performed at regular intervals (15-35 cm) along samples of the half core. Based on a visual inspection by the exploration geologist (Hayward, 2006), the transition from "altered" to "fresh" ore was taken at ~ 40 m from surface.

Each selected half core sample was dried, weighed and then reweighed in air. The mass of the halved core was denoted (M1) and measured in air. The second mass was measured in displaced water and denoted (M2). Then the in situ dry bulk density was determined by the following formula:

Equation 25:

$$\text{Relative Density} = \frac{m_1}{m_1 - m_2}$$

Since core pieces from the "fresh" core were not porous, the specimen was not sealed prior to water immersion. Although this technique works well for "fresh" material, the friable and porous nature of the altered material often precluded this method and hence down-hole geophysical surveys were utilised.

Down-hole geophysical surveys were conducted in 95 of the exploration drill cores to measure the density of "altered" PPM ore. An in-situ wall-rock density was calculated using a density probe that measures the absorption of gamma rays emitted from a radioactive crystal within the probe. According to Selfe (2006), this technique works well for rock densities ranging from 2 – 3.2 $g \cdot cm^{-3}$, and is therefore appropriate for the PPM silicate reef. Two commercial companies (Reeves and Quiklog) were commissioned to do these measurements and then statistically

compared with one another. The actual measured spot densities as reported by Hayward (2006), were used for both comparison and adjustments of the two data sets from Reeves and Quiklog. The average density over any specific depth zone was calculated with the Wellcad™ software (Selfe, 2006).

3.1.2. SAMPLING: IN SITU METALLURGICAL PROFILING

The solid samples of PPM Silicates reef were drawn initially from the reverse circulation drill samples across the mine property. Reverse circulation (RC) drilling uses a dual-walled drill pipe (rod) with a solid drill bit to produce a hole in a formation and delivers rock chips (cuttings) to the surface for subsequent analysis. The RC drilling procedure prevents the upcoming sample from being contaminated with material broken off from the sides of the hole and so can potentially provide a sample whose down-hole position is exactly known. Because it is important to collect almost all the rock drilled, the hole is normally sealed at the collar, so the sample is forced to travel through the drill stem and into the collector at the top of the rod. The technique also applies high pressure air for a period after each advance, which is 1m, in order to clear all the cuttings from the drill stem before continuing with the next advance. There is a centrifugal classifier through which the air exhausts, which captures rock chippings into the sampler. The sample from each RC hole is then manually riffled to obtain sizable sample of about 2.5kg. It is these samples that were taken for both, PGE analysis and to metallurgical test work.

The primary purpose of the RC drilling was to generate auxiliary information regarding the geology of the mine area ahead of mining. The RC pulp samples were taken every meter down the drill core and samples that intersect the reef were withdrawn for PGE content analysis. After the PGE analysis, the samples were further taken to metallurgical test work to determine recovery profiling relative to the position of the mining depth. The results would then be used to forecast the recovery profile with respect to the mine plan and cash flow requirements.

The mining bench (or levels) considered were from surface elevation to 45 m below surface. A bench is made up of 5 m where a flinch of 2.5 m is mined at any give instance. The assumption here was that within a bench (i.e. 5m mining intervals) the

recovery will largely remain the same. The RC sampling was able to afford the project the opportunity to bulk sample the in-situ ore prior to mining. Making use of the RC samples made it easier to take planned sample in such a way that the sampling covered the whole mine property. Within each bench, the ore was classified according to the headgrade deliverable to the plant as shown in Table 4 below.

TABLE 4: ORE CLASSIFICATION BASED ON HEADGRADE DELIVERABLE TO THE PLANT

MATERIAL TYPE	ORE TYPE	Headgrade	COLOUR
Overburden	Overburden	0	-
Internal Waste	MR; MRFW; UPR; PRHZB; LPR	<0.35	White
Trace	MR; MRFW; UPR; PRHZB; LPR	0.35 - 0.60	Blue
V. low Grade	MR; MRFW; UPR; PRHZB; LPR	0.60 - 1.10	Green
Low Grade	MR; MRFW; UPR; PRHZB; LPR	1.10 - 1.60	Yellow
Medium Grade	MR; MRFW; UPR; PRHZB; LPR	1.60 - 2.40	Red
High Grade	MR; MRFW; UPR; PRHZB; LPR	> 2.40	Pink

For instance, if the mined ore within any particular bench had a grade between 0.35 – 0.60 g/t, such ore would be classified as “blue (0.35 - 0.60 g/t)” ore and stockpiled accordingly. The samples from different lithological types: Merensky footwall (MRFW), Upper pseudo (UPR), Lower pseudo (LPR), and Harzburgite (PRHZB) were all treated as one reef package, Silicate reef.

The RC pulp samples were drilled ahead of mining at a grid of 10 by 10 m spacing. The samples derived from this RC campaign were assumed to closely represent the geology of the pit area, and could provide the closest view as to how the ore would behave. At least 4 samples from each mining bench (flinch) were composited into one metallurgical sample. The actual strategy that was followed to sample each mining bench using RC samples is shown in Appendix 1. The mine pit was subdivided into 6 main regions, from the north end southwards: UN region, RFN Region, RFS region, TP region, U3 Region, and U5 Region in the south end.

3.1.3. Mineralogical Characterisation

Mineralogical analyses of the PPM silicate reef ore were performed on a series of samples taken from the PPM plant. At the time of sampling, the ore that was being

processed by the plant was representative of the material tracked from the initial RC sampling work prior to mining. Samples of the primary rougher feed, final concentrate and secondary rougher tails were sent for mineralogical analysis. Figure 22 show the process flow diagram showing where sampling points were taken for mineralogical study.

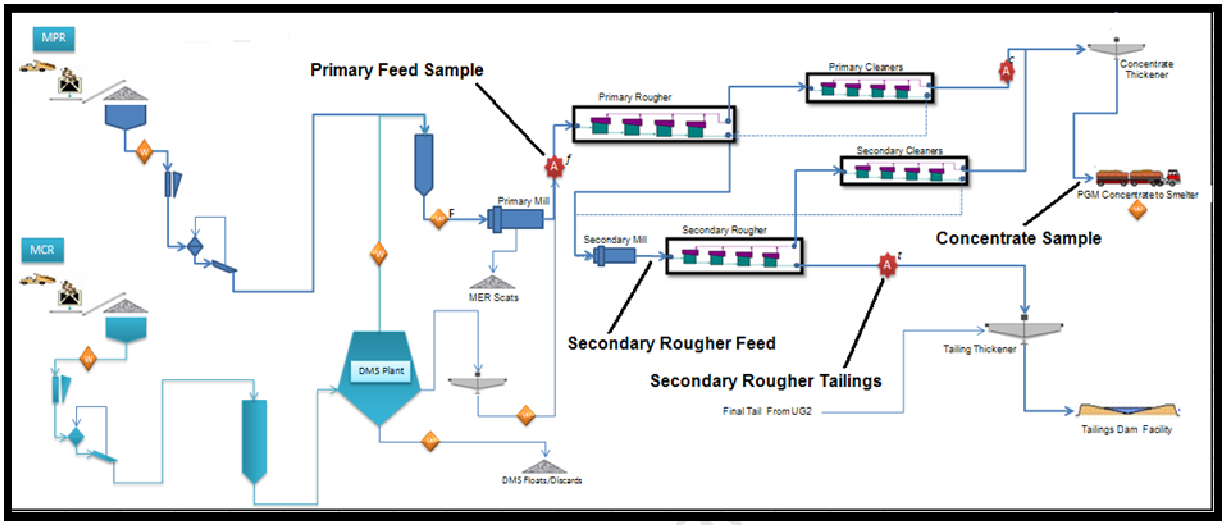

FIGURE 22: PPM SILICATE PROCESS FLOW DIAGRAM SHOWING WHERE SAMPLING POINTS WERE TAKEN FOR BOTH MINERALOGICAL STUDY AND METALLURGICAL TEST WORK

The plant is divided into two feed streams (high grade stream and low grade steam). The low grade stream goes through the dense media separation (DMS) plant to upgrade the ore. The upgraded ore is then combined with the high grade stream into the silo before being sent to primary milling.

TABLE 5: LIST OF SAMPLES SENT FOR OVERALL MINERALOGICAL ANALYSIS

Sample ID	Description	Test
C - 21	Silicate Final Concentrate	SEM
C - 22	Silicate Secondary Rougher Tails	SEM /MLA
C - 23	Silicate Primary Rougher Feed	MLA
A- 25	Silicate Final Concentrate	Q-XRD

The feed assay sample is taken just after the primary mill and the tailings sample is taken just after secondary rougher cells. Table 5 shows the list of samples which were taken for mineralogical investigation.

Quantitative X-ray Diffraction

Quantitative X-ray diffraction (QXRD) was performed on of final concentrate sample (Grobler, 2010). The analyses were run at the Council for Geoscience and the identification and quantification performed by XRD Analytical and Consulting.

Scanning Electron Microscopy

A scanning electron microscopy (SEM) study was done by Betachem (Grobler, 2010) as a qualitative evaluation of the mineralogy of the final concentrate and the secondary rougher tails. The work was aimed at providing SEM images that can help in the understanding of the deportment of the valuable minerals and problematic gangue minerals. The sample preparation was done at the Industrial Metal and Mineral Research Institute (IMMRI) located at the University of Pretoria (Grobler, 2010).

Mineral Liberation Analysis (MLA)

In order to investigate mineralogy of the PGMs, their grain size distribution, their liberation and their association; samples of the silicate reef primary rougher feed and secondary rougher tails were sent for Mineral Liberation Analysis (MLA) at ALS Laboratory Group in Johannesburg. Samples were analysed using the spare phase liberation (SPL) routine ((Fandrich et al., 2007) and (Lastra, 2007)). It should be noted that PGEs present in low concentration as part of a solid solution series, and PGMs present as sub-micron grains were not detected by the MLA analysis.

3.1.4. Batch Flotation Test

Recovery Depth Profiling

Samples of the PPM silicate reef were collected for the recovery depth profiling as described in section 3.1.2. As indicated in section 3.1.2, a minimum of 4 samples from each bench (see Appendix 1) were composited and pulverised in a vertical spindle pulveriser. The pulveriser was timed to produce a grind of about 80% passing 75 microns. The pulverised sample was sub-sampled using a rotary sample splitter followed by random scooping to make up 1.54 kg samples for each batch float.

Flotation tests were done in a 4 L 12D Denver flotation machine, run at approximately 30 % solids, with the agitator running at 986 rev/min for all the tests. The air supply was controlled by opening the air nozzle completely for all the float

tests. The conditions of the air flow and agitation were chosen such that the froth level just reaches the brim of the flotation cell. Flotation tests were done using plant water which is known to contain several salts of magnesium, calcium and other contaminants (Appendix 2). Table 6 summarises the reagents used, their dosages and conditioning times. The normal reagent suite consists of sodium isobutyl-xanthate (SIBX) as a collector, the Sendep as CMC depressant and sasfroth (triethylene glycol monobutyl ether) as a Frother. All normal flotation reagents were supplied by Senmin.

TABLE 6: REAGENT SUITE ADDITION FOR FLOTATION TEST RUN

Reagent addition sequence	Reagent Merensky	Dosage (g/t)	Conditioning Time (min)	Required Volume (mL)
0	**$CuSO_4$***	50	5	27
1	**SIBX**	100	2	53.90
3	**Sendep**	50	3	26.95
4	**Frother**	50	0.5	26.95

*$CuSO_4$ was only used for recovery profiling; subsequent tests showed copper sulphate did not add any benefits and the addition of $CuSO_4$ was discontinued for subsequent float tests.

Four concentrates were collected for each flotation tests over 0-1, 1-3, 3-7, and 7-20 minute, where the froth was scraped off every 15 seconds into the collection tray. Samples of the concentrates and final tailings were filtered and dried in an oven over night at 107°C. The dried concentrates and tailings were then weighed and the masses reconciled for mass balance. Only when the flotation mass balance fell within 1% error, was the material then deemed suitable to be sent for assaying. The samples were assayed for the 3PGE and gold using a lead collection fire assay technique (see Appendix 2 for more details).

RECOVERY IMPROVEMENT STRATEGIES

After the in-situ RC sampling (see section 3.1.2), the silicate reef was mined and then re-sampled after the primary roughers (secondary rougher feed) in the metallurgical plant (see Figure 22). The aim of this secondary sampling was to investigate the

feasibility of improving flotation performance of the altered ore material. The material for the metallurgical investigation was chosen at the secondary rougher feed, in order to target material that has already shown resistance to flotation recovery in the primary rougher circuit. About 70 kg of the secondary rougher feed sample was taken, and then prepared for batch flotation tests. The sample was dried in an oven at 107°C overnight. The lumps of the dry sample were broken and then ground through a 1 mm sieve. The 70 kg lump free sample was then blended in the v-blender for 12 hours. This sample was then considered ready for metallurgical test work. In order to determine the grind of the sample, about 100 g of the blended sample was wet screened at 75 µm in triplicate to determine the grind size, which was found to be 80 wt% passing 75 µm. A further sub-sample of this sample was reground in an Essa laboratory pulverising (LM5-C) mill to increase the grind from 80 to 90 wt% passing 75µm

The use of oxide co-collectors and an acid pre-leach were investigated as strategies to improve PGE recovery of the altered ore, using the standard procedure described above.

Acid Pre-Leach

The aim of acid pre-leach was to see whether pre-leach could assist in cleaning the surfaces of the altered valuable minerals. Pre-leaching was done prior to normal flotation reagent addition, and the leaching times varied between 90 and 120 minutes (Table 7). A series of acid dosages were tested in order to determine the optimum dosage appropriate to polish the silicate reef ore PGM bearing mineral surface. Since both the flotation cell and the agitator shaft were made out of stainless steel 316, and the agitators themselves made out of polyethylene material; the flotation rig was also found suitable to conduct acid leach reactions. The pH meter was inserted in the cell to measure the pH as the test proceeded. At the end of the each leach reaction, the pH was raised using KOH pebbles to approximately pH of 8. This was done in view that the sulphide collector (SIBX) decomposes at pH 4. Once the pre-leaching had been completed, the normal flotation reagent suite was added as shown in Table 6.

In order to determine the best required acid dosage, varying amounts of sulphuric acid were used for this purpose. Table 7 shows the quantities and the reaction times allowed for each exploratory pre-leach test.

TABLE 7: ACID DOSAGE AND REACTION TIMES FOR ACID PRE-TREATMENT

Test Number	Volume of H_2SO_4 Added (mL)	Acid Dosage Rate (g/kg)	Pre-leach time (min)
1	0.00	0.00	0.00
2	20.00	23.42	120
3	30.00	35.14	110
4	40.00	46.85	90

In order to maintain the same flotation standard as with the RC pulps, the slurry solids percentage was still maintained at 30% (see Appendix 7.1).

The acid was added slowly using a 20 ml syringe while agitating the slurry. The pH meter was held inside the slurry to measure the pH of the slurry. As the acid was added the pH dropped from 7.6 to about 1.4. The pH slowly rose with increasing reaction time and stabilised at around pH 4.4. However, when 40 ml of acid was added, the pH dropped to below 1 and finally settled at around pH 3.7. During the addition of acid, it was observed that there was an effervescence of tiny bubbles being produced.

TABLE 8: FLOTATION REAGENT SUITE ADDITION SEQUENCE, DOSAGE AND THE CONDITIONING TIME

Reagent addition sequence	Reagent Merensky	Dosage (g/t)	Conditioning Time (min)	Required Volume (mL)
1	**H_2SO_4**	35136	120	30.00*
2	**SIBX**	100	2	53.90
3	**Sendep**	50	3	26.95
4	**Frother**	50	0.5	26.95

*Different acid volumes as shown in Table 7 were used but 30 mL was subsequently used for further test.

Subsequent to the acid pre-leaching, the normal flotation reagent suites were added and the flotation tests carried out as normal.

CO-COLLECTORS

The co-collectors that were investigated are listed in Table 9. These co-collectors were respectively added just after the primary collector, and allowed to condition for 2 minutes, then followed by the frother addition. Flotation tests were conducted in triplicates.

TABLE 9: LIST OF CO-COLLECTORS EVALUATED FOR RECOVERY IMPROVEMENTS

Code Name	Primary Reagent	Secondary Reagent	Dosage	Supplier
AM28	Hydroxamate	None	100 g/t	Axis house
TC1000	Thionocarbamate	None	30 g/t	Tecrich
TC2000	Fatty Acid	Xanthate	15 g/t	Tecrich
TC3000	Thionocarbamate	Xanthate	30 g/t	Tecrich
TC6000	Thionocarbamate	Xanthogen Formate	30 g/t	Tecrich
BC364	Fatty Acid	Unknown	15 g/t	Betachem

For hydroxamate reagent, AM28 (potassium alkyl hydroxamate) supplied by commercial company, Axis House was used for this study. The reagent was prepared according to the method prescribed by the supplier. The supplier recommended that AM28 be prepared to 2% solution strength in a 1% solution of potassium hydroxide. This was achieved by first dissolving 1.52 g of Activator (KOH) in 194.48g of water and then adding 4 g of AM28. On flotation rig, SIBX was added first and followed by addition of AM28 as shown in Table 16 (Appendix 4).

For thionocarbamates, a Chinese reagent supplier (Beijing Tecrich Development Co., Ltd) provided a series of co-collectors branded TC1000, TC3000 and TC6000. These reagents were touted as effective co-collectors for the flotation of base metal sulfide ores such as Lead, zinc, copper, Molybdenum, gold, platinum and palladium.

The material safety data sheet on these reagents revealed that the major chemical compounds in these reagents are modified thionocarbamates (TC). The ingredients in TC1000 were listed as Thionocabamate (>90%) and isobutanol (<10%). TC3000 contained thionocabamate (>60%), xanthate (~30%) and Isobutanol (<10%). Similarly, TC6000 contained thionocabamate (>60%), Xanthogen formate (~30%) and Isobutanol (<10%). The supplier further claimed that the molecular compositions of

TC reagents are similar to natural mustard oil and they are biodegradable (Huang, 2010). Furthermore, the TC reagents were said to have modifying characteristics that promote the effect of xanthate collector (Huang, 2010).

These chemicals reagents are oil based with varying transparent colours; TC1000 appeared amber, TC3000 appeared yellowish, and TC6000 appeared light orange. The chemicals did not dissolve in water, but were said (Huang, 2010) to dissolve in alcohol, ester and ether.

The supplier did not give any recommendations as to the dosage method and reagent flotation preparation; therefore a dosage screen was carried out with results shown in Appendix 7.4 (28 g/t added after xanthate was found to produce the best results). The reagent suite with the TC co-collectors was prepared and conditioned as shown in Table 16.

For fatty acids, the supplier of BC364 recommended 30 g/t, and this dosage was used for TC2000 as well. The fatty acid was added after conditioning with SIBX for two minutes. The conditioning time for fatty acids was also maintained at 2 minutes.

The last test that was done with co-collectors was the combination of fatty acids and thionocarbamates. The dosage procedure that was followed for this test was as follows; conditioning with SIBX for 2 minutes, BC-364 (fatty acid based co-collector) was added and also conditioned for 2 minutes. And lastly, the thionocarbamate was added and similarly conditions for 2 minutes.

3.2. Analysis of Flotation Data

The flotation assay results were collated together for each float test and mass balance calculations were conducted to verify metal accountability. Detail account of the process followed to analyse flotation results can be found in Appendix 4. The flotation recovery results were then fitted to Kelsall model (Kelsall, 1961) and Klimpel model (Dowling et al., 1985) in order to determine flotation kinetic data (see the results in Appendix 5.2).

Furthermore, a statistical evaluation of the results was conducted using ANOM (ANOVA analysis of means) in Minitab™ statistical software. The results of statistical evaluation were also plotted in a graph for presentation. The one way analysis of means (ANOM)

uses the ANOVA statistical technique, which is based on the hypothesis that there is no significant difference between the means of the variables under study. The boundary limits for the 95 % confidence interval ($\alpha = 0.05$) are depicted by two boundary lines. The centre line bounded by the decision limits of the boundaries represents the average of the all means. The vertical stick plot represents the mean for a particular test. If the stick plot for a particular test falls outside the boundary limits, this shows the results obtained are significantly different from the other results that falls within the boundary limits (see Figure 23 for illustration of ANOM technique).

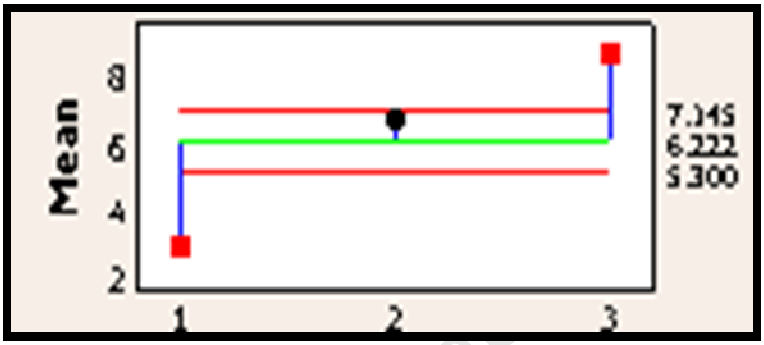

FIGURE 23: AN ILLUSTRATION OF ANOM SHOWNG "1" AND "3" ARE SIGNIFICANTLY DIFFERENT FROM THE AVERAGE MEAN, "1" - SIGNIFICANTLY BELOW AND "3"-SIGNIFICANTLY ABOVE

4. CHAPTER FOUR: RESULTS

This chapter presents the results obtained from field work, the laboratory test work and mineralogical investigations. The first part of this chapter will begin by showing how the density of the country rock changes with increasing depth (section 4.1) and which rock types were most affected by weathering. The results of metallurgical profile of the ore body will then be presented in section 4.2. This will then be followed by the results of mineralogical investigation on the run-of-mine, the tailings, and the final concentrate in section 4.3.

Having presented the results of weathering profile on the mine property and looked into the mineralogy, the second part of this chapter will present the results of the investigation into ways of improving the metallurgical performance. The first set of result in the second part will present the pre-leaching results showing the metallurgical response of the weathered ore after selective leaching (section 4.4.1). Then the results of the metallurgical response of selected co-collectors will be presented in section 4.4. Section 4.4 will begin by presenting the results of hydroxamate then followed by the results of thionocarbamates based reagent. Fatty acid results will be presented in section 4.4.4 and finally the results of combining both the fatty acids and thionocarbamates will be presented.

The complete set of results from both the field work and laboratory test work can be seen in Appendix 7.

4.1. DENSITY PROFILE

The first strategy that was employed to assess the extent of weathering and alteration on the in situ ore body, was the use of both the down-hole geophysical surveys (Selfe, 2006), and the specific gravity measurements of the diamond drill core samples (Hayward, 2006). Figure 24 illustrates the change in specific gravity with depth for the various lithologies of ore comprising the silicate reef. The density of the rocks gradually increases with increasing depth suggesting that the primary rock transformed closer to the surface. The results also show some scatter and this is generally attributed to the heterogeneity of the weathering and alteration processes. In particular, the UPR pegmatoidal pyroxenite shows considerable scatter and has a high standard deviation

(SD = 0.107). This is most likely since the UPR is often thin and poorly developed, and hence it is difficult to obtain good density measurements (Selfe, 2006). The density of anorthosite on the other hand did not respond appreciably with depth. This rock type was well developed in the property with the thickness ranging from 10 to 15 m.

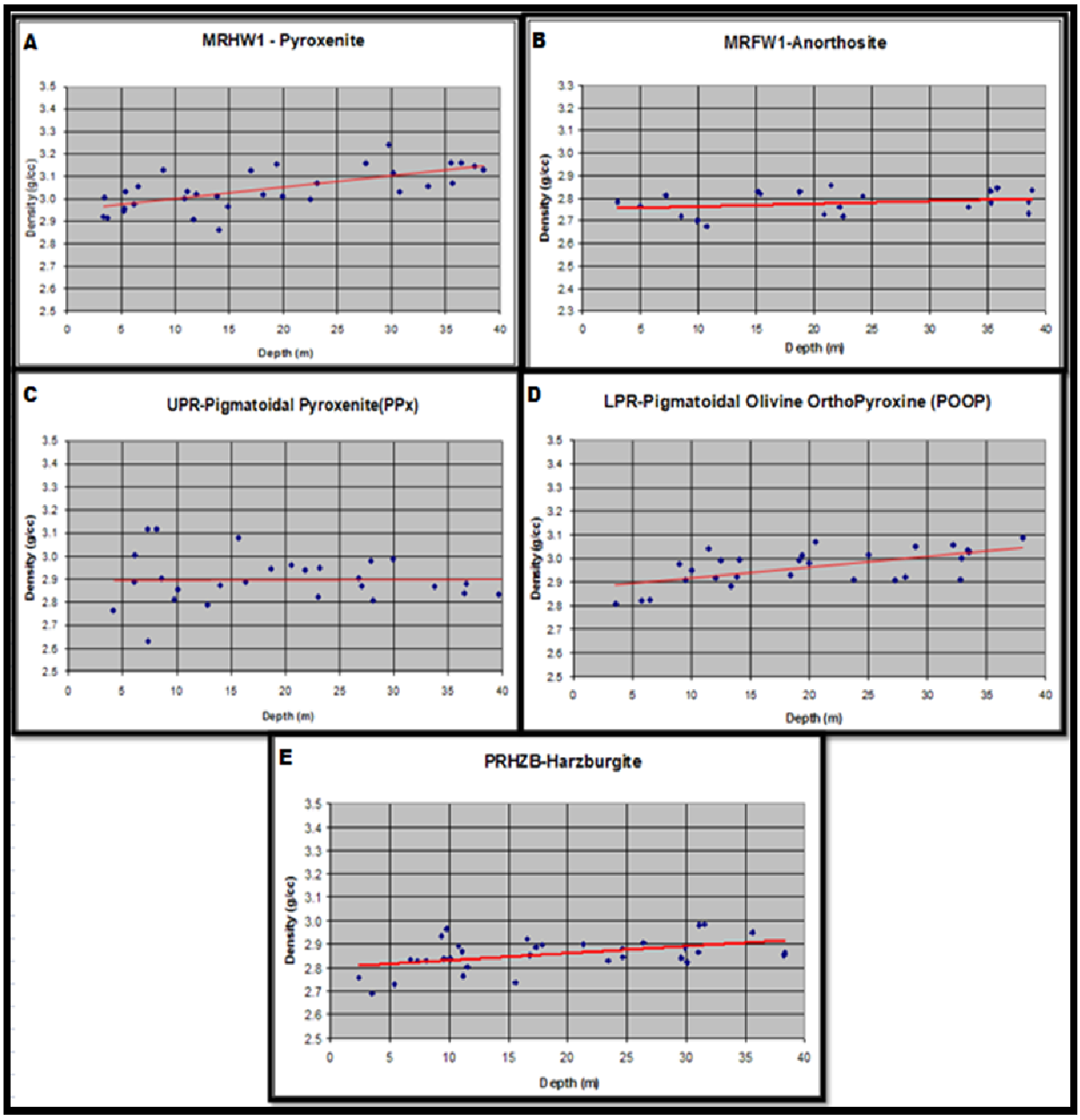

FIGURE 24: ROCK DENSITY VERSUS DEPTH (PYROXENITE (PX), ANORTHOSITE (ANS), PEGMATOIDAL PYROXENITE (PPX), PEGMATOIDAL OLIVINE ORTHOPYROXENITE (POOP), PSEUDO HARZBURGITE (PRHZB))

Average density measurements for the various lithologies of silicate reef are given in Table 10 and Table 11, for ore sampled from less than and greater than 40 m depth from surface, respectively.

TABLE 10: AVERAGE DENSITY IN THE WEATHERED SILICATE ZONE - SHALLOWER THAN 40 M

<40m	MRHW1 PX	MRFW1 An	UPR PPx	PRHZB Hz	LPR Poop
N=	32	21	27	33	29
Av Density g/cc	3.044	2.779	2.901	2.856	2.964
SD	0.090	0.052	0.107	0.070	0.076

TABLE 11: AVERAGE DENSITY IN THE UNWEATHERED SILICATE ZONE – DEEPER THAN 40 M

>40m	MRHW1 PX	MRFW1 An	UPR PPx	PRHZB Hz	LPR Poop
N =	45	33	36	46	31
Av Density g/cc	3.163	2.811	3.084	2.939	3.068
SD	0.057	0.053	0.081	0.065	0.091

For ore sampled shallower than 40 m, the highest density was obtained for the pyroxenite (3.044 $g \cdot cm^{-3}$), and the lowest for the anorthosite (2.779 $g \cdot cm^{-3}$). The average density of the country rock greater than 40 m depth (Table 11) showed a small, yet clear increase in density relative to the same lithology sampled less than 40 m depth. For example, the pegmatoidal pyroxenite showed an increase in density from 2.901 to 3.084 $g \cdot cm^{-3}$. The data in Table 10 and Table 11 also shows that the standard deviations (SD) of the rock density sampled from less than 40 m depth are generally larger than for those sampled greater than 40 m depth. The standard deviations indicate the amount of variability, or scatter, in the data. This indicates that the data shallower than 40 m are more inconsistent, which may be expected given the heterogeneity of the near-surface weathering and alteration processes. The standard deviation of the anorthosite however, for both altered and unaltered zones remained fairly consistent, indicating that plagioclase-rich rocks are more resilient to weathering than rocks rich in Mg-Fe silicates.

4.2. IN SITU METALLURGICAL PROFILE

Based on the RC samples taken from different depths on the mine property, it was decided to conduct standard flotation tests to profile the metallurgical response of the PPM silicate ore relative to its in situ depth in the mine area. As shown in Appendix 1 Table 15, the RC samples were divided according to their location in the mine area, sampling depth, and grade category.

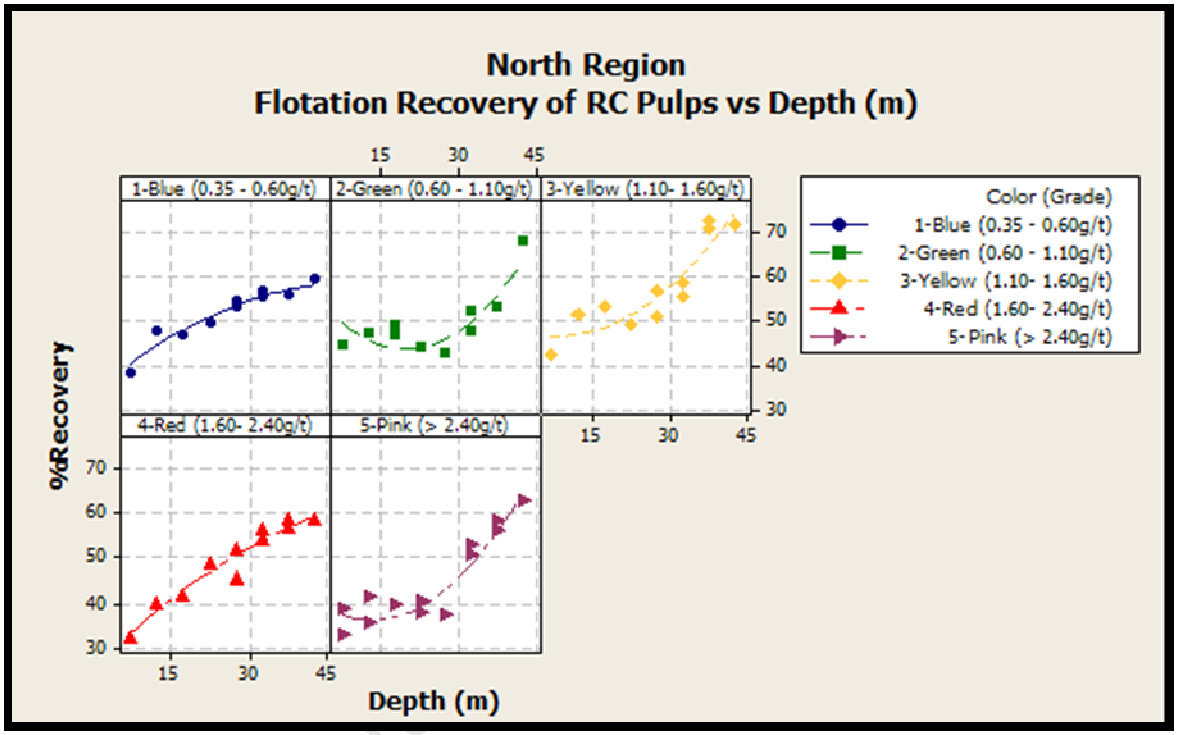

FIGURE 25: COMPARISON OF THE PGE RECOVERY VERSUS DEPTH FOR SILICATE REEF CLASSIFIED IN VARIOUS GRADE CATEGORIES. RESULTS ARE SHOWN FOR THE NORTH REGION OF THE PPM ORE

The results of flotation tests showing the change in PGE recovery versus mining depth for silicate reef ore from the North Region of the mine are shown in Figure 25. Overall, low recoveries are obtained for ore sampled from less than 20 m depth (< 45% recovery). For the ore sampled from greater than 20 m depth, there is a gradual increase in recovery up to 70 %. It is noteworthy that the flotation response for ore in the blue and red grade categories showed a different flotation response to that in the green, yellow and pink grade categories. The blue and red ore showed gradual increase of recovery at diminishing rate from surface to the depth of 45m, while the recovery profile of green, yellow and pink remain fairly constant at shallow depth and seem to increase rapidly beyond 25m depth. During the flotation tests for the ore from the blue and red

grade categories, the colour of the pulp was noted to be significantly lighter, suggesting the presence of abundant plagioclase instead of orthopyroxene

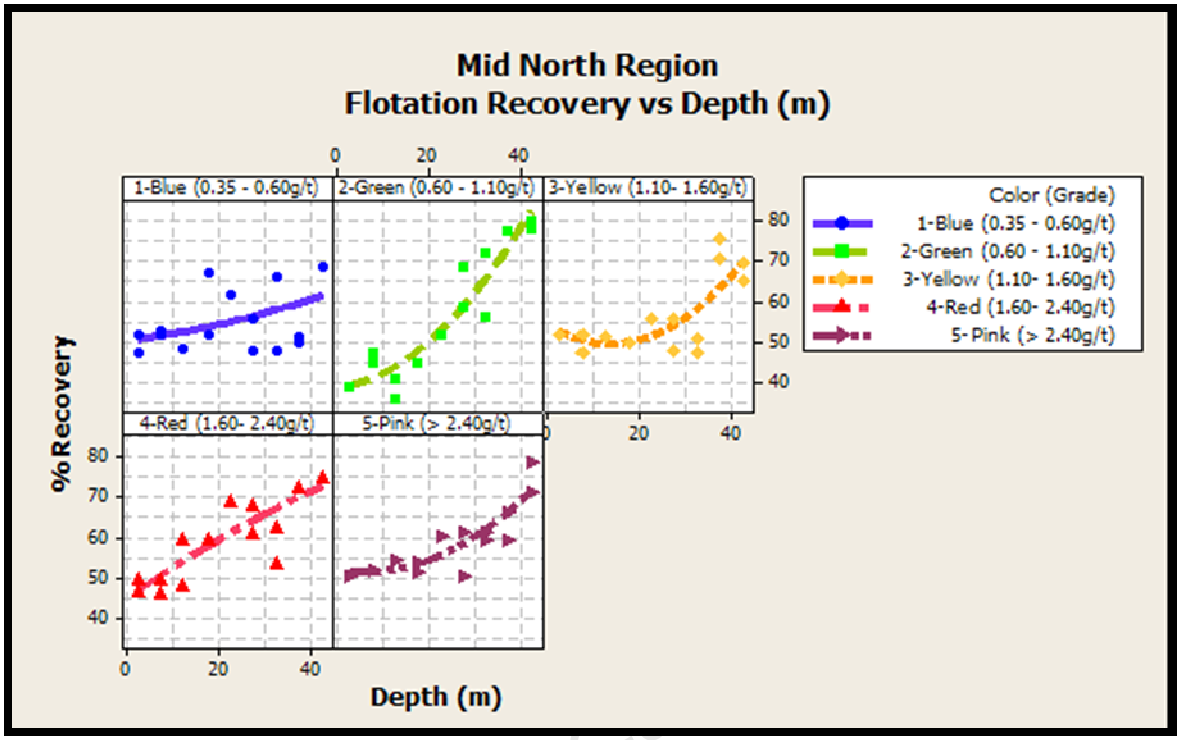

FIGURE 26: COMPARISON OF THE PGE RECOVERY VERSUS DEPTH FOR SILICATE REEF CLASSIFIED IN VARIOUS GRADE CATEGORIES. RESULTS ARE SHOWN FOR THE REGION SANDWITCHED BY BOTH THE CENTRAL AND THE NORTH REGION (MID NORTH REGION)

The mid north region was also found to suggest the presence of geological structure, perhaps fault line around 20 m depth with an increasing recovery at increasing depth (Figure 26). This was more vivid on both “yellow (1.10 – 1.60g/t)” and “pink (>2.40g/t)” headgrades. It was difficult to infer any form of pattern or profile with regard to the “blue (0.35 – 0.60g/t)” material as the recoveries seem to have been dominated by entrainment as opposed to true flotation. The recovery data appeared somewhat more scattered compared to the other grades from the same region.

A similar pattern of recovery profile is observed in central region as with the north regions and mid north region (Figure 27). However, some ore grades seem to follow exponential growth type curve (see “yellow (1.10 – 1.60g/t)” and “pink (>2.40g/t)”, while others such as “red (1.60 – 2.40g/t)” and “green (0.60 – 1.10g/t)” seem to follow logarithmic grow curve (see Figure 27).

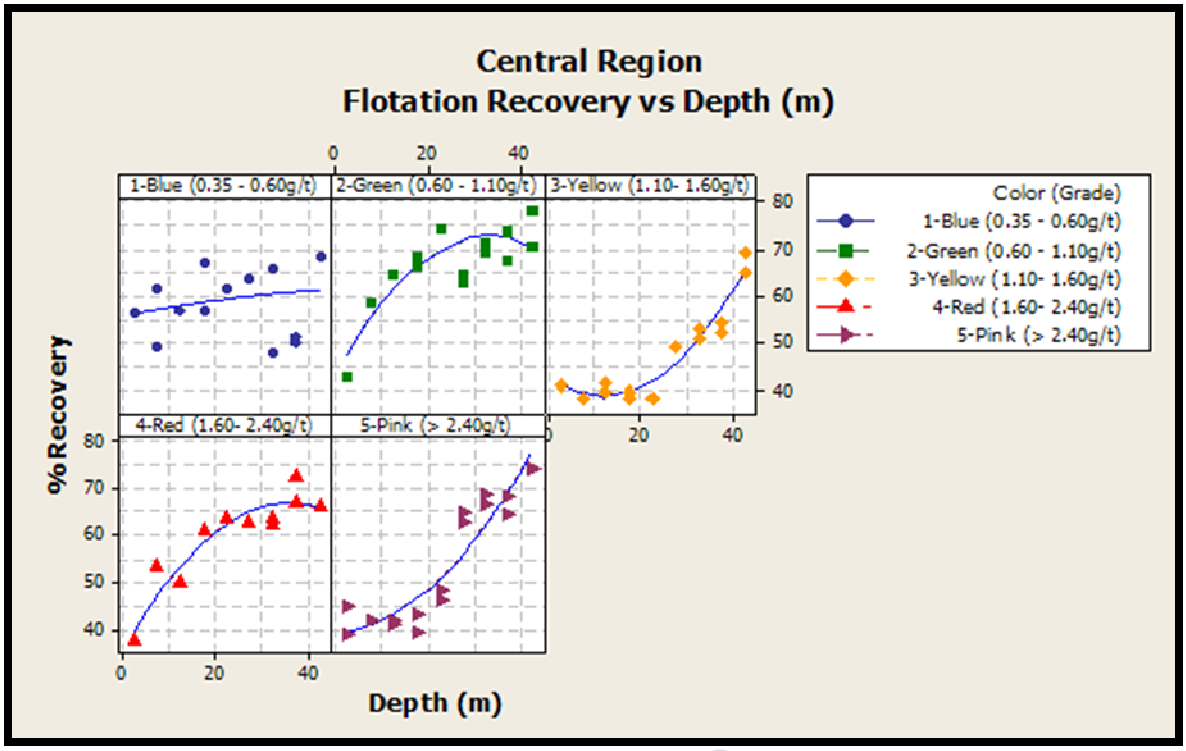

FIGURE 27: COMPARISON OF THE PGE RECOVERY VERSUS DEPTH FOR SILICATE REEF CLASSIFIED IN VARIOUS GRADE CATEGORIES. RESULTS ARE SHOWN FOR THE CENTRAL REGION OF THE PPM ORE BODY

This behaviour is suspected to be due to lithological variance based on the individual samples within a composite. The "blue (0.35 – 0.60g/t)" ore again showed high entrainment, probably due to high content of talc material.

There was hardly any potholing noticed in the south region. This was accompanied by better recoveries profile than the ore from the northwards regions (Figure 28). Although there was some oxidation that was noticed and the high talc in the material closer to the surface, there was less geological alteration in the south region compared to the regions toward the north.

The north region was dominated by potholing, and more serpentinisation was observed at the north region compared to the south region.

As seen in Figure 28, the recovery at the south region seems to increase beyond 80% with increasing depth. Although there was some incidence of higher recovery in the north regions, the recovery around the depth of 40 m in the south region were firmly in the 80% range.

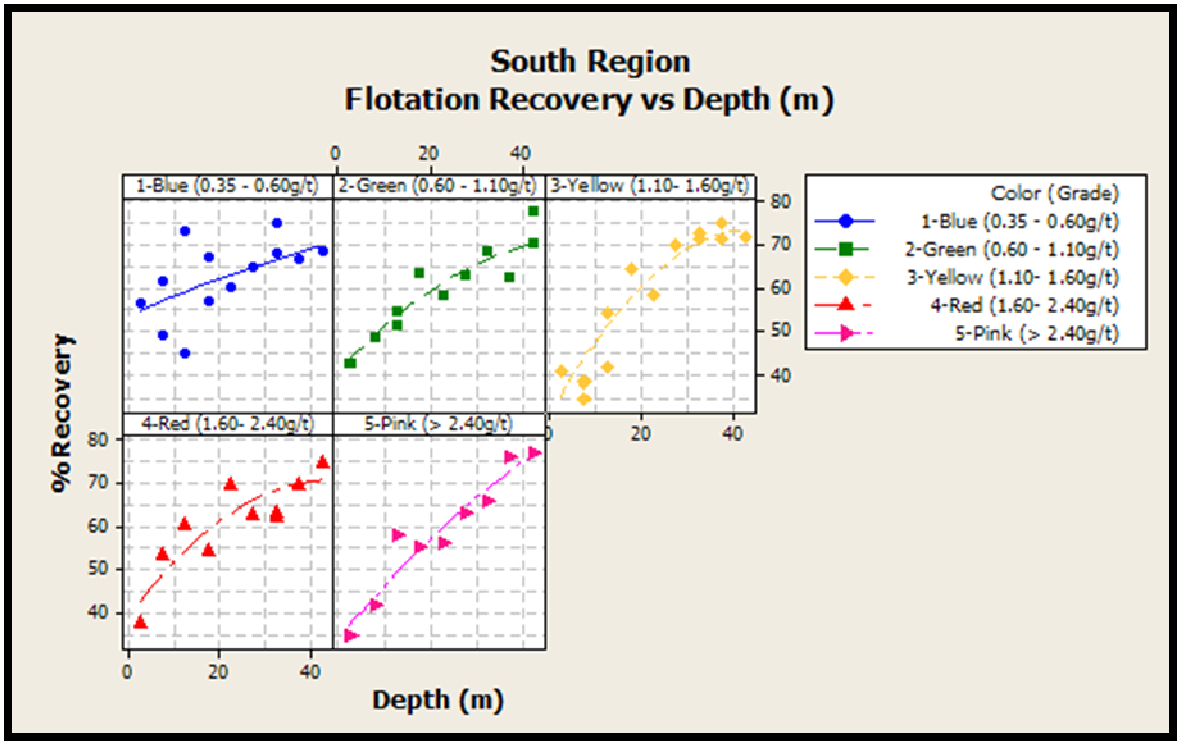

FIGURE 28: COMPARISON OF THE PGE RECOVERY VERSUS DEPTH FOR SILICATE REEF CLASSIFIED IN VARIOUS GRADE CATEGORIES. RESULTS ARE SHOWN FOR THE SOUGH REGION OF THE PPM ORE BODY

The silicates reef recovery profile results, (Figure 26, Figure 27, and Figure 28) also shows the increasing recovery with increasing depth for all regions. This observation further support the argument that the ore near surface is somewhat passivated compared to the material deep into the earth.

4.3. MINERALOGY

Mineralogical analyses were conducted on silicate reef samples obtained from the primary rougher feed, final concentrate and secondary rougher tailings at PPM plant. The material was the follow on from the same material that was sampled in situ with RC samples, also, the same material that was covered by diamond drill sample which got used for density profiling. Having established the weathering profile using density and flotation profile with depth, the material near surface was treated through the plant and sampled at the points shown in Figure 22 (Primary Rougher Feed, Secondary Rougher tails and Final concentrate). Mineralogical analysis was aimed at finding complementary evidence of PPM ore weathering in order to characterise the type of PGM minerals found in the head-grade, the tailings and the final concentrate.

4.3.1. Bulk Mineralogy

The mineral identification and quantification by XRD of silicate reef in the final concentrate is shown in Table 13 and represents altered ore derived from less than 40 m depth.

TABLE 12: QUANTITATIVE XRD RESULTS OF THE SILICATE REEF FINAL CONCENTRATE (GROBLER, 2010)

Minerals	Weight % in Sample
Chalcopyrite	< lld*
Pentlandite	< 1.0
Pyrrhotite	2.3
Chlorite	6.5
Clinopyroxene	3.8
Orthopyroxene	39.2
Plagioclase	21.1
Talc	9.8
Olivine	2.4
Hornblende	5.1
Serpentine	5.6
Magnetite	2.8
Quartz	< 1 .0

* lld indicates the detection limit of XRD

The dominant minerals present in the silicate reef final concentrate are orthopyroxene (39.2 wt%) and plagioclase (21.1 wt%). Significant amounts of the alteration minerals; talc, chlorite and serpentine are also present. The abundance of talc in the concentrate is attributed to its natural hydrophobicity ((Fuerstenau et al., 1988), (Leterme et al., 2004) and (van Oss, 2008)). Other secondary minerals such as magnetite and quartz are also present, although only in minor quantities.

The concentration of the base metal sulphides as measured by XRD in the final concentrate was particularly low (< 2.5 wt%), and chalcopyrite was not even detected during the measurement. This observation was surprising given the known presence of chalcopyrite in the feed, and its good floatability ((Bulatovic, 2007), (Gu et al., 2010), (Ansari and Pawlik, 2007) and (Guo and Yen, 2003)).

A qualitative SEM analysis of the tailings showed the presence of liberated chalcopyrite (Figure 29 A). This would suggest that the poor recovery of chalcopyrite

may be due to its surface passivation as a result of the weathering and alteration processes.

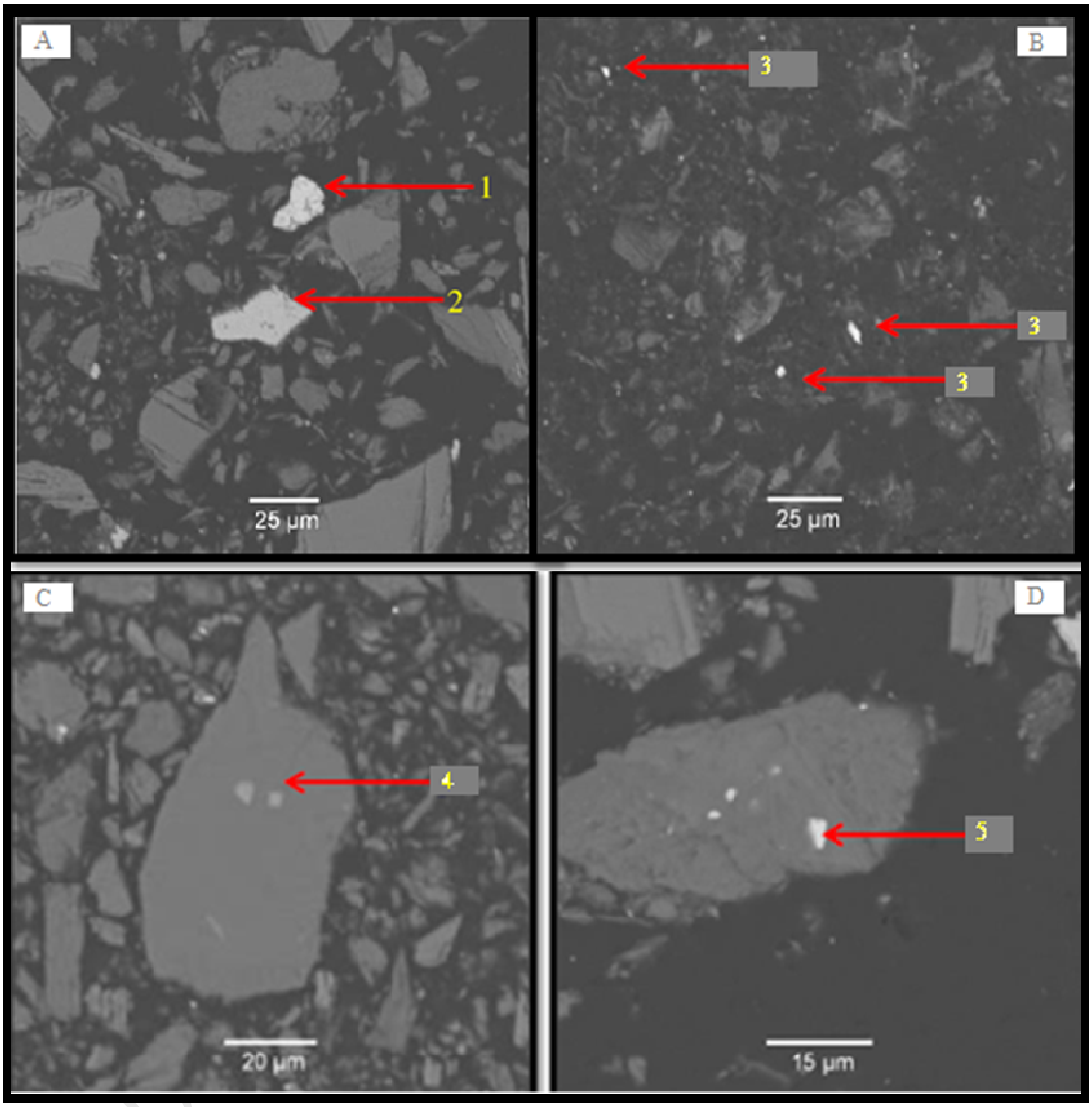

FIGURE 29:THE SEM IMAGE OF THE SILICATE FINAL TAILINGS: A SHOWS EVIDENCE OF (1)-CHALCOPYRITE, (2)-PYRRHOTITE, B SHOWS EVIDENCE OF (3)-COPPER AND ZINC OXIDE, C SHOWS (4)-NICKEL OXIDE OCCLUDED IN ENSTATITE, AND D SHOWS (5)-PENTLANDITE (36-WT%) OCCLUDED IN ENSTATITE.

A significant amount of copper and zinc oxides (Figure 29 B) were detected in the final tails, providing further support that the ore has been altered. Appreciable amounts of pentlandite and pyrrhotite were also detected in the tails during the SEM investigation (Figure 29 A and D). The Ni-rich character (36 wt %) of the pentlandite indicates it is nearing violarite ($FeNi_2S_4$) structure, which is known to be an alteration product of pentlandite (Lamya, 2007). The presence of millerite in the tails (NiS), also provided further evidence that the pentlandite has been altered possibly through

oxidation. Given that the base metals sulfides show a strong association to the platinum group minerals ((Zhu et al., 2010), (Liddell, 2009), (Chetty et al., 2009), and (Holwell et al., 2006)), their presence in the tailings sample indicated significant losses of the PGM during the flotation.

4.3.2. PGM MINERALOGY

MLA analyses of the silicate reef primary rougher feed indicated that the PGM contingent consisted primarily of PGE-arsenides (36%), PGE-alloys (26%) and PGE-sulphides (24%) and lesser amounts of PGE-tellurides (7%) and electrum (5%). The tailings contained more PGE-alloys (44%) and PGE-sulphides (32%), with 13% PGE-arsenides and 10% PGE-tellurides.

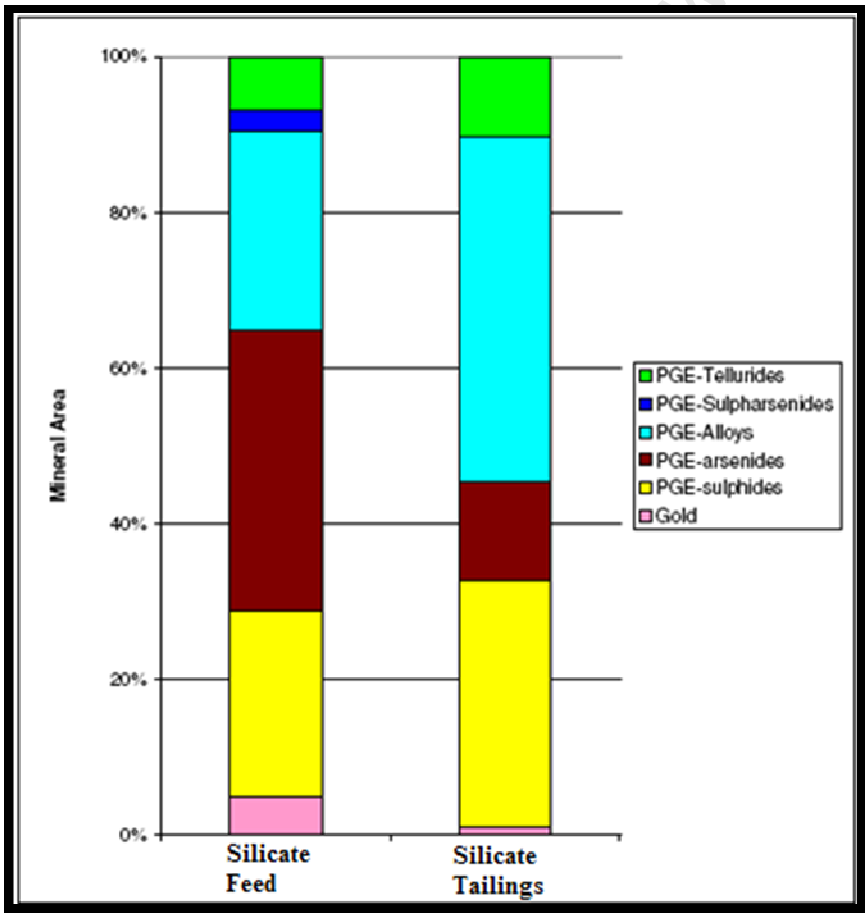

FIGURE 30: RELETIVE PGM ABANDANCE IN THE SILICATE FEED AND TAILINGS MATERIAL (SMITH, 2010)

MLA analyses (Table 13) also showed a higher degree of liberation of PGMs in the feed (62.4%) than the tailings (55.4%). The PGM association for un-liberated PGM

bearing minerals was then determined based on the percentage of the total phase boundary of the valuable mineral in contact with other mineral phases.

TABLE 13: PERCENTAGE LOCKING AND LIBERATION OF PGM'S IN MERENKSY FEED AND TAIL

	Merensky Feed	Merensky Tail
Liberated	62.4	55.4
Middlings	3.9	13.0
Locked	33.7	31.6
Total	100.0	100.0

Figure 31 shows graphically the PGM association data and the accompanying table may be viewed in Appendix 6. The middlings and locked PGMs in all of the samples were mostly associated with the silicates. For the silicate reef feed, 69 % of the locked and middling PGMs were enclosed in or attached to silicates; a further 17 % of the PGMs were locked in gangue, or occurred on grain boundaries (mostly between silicates and oxides).

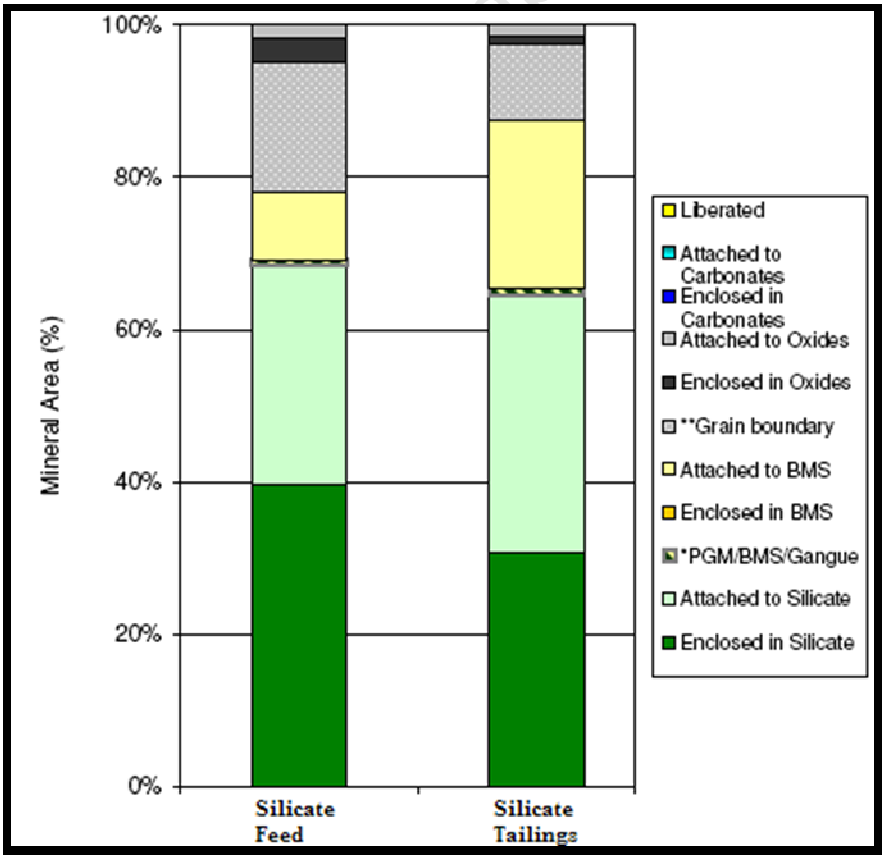

FIGURE 31: SILICATE PGM ASSOCIATION IN THE FEED AND TAILS

Only 9% of the PGMs were attached to liberated BMS. In the silicate reef tailings, 64% of the un-liberated PGMs were attached to the silicates, with a further 9% occurring on grain boundaries (mostly between silicates and oxides). Significant proportions (22 %) of the PGMs were associated with liberated BMS.

TABLE 14: GRAIN SIZE DISTRIBUTION SHOWING WEIGHT PERCENTAGE PASSING DATA FOR PPM PGM ORE

P-value	Silicate Feed	Silicate Tailings
P20	3	3
P50	7	7
P80	23	11

Table 14 shows the cumulative percent passing of the PGM both from the feed and the tailings sample. The weight percent distributions include 20, 50 and 80 percent passing data. The grain size data was calculated, whereas the particle size was based on screening data (Smith, 2010). The grain size distribution (Table 14) indicates that the P50 was 7 microns both in the feed and the tailings. The P80 improved from 23 microns in the feed to 11 microns in the tailings.

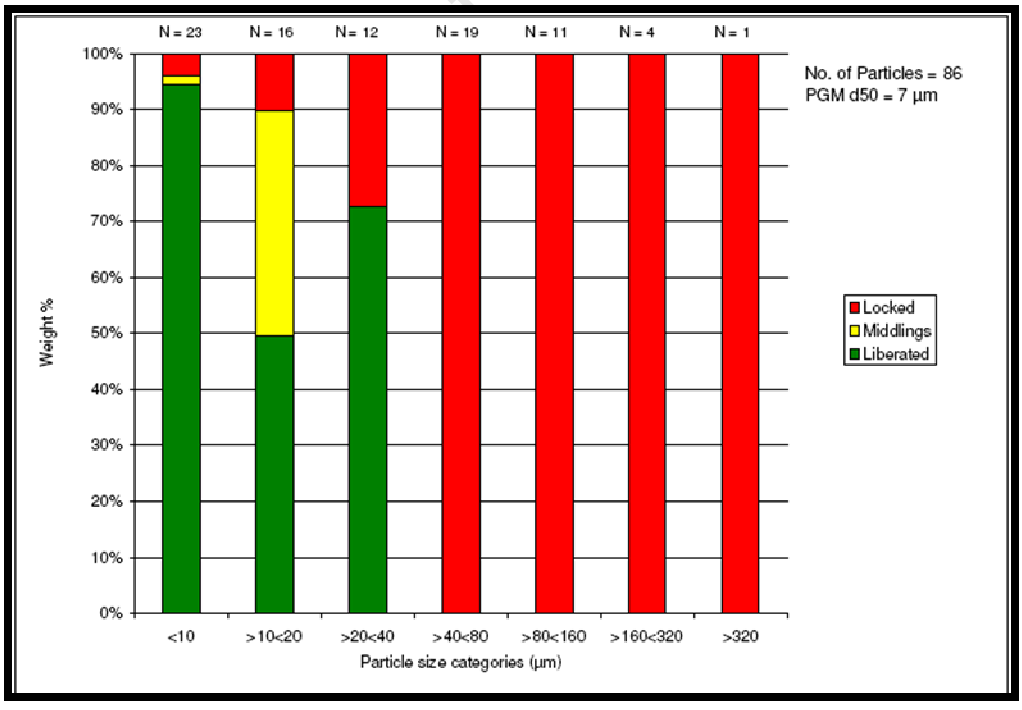

FIGURE 32: PPM PGM DEPORTMENT IN SILICATE TAILINGS. SHOWING 72% (WT%) OF PGMS FALLING WITHIN A FLOATABLE RANGE OF >20<40 MICRONS WERE LIBERATED

Even though +20 µm to -40 µm are known to float reasonably well, Figure 32 shows over 70 wt% of PGMs in the tailings were liberated. Details grain size distribution curve is shown in Appendix 6.

4.4. METALLURGICAL STRATEGIES TO IMPROVE FLOTATION RECOVERY OF ALTERED SILICATE REEF

Having established several indications of alteration of the silicate reef ore derived from near surface, this study now focuses on investigating some potential remedies to improve flotation performance. In this section, the results of deferent flotation techniques employed in the study to improve metallurgical performance of the altered ore are presented.

4.4.1. PRE-LEACHING

The aim of the acid pre-leaching or acid etching of the ore prior to standard flotation was to try removing the passivating layer surrounding the valuable mineral. The oxide layer around the PGM mineral particle is thought to be responsible for the passsivation of the PGM bearing minerals, preventing them from floating with normal sulphide collectors.

The etching of oxide layer on the PGM bearing mineral particle surface with sulfuric acid is fairly rapid once the acid arrives at the particle surface. This is the reason why this reaction can be performed at ambient temperature in a standard reactor equipped with just a mechanical agitator (Luszczkiewicz and Chmielewski, 2008).

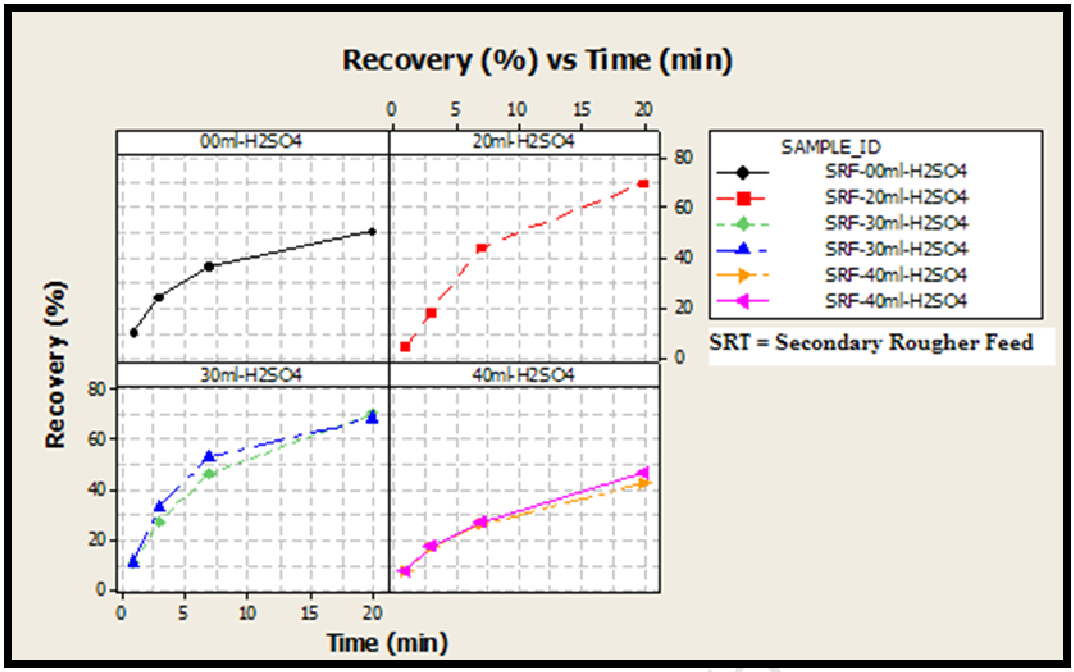

FIGURE 33: FLOTATION RECOVERY VERSUS TIME FOR PRE-LEACHED SILICATE REEF ORE. RESULTS ARE SHOWN FOR DIFFERENT ACID DOSAGES

The flotation recovery curve of the pre-leached samples is shown in Figure 33. The control curve in Figure 33 was the case with no acid addition, "00ml-H2SO4". The results for the 20 and 30 ml acid leaches showed similar flotation kinetics and overall recovery at about 70%.

Figure 34 shows the mean recovery of the acid pre-leach tests for different sulphuric acid dosages. The ANOM (one way analysis of the means) shown in Figure 34 compares the average recoveries for each scenario and shows the mean recovery. The mean recovery for all four tests shown in Figure 34 is represented by the middle line. From Figure 34, it is apparent that the mean recovery of the 30 ml acid pre-leach falls outside the decision boundary limits indicating a significant difference compared to the results with other acid dosages.

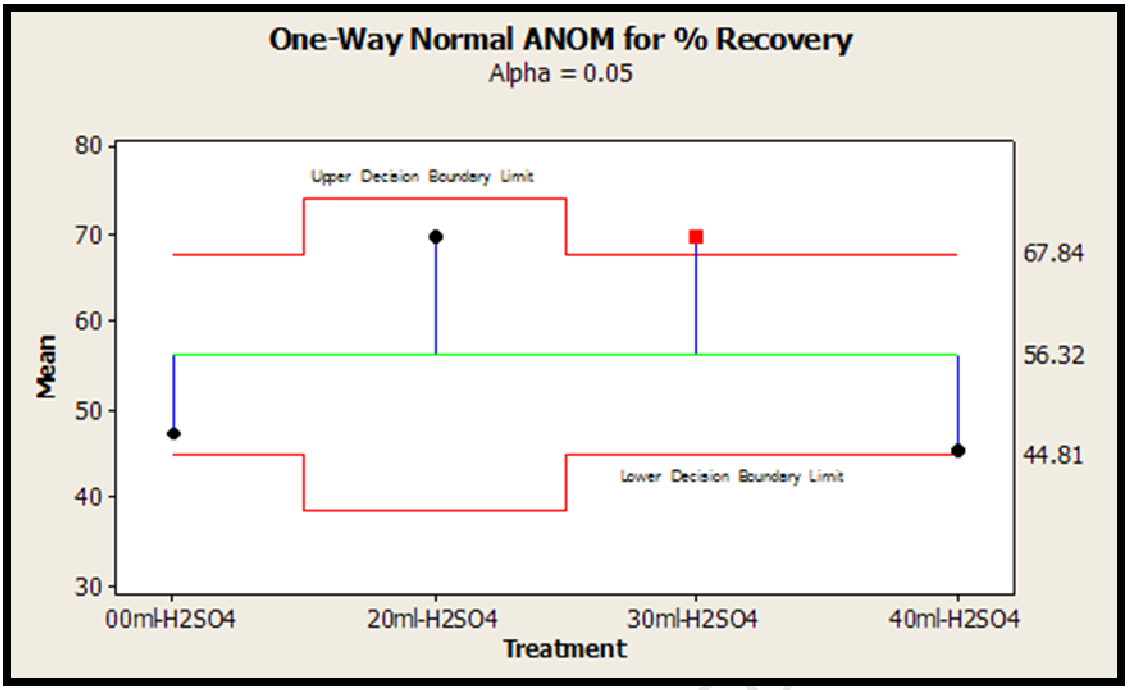

FIGURE 34: ONE-WAY NORMAL ANALYSIS OF MEANS USING ANOVA STATISTICAL TECHNIQUE. THE RESULTS SHOWS 20 AND 30 mL ACID DOSAGE GIVES RESULTS WELL ABOVE THE AVERAGE MEAN OF ALL TESTS. ACID DOSAGE OF 30 mL IS SIGNIFICATLY HIGHER THAN THE AVERAGE MEAN AT 95% CONFIDENCE LEVEL.

Comparison of the recovery versus mass (Figure 35 C) and grade - recovery curves (Figure 35 B) for the acid pre-leach conducted at this acid dosage (30 ml), confirm its improved recovery relative to the tests with no acid pre-leaching. The one-way ANOM graph shown in Figure 35 D depict that recovery achieved by acid treatment is significantly higher that the recovery achieved with normal treatment with 95% confidence (α = 0.05). The selectivity however was somewhat poorer for the pre-leached ore as evidenced by the downward shift in the grade-recovery curve. Similarly, the mass recovery curves illustrated in Figure 35 C show the same difference. The fact that acid treated material produced a higher mass recovery, with higher PGE recovery (~ 20 % improvement), is viewed as positive because it shows the acid treatment encourages the flotation of the PGM. The seemingly poor selectivity compared to the untreated material suggests the pre-leach activated other undesirable gangue minerals, or perhaps the residual effect of pre-leach interfered with the activity of the depressant, which was added as normal, after the pre-leach.

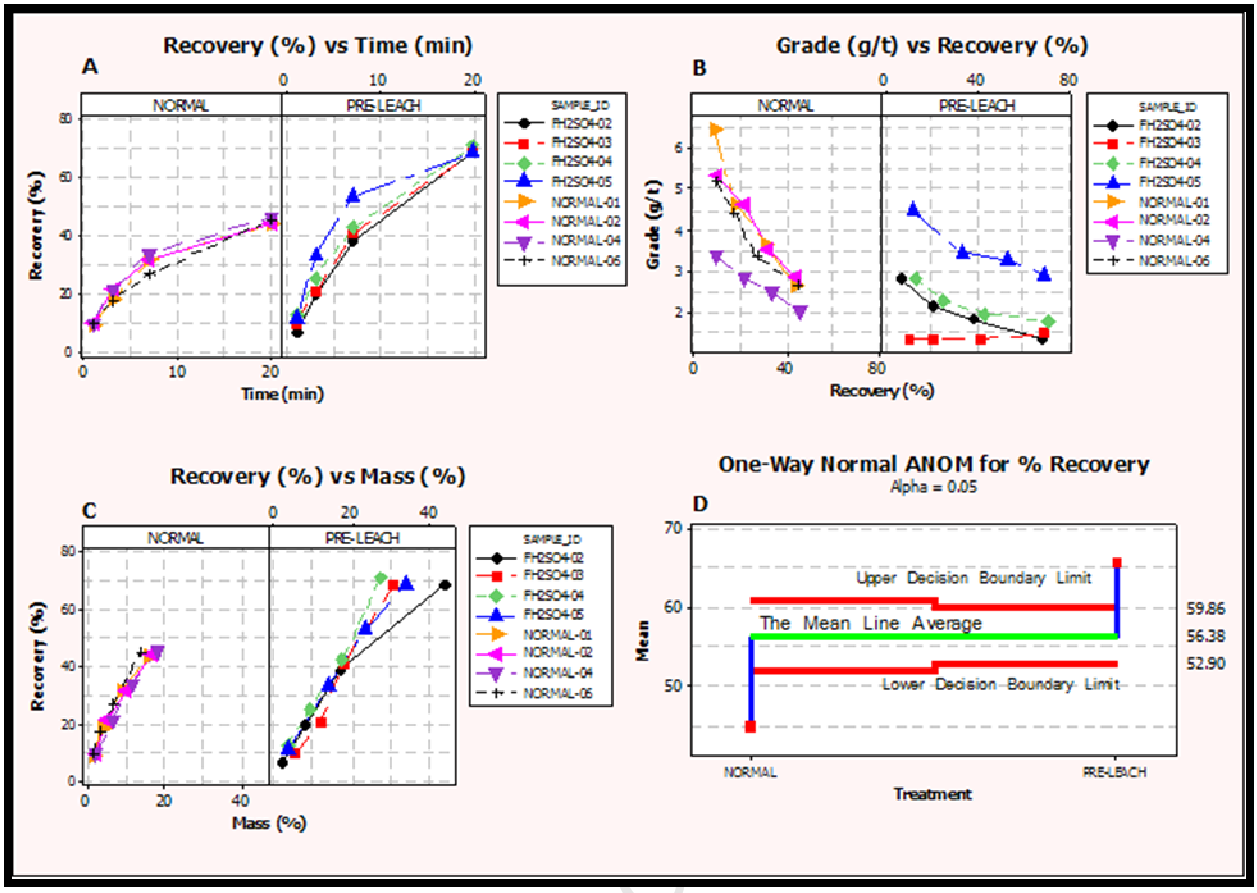

FIGURE 35: SHOWING FOUR GRAPH COMPARING ACID TREATED MATERIAL WITH NORMAL FLOTATION PROCEDURE: GRAPH "A" IS PGE RECOVERY CURVE, GRAPH "B" IS GRADE RECOVERY CURVE, GRAPH "C" IS MASS PULL CURVE, AND GRAPH "D" IS ONE- WAY ANOVA COMPARING THE MEAN RECOVERY FOR ORE TREATED WITH ACID AND NORMAL TREATMENT

4.4.2. HYDROXAMATE BASED CO-COLLECTOR

Hydroxamate based reagents are believed to be effective especially on oxidised copper minerals. Addition of AM28 as a flotation co-collector with xanthate seemed to increase the mass pull when compared with the base case (normal reagent suite). Figure 36 shows the kinetic recovery curve with and without AM28 at the grind of 80% passing 75 microns and 90% passing 75 microns respectively. The aim of grinding finer (from 80% passing to 90% passing) was to determine if high liberation would also assist to improve the recovery with AM28 as co-collector.

As shown in Figure 36, the recoveries seemed to improve compared to a case where AM28 was not added (compare "80-AM28"with "80-NOAM" and "90-AM28" with "90-NOAM" in Figure 36). Figure 36 also shows that increasing the grind from 80% passing 75 microns to 90% passing 75 microns had slightly negative effect in terms of metallurgical performance when comparing the case where AM28 for both grinds.

But comparing the case of adding AM28 together on finer grind (90% passing 75 microns) with the case where AM28 was not used at 80% passing 75 microns, the results shows that AM28 still improved the recovery. This shows that AM28 was still able to improve metallurgical performance over a finer ground material; even so, not to the level of optimal grind of 80% passing 75 microns.

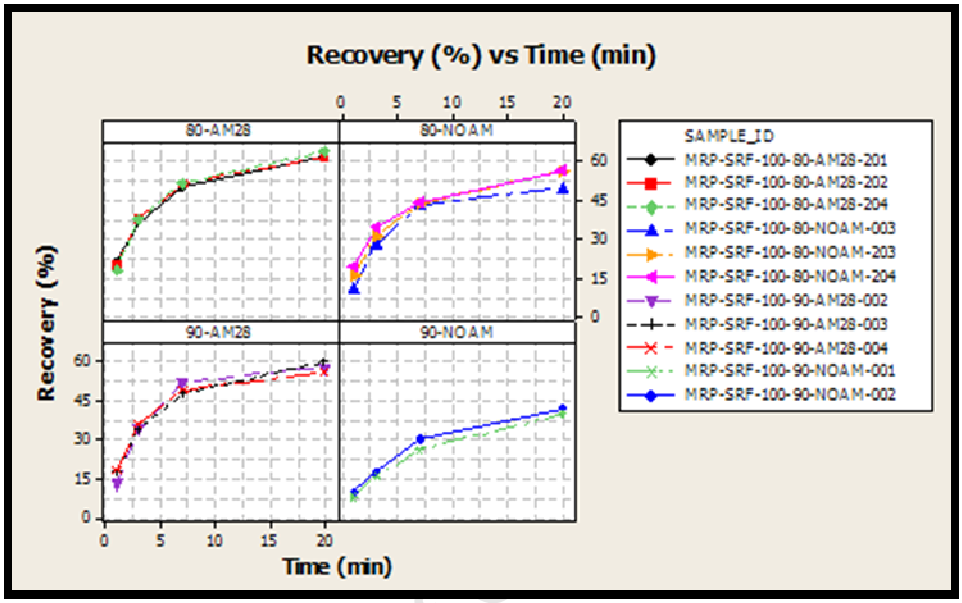

FIGURE 36: FLOTATION KINETICS CURVE WITH AND WITHOUT AM28 (AT 80% GRIND AND 90% GRIND)

[NOAM MEANS AM28 WAS NOT ADDED]

The grade-recovery curve (Figure 37) shows the PGM recovery versus the product grade. Figure 37 is particularly useful to compare separation where both the grade and the recovery are different.

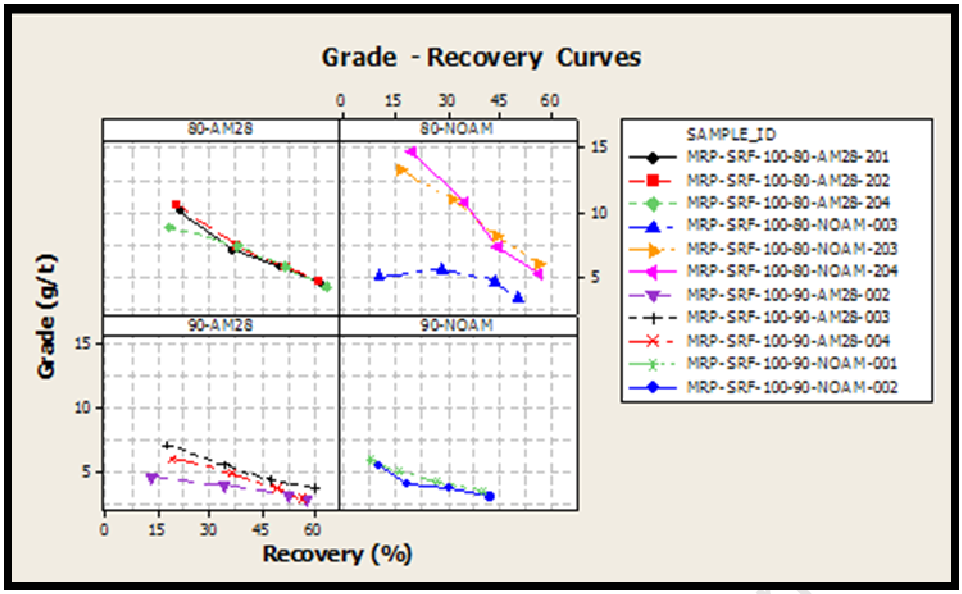

FIGURE 37: GRADE RECOVERY CURVE WITH AND WITHOUT AM28 AT 80 AND 90% GRIND SHOWING AM28 AT 80% GRIND SHIFTED THE GRADE RECOVERY CURVE TO THE RIGHT.

From Figure 37, the flotation results of material treated with AM28 ("80-AM28" and "90-AM28") seem to be shifted lower and to the right, indicating the drop in concentrate grade with slightly higher recovery. On the other hand, the base case ("80-NOAM" and "90-NOAM") seems to be shifted higher and to the left. This suggests that AM28 was able to improve the recovery but selectivity was somewhat subdued.

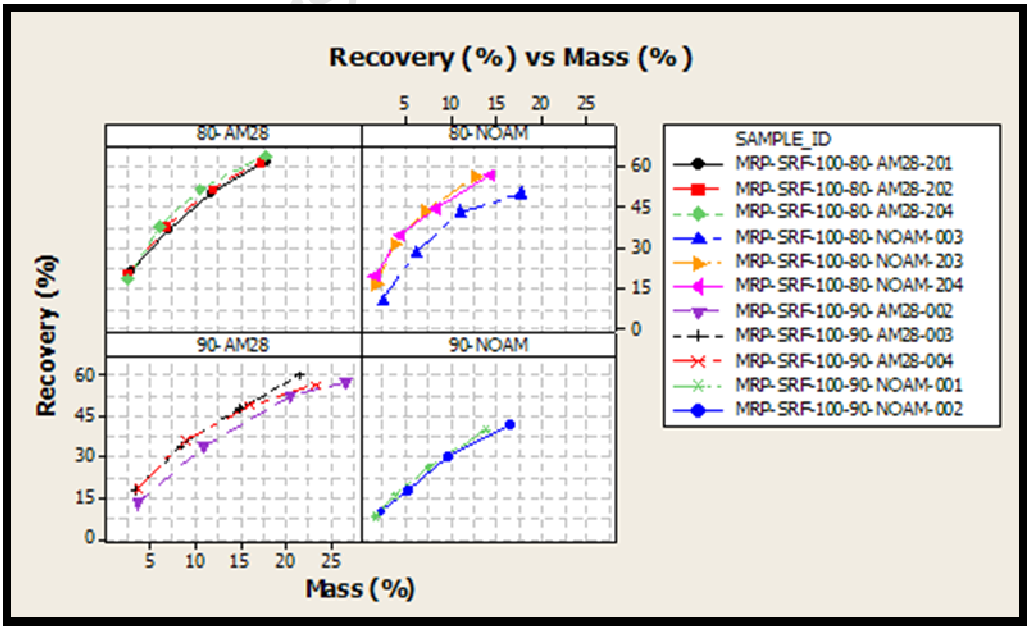

FIGURE 38: THE MASS PULL CURVE WITH OR WITHOUT AM28 AT 80 AND 90% GRIND SHOWING 80% GRIND PRODUCED HIGHER GRADE CONCENTRATE.

The mass pull curves depicted in Figure 38, shows that AM28 eventually had higher mass pull at finer grind, but at 80% passing, the mass pull was comparable to the normal reagent suite. This confirms the observations that were done during the flotation test. The higher mass pull curves are generally shifted higher and to the right. It is not possible to deduce from the analysis done as to what other particles were collected by AM28 at finer grind.

Figure 39 clearly shows that the highest recovery was achieved when AM28 as co-collector was added over and above the normal reagent suite. As shown in Figure 39; one way analysis of means derived from ANOVA statistical technique shows that AM28 improves metallurgical performance significantly, with or without fine grinding.

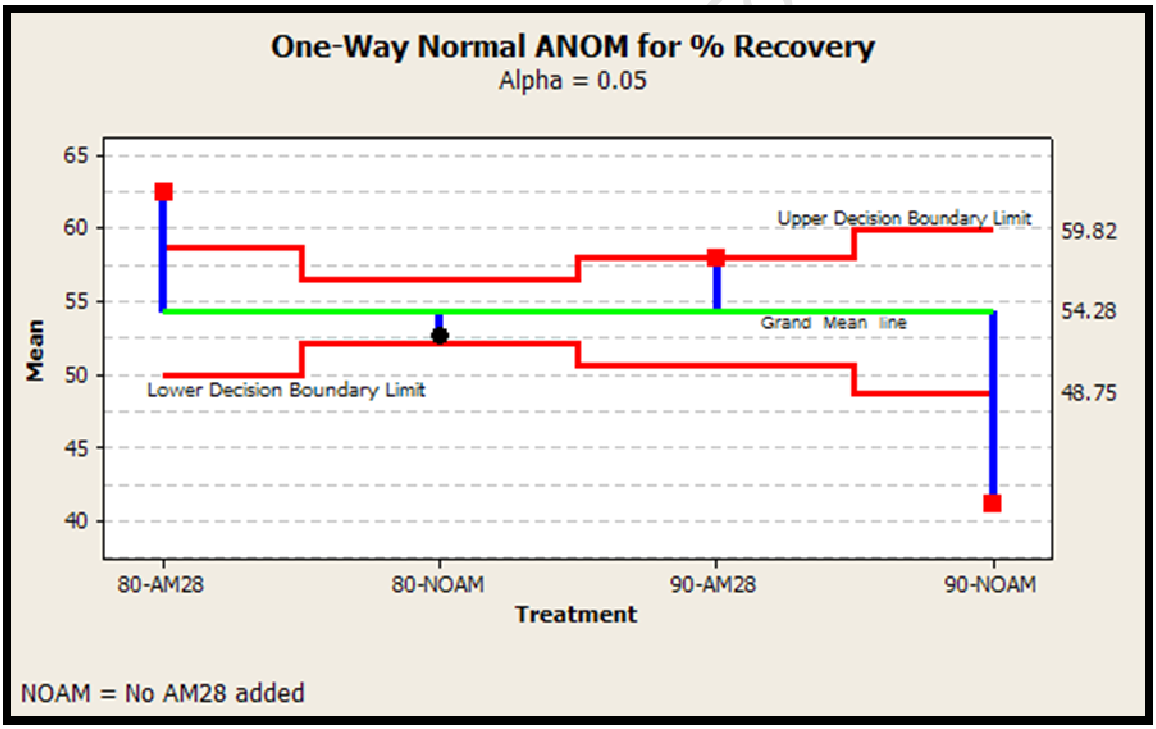

FIGURE 39: ANOVA ANALYSIS OF MEAN SHOWING TREATMENT WITH AM28 AT 80% GRIND PRODUCED SIGNIFICANTLY HIGHER RECOVERY COMPARED TO THE AVERAGE MEAN OF ALL TEST. NORMAL REAGENT SUITE AT 90% GRIND WAS THE LEAST EFFECTIVE

Although the recovery drops substantially when the material is finely ground, AM28 seems to improve the recovery irrespective of the grind. However, even AM28 was unable to restore floatability of the over ground material (see Figure 39).

4.4.3. THIONOCARBAMATE BASED CO-COLLECTORS

Figure 40 shows the kinetic recovery curve for the three thionocarbamates based co-collectors supplied by Tecrich Development Corporation. The results of 20 minutes recoveries for three reagents ("TC1000", "TC3000", and "TC6000") seemed to be similar to the results obtained from the base case ("Normal"). However, there was a slight metallurgical performance improvement on the material treated with TC6000 (~50% recovery compared to 45% recovery from the control test).

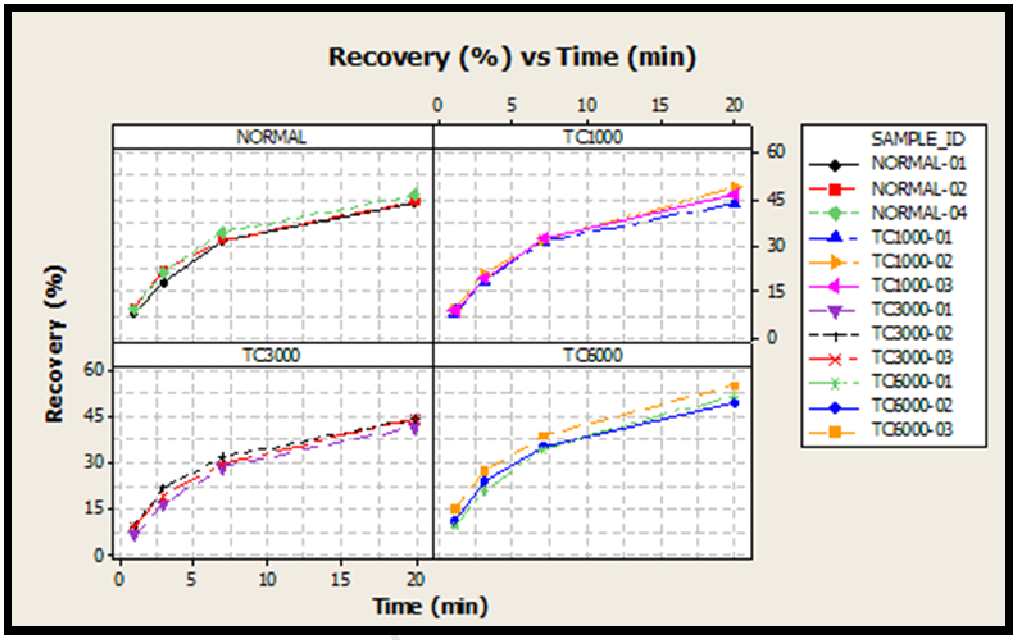

FIGURE 40: FLOTATION KINETICS CURVE FOR THIONOCARBAMATE BASED CO-COLLECTORS WITH NORMAL REAGENT SUITE

Although adding TC1000 did not seem to affect the ultimate recovery, TC3000 on the other hand showed a marginal decline of recovery. By visual inspection of the froth during the test run, these reagents changed the stability of the bubbles and the froth appeared more brittle compared to froth generated by the normal reagent suite. TC6000 appeared to have the greatest impact in terms of destabilising the froth bed, followed by TC3000 and TC1000 respectively. The major difference noticed amongst these reagents was the secondary active chemical component. Over and above thionocarbamates, TC6000 also contained xanthogen formate whereas TC3000 contained some form of xanthate. Perhaps it was the interaction of thionocarbamates with the secondary active reagent that informed the collecting power of the reagent.

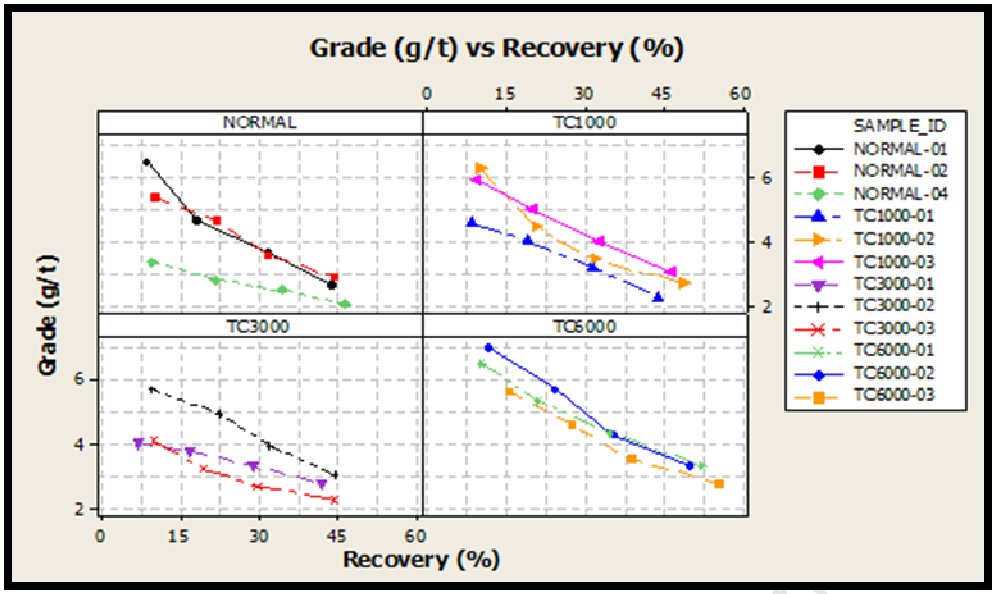

FIGURE 41: GRADE RECOVERY CURVE OF TC-SERIES REAGENTS COMPARED TO NORMAL REAGENT SUITE. THE RESULTS SHOW TC6000 AND TC1000 HAVE SIMILAR OR SLIGHTLY STEEPER CURVER COMPARED TO NORMAL

The grade-recovery curve (Figure 41) shows that the TC reagents improved the selectivity slightly but TC3000 again showed no impact on selectivity (in fact slightly worsened). In terms of shifting the grade-recovery curve to the right and upwards, TC6000 showed relatively better performance. It is not possible based on the analysis carried out in this study to determine whether there were other active chemicals in the TC reagents. However, there is some indication that thionocarbamates together with xanthogen formate may have something to offer. Comparison of the result of TC1000 and TC6000 shows that thionocarbamates alone does not have that much impact in terms of flotation performance. TC3000 contained additional xanthate with thionocarbamates, and this combination did not improve flotation recovery. It is also not known whether the ratio of thionocarbammate to xanthogen formate used was sufficiently optimal.

Grade-recovery curve (Figure 41) when read in isolation, suggests that at concentrate grade say of 5g/t, the recovery moved from 15% to 30% when using TC600 compared to normal reagent suite. However, combining grade-recovery curve with recovery-mass pull curve (Figure 42), the normal reagent suite achieved 15% recovery at the mass pull of 2.5%, but TC6000 achieved the same 15% recovery at the mass pull of 5% (by doubling mass pull), indicating the metallurgical performance did not materially improve.

Although the TC reagents did not show significant metallurgical improvements (Figure 43), there were some indications that these reagents had some desirable promoting qualities as depicted by slightly lower or virtually unchanged mass pull without loss of substantial recovery (Figure 42).

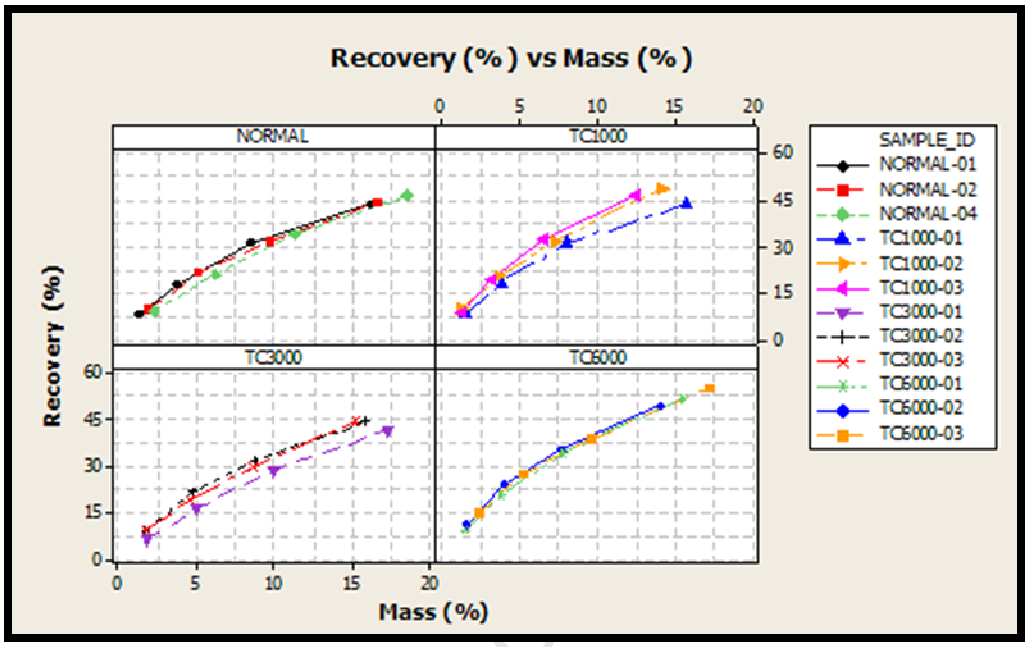

FIGURE 42: MASS PULL CURVE OF TC-SERIES REAGENTS SHOWING BOTH TC6000 AND TC1000 SHIFTED THE MASS PULL CURVE TO THE LEFT AND SLIGHTLY HIGHER RELATIVE TO THE NORMAL REAGENTS.

TC6000 showed slight improvement on recovery with noticeable improved selectivity (Figure 43). Perhaps the xanthate used in TC3000 may have been responsible for negative influence on the metallurgical performance.

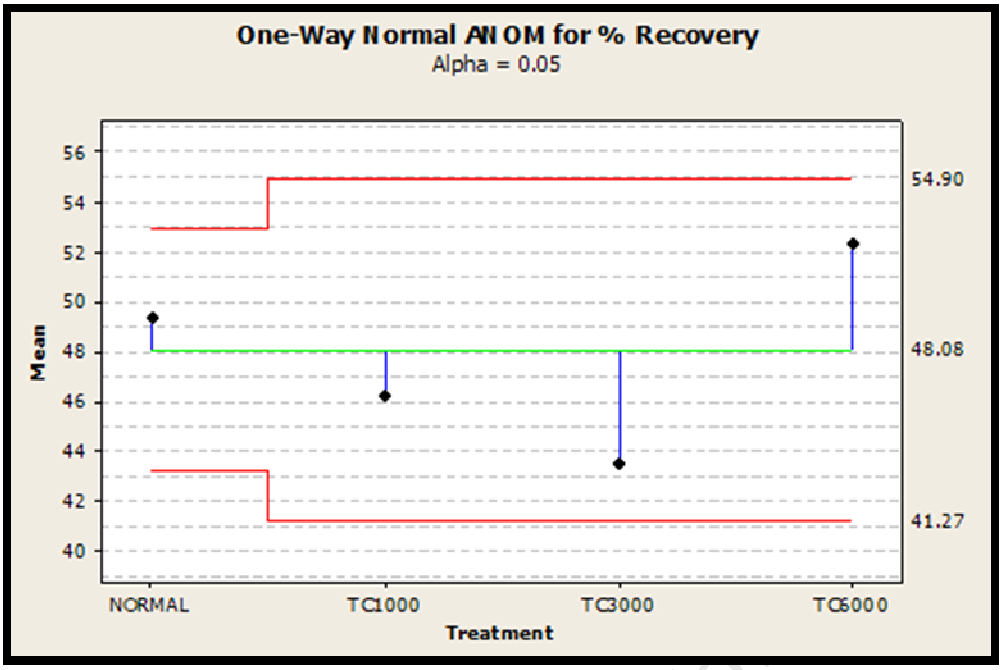

FIGURE 43: ANOVA ANALYSIS OF MEANS FOR RECOVERIES OF TC1000, TC3000 AND TC6000 SHOWING THERE IS NO SIGNIFICANT DIFFERENCE BETWEEN THE AVERAGE RECOVERIES BUT TC6000 YIELDED SLIGHTLY HIGHER RECOVERY THAN OTHER REAGENTS

Figure 43 shows that the mean recoveries for all TC reagents including the control test ("NORMAL") falls within the decision boundary limits; meaning there was no significant difference between all recoveries within 95% confidence.

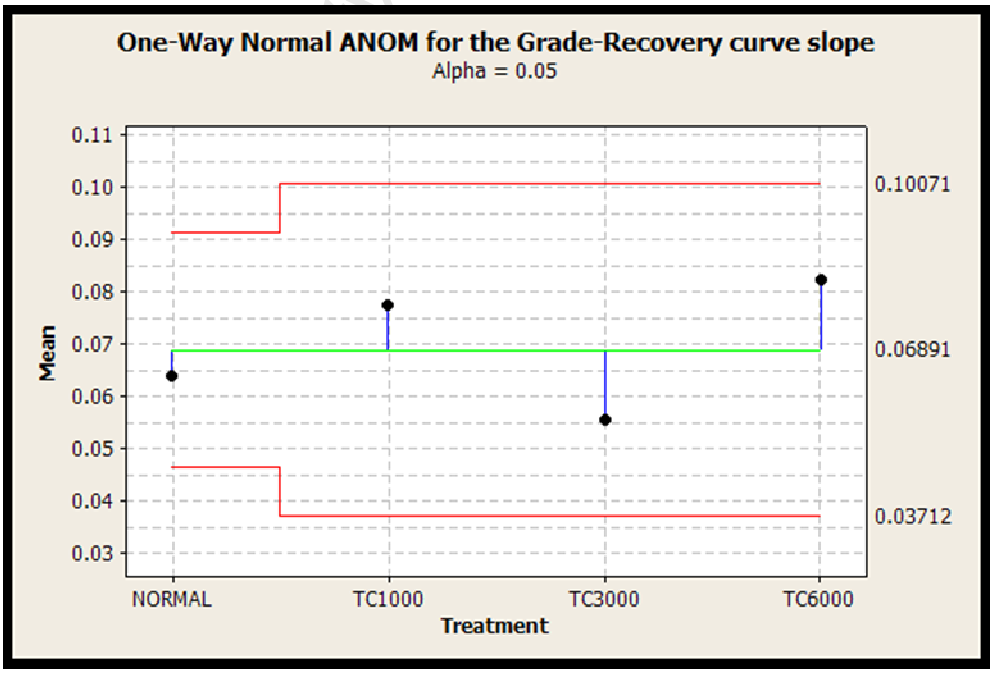

FIGURE 44: ANOVA ANALYSIS OF MEANS FOR THE SLOPES OF GRADE-RECOVERIES CURVE OF TC1000, TC3000 AND TC6000 SHOWING NO SIGNIFICANT DIFFERENCE BETWEEN THE REAGENTS BUT TC6000 AND TC1000 YIELDED SLIGHTLY HIGHER SLOPE

The TC reagents were found not to be as effective in improving recoveries of PPM material but rather slightly suited for improving selectivity especially TC6000 followed by TC1000 (Figure 44).

4.4.4. Fatty Acid based Co-Collectors

There are two categories of fatty acids, saturated and unsaturated fatty acids. Saturated fatty acids are of the general form, $C_nH_{2n+1}COOH$ whereas saturated fatty acids have a formula of form $C_nH_{2n-1}COOH$ (Bulatovic, 2007). The best known saturated fatty acids are stearic acid, $C_{17}H_{35}COOH$, and palmitic acid, $C_{15}H_{31}COOH$ (Bulatovic, 2007). Oleic acid $CH(CH_2)_7COOH$, is probably the most commonly used flotation unsaturated fatty acid reagent. Fatty acids are generally not very selective as flotation reagents but unsaturated fatty acids are much more selective than saturated fatty acids (Bulatovic, 2007).

In this study, the results of two commercial suppliers of fatty acid flotation reagents are presented. The reagent TC2000, which behaved more like unsaturated fatty acid, supplied by Tecrich Corporation in China, was treated as such. The other reagent supplied by Betachem, BC364, was expressly presented as a unsaturated fatty acid.

Figure 45 shows the flotation recovery curve of the two reagents (BC364 and TC2000), compared to the normal reagent suite case (“NORMAL”). The recovery obtained from TC2000 was slightly higher than the recovery obtained from BC364, however, TC2000 also gave the highest mass pull. Both fatty acids improved metallurgical recovery of the PGMs by over 35%.

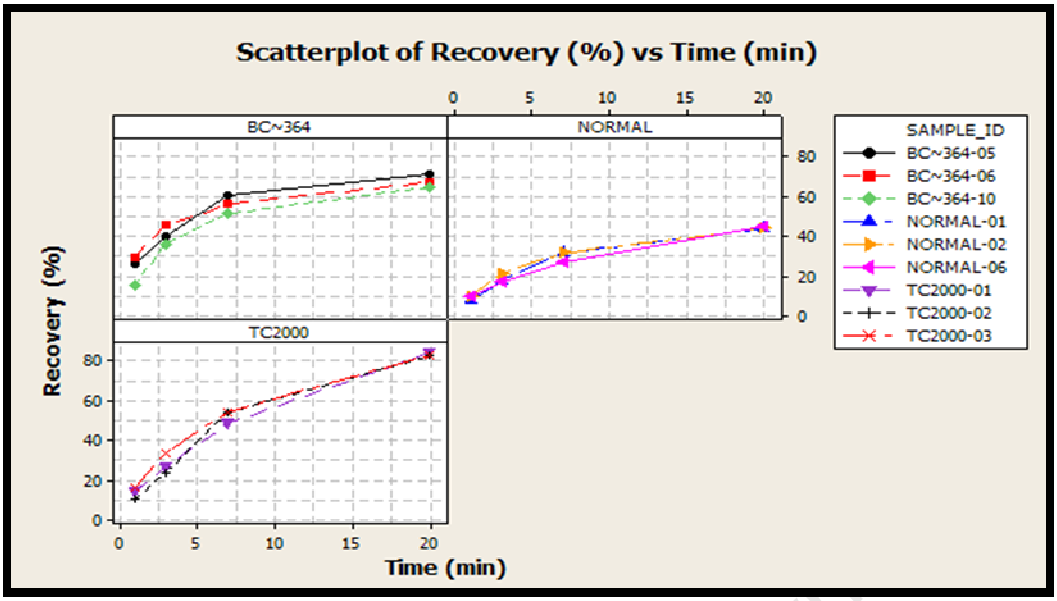

FIGURE 45: FLOTATION KINETICS CURVE WITH FOR TC2000 AND BC364 AGAINST NORMAL REAGENTS SHOWING HIGH RECOVERY COMPARED TO NORMAL REAGENTS

The grade-recovery curve (Figure 47) shows that these two reagents (TC2000 and BC364) produced high recovery at the expense of selectivity. The grade-recovery plots although shifted to the left, the slope of the curves had reduced considerably. These flatter curves of grade-recovery curve on both reagents indicate poor selectivity (Figure 46).

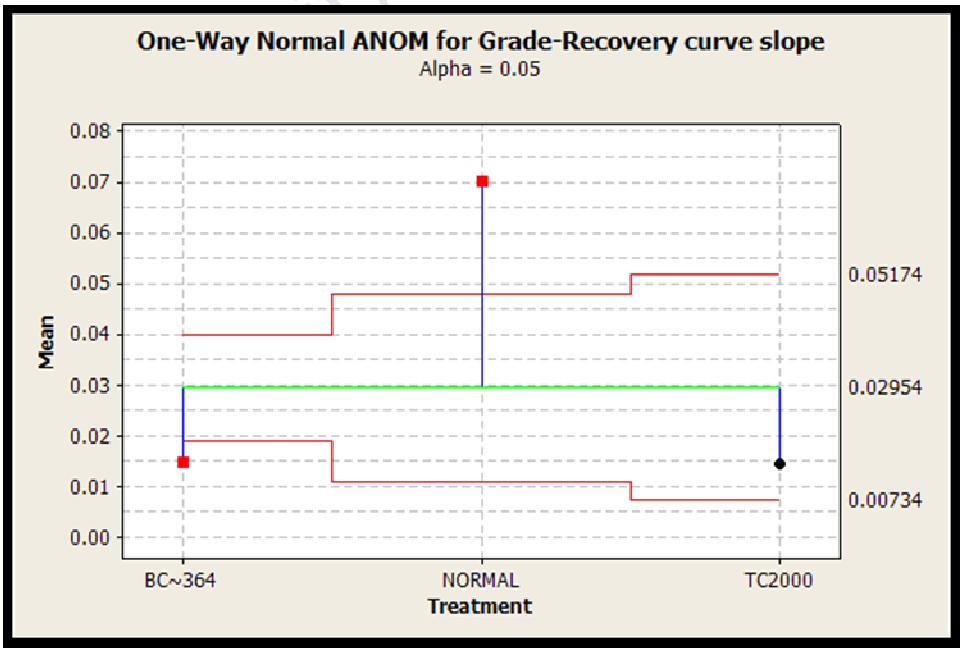

FIGURE 46: ANOVA ANALYSIS OF MEANS FOR THE SLOPES OF GRADE-RECOVERIES CURVE OF BC364, TC2000 AND "NORMAL" SHOWING SIGNIFICANT DIFFERENCE BETWEEN THE AVERAGE WITH BC364 AND TC2000 YIELDED SIGNIFICANTLY LOWER SLOPE (SELECTIVITY)

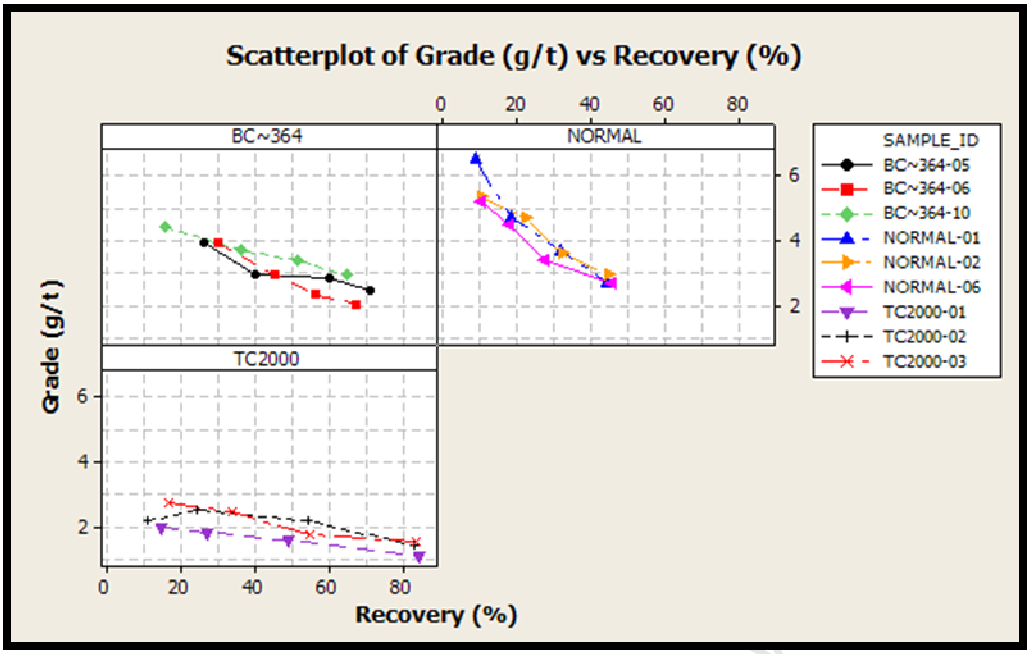

FIGURE 47: GRADE-RECOVERY CURVE OF TC2000 AND BC364 AGAINST THE NORMAL REAGENTS, SHOWING THE TWO REAGENTS HAVE CONSIDERABLY LOW SELECTIVITY (SLOPE OF THE CURVES IS MUCH FLATTER)

It would appear as if the fatty acids were able to activate particle surfaces indiscriminately. Based on the tests and analysis done for this study, it is not possible to deduce if these reagents acted solely as frothers or if a truly unselective flotation mechanism occurred.

It is important to note that fatty acids can also be classified as frothers because of the polar COOH group they possess. Frothers are known be heteropolar surface-active compounds containing a polar group (OH, COOH, C=O, OSO_2 and SO_2OH) and a hydrocarbon chain (Bulatovic, 2007).

Both TC2000 and BC-364 showed rather flat grade-recovery curves compared to the base case scenario, the "Normal" case. The mass pull (see also Figure 48), as observed during the test with both reagents, was significantly higher judging by the mass of concentrates achieved. Although recovery is important, the selectivity of the reagents is also important as it determine the final grades that can be achieved.

Fatty acids are normally favoured for flotation of minerals such as phosphates, lithium, silicates and rare earths. Fatty acids were found to be effective on ores that

has simple gangues, and free from both clay as well as slimes (Bulatovic, 2007).

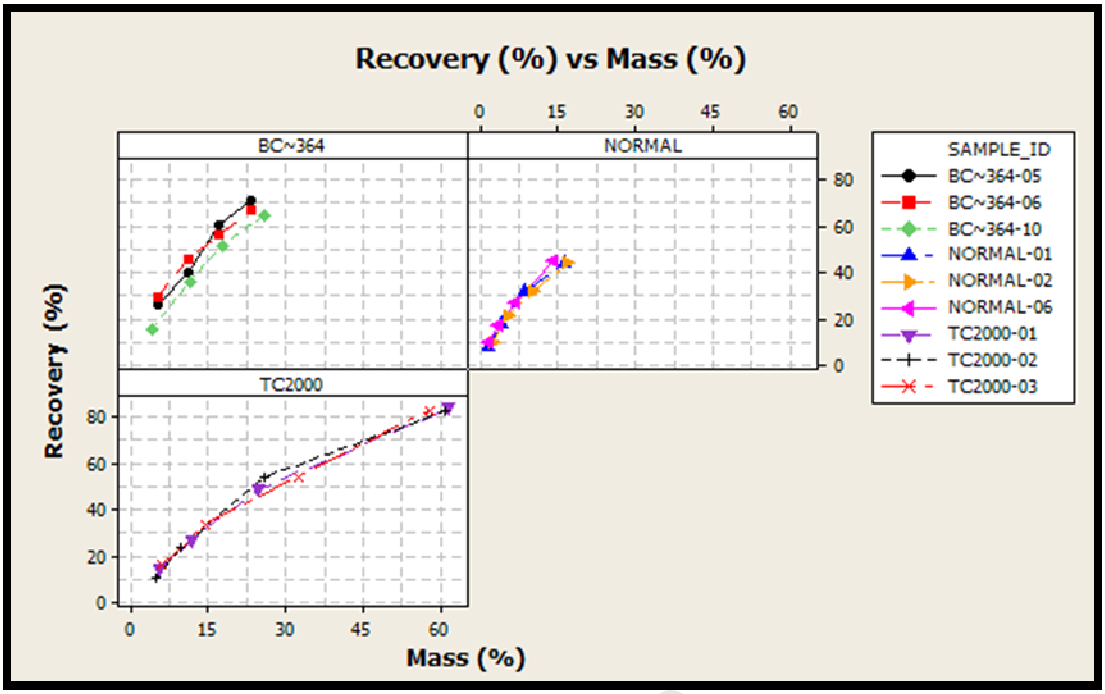

FIGURE 48: MASS PULL GRAPH FOR FATTY ACIDS (TC2000 AND BC364) VS. NORMAL REAGENT SUITE

In terms of the mass pull curves (Figure 48), the two fatty acids ("BC364 and TC2000) seem to have their curves shifted higher and toward the right hand side relative to the control test ("NORMAL"). The mass pull curves also confirm visual observations made during the test. It has indeed been noted in the literature (Hosseini, 2008) that the flotation of oxide minerals with conventional collectors, such as long chain alkyl amines and fatty acids, is not very selective because there are some similarities in the surface chemistry of the most oxidised valuable minerals and gangue minerals.

4.4.5. Combing Fatty Acids and Thionocarbamates

The results presented in sections 4.4.3 and 4.4.4 indicate improved selectivity of thionocarbamates and lack of selectivity of fatty acids, respectively. Irrespective of whether the fatty acids were merely acting as strong frothers or positively inducing hydrophobicity on the targeted mineral surface, thionocarbamates seemed to destabilise the froth somewhat. It was then decided to combine the apparent properties of these two collectors in order to manipulate the froth and hopefully improve both recovery and selectivity. BC364 was the chosen fatty acid and was tested in combination with the two thionocarbamates based collectors (TC1000 and

TC6000). The reason for the choice of the two thionocarbamates reagents was based on the fact that TC1000 and TC6000 showed improved selectivity (Figure 41).

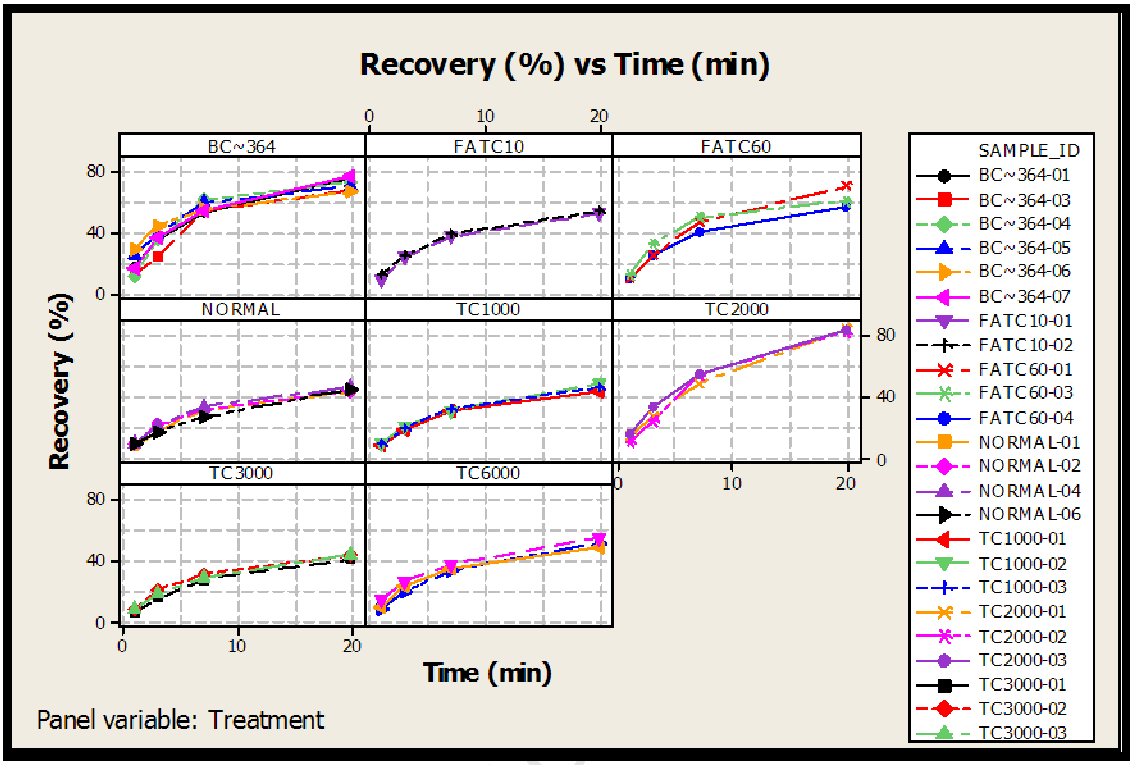

FIGURE 49: RECOVERY CURVES OF FATTY ACIDS BASED COLLECTOR AND THIONOCARBAMATE BASED CO-COLLECTORS, ALSO SHOWING THE RECOVERY CURVE THAT RESULTED FROM COMBINING BC364 WITH TC1000 AND TC6000 (FATC10 AND FATC60 RESPECTIVELY)

Figure 49 presents flotation recovery curves results of the two fatty acid (BC-364 and TC2000), the three thionocarbamates (TC1000, TC3000, and TC6000), and flotation recovery curve results of material treated with the combination of BC364 and TC1000 (FATC10) , as well as material treated with the combination of BC364 and TC6000, (FATC60) respectively.

Metallurgical performance in terms of recovery of the ore improved slightly when both fatty acids and thionocarbamate were added concurrently as co-collectors (Figure 49). The combination of TC6000 and BC364 (FAT60) improved recovery by about 5% against the control test ("NORMAL"). On the other hand the combination of TC1000 and BC364 (FAT10) marginally improved recovery (~3%).

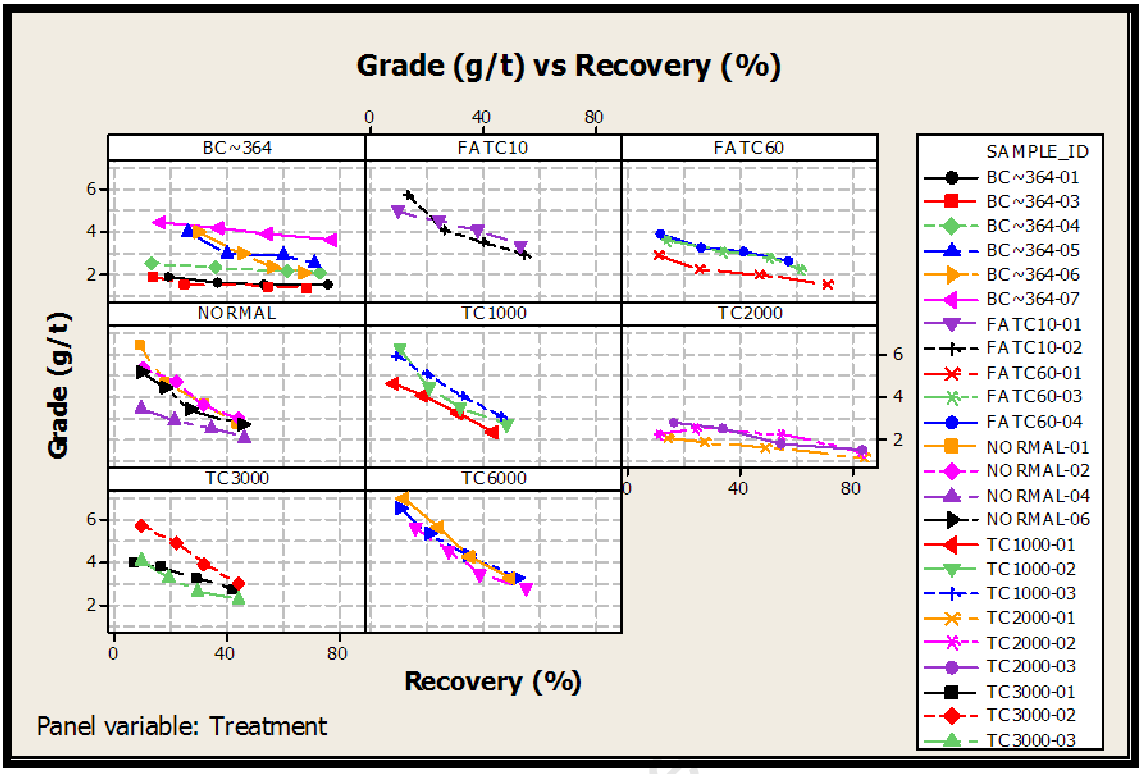

FIGURE 50: GRADE-RECOVERY CURVE OF BOTH FATTY ACIDS AND THIONOCARBAMATES BASED REAGENTS

Also in Figure 50, the grade recovery curve of the combination of BC364 and TC1000 is denoted as FAT10. And FATC60 denotes the combination of BC364 and TC6000. FAT10 seemed to maintain the selectivity compared to control test ("NORMAL") while FAT60 seemed to subdue selectivity somewhat. Accompanying fatty acids with thionocarbamates as co-collector seem to affect either the frothing power or the floating power of the fatty acids. The bubbles generated by BC364 alone as co-collector were sticky and elastic, while the bubbles generated by adding thionocarbamates based co-collector seemed more brittle.

The ANOVA analysis of mean shown in Figure 51, again highlight the high recovery induced by fatty acids based but with limited selectivity (Figure 50).

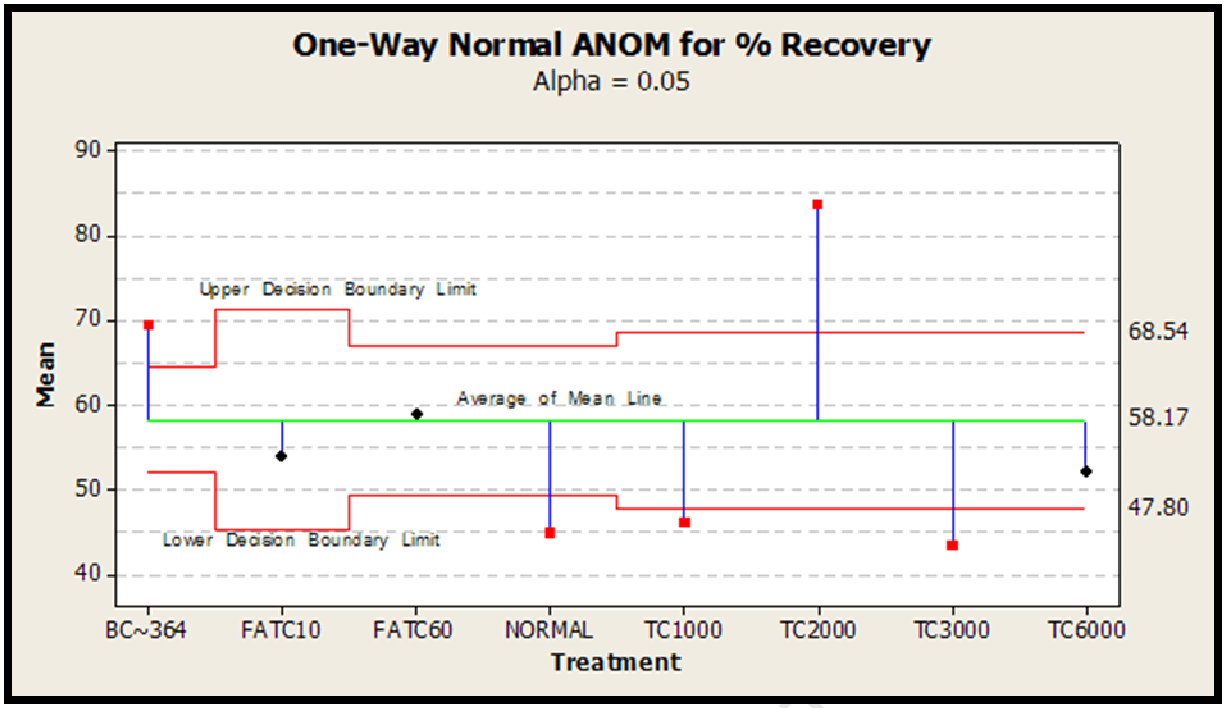

FIGURE 51: ANOVA ANALYSIS OF MEANS FOR RECOVERIES FOR FATTY ACID AND THIONOCARBAMATES BASED REAGENTS

However, within 95% confidence as bounded by the "Decision Boundary Limits" shown in Figure 51, there was no significant different between FATC10, FATC60 and TC6000, in terms of average recoveries. The control test ("NORMAL"), TC1000 and TC3000 were significantly lower than the case where fatty acid was used together with thionocarbamate (FATC10 and FATC60).

Comparing the recovery in the two cases where fatty acid based co-collector was added in conjunction with thionocarbamate; the combination of BC364 and TC6000 (FATC60) seemed more effective than the combination of BC-364 and TC1000 (FATC10).

5. CHAPTER FIVE: DISCUSSIONS

The aim of this chapter is to discuss the results in view of the three key questions raised (see section 2.5). The relationship and the effects of weathering with rock density profiles, as shown in Figure 24 will be discussed in terms of mineral mineralogy. This will then be followed by the discussion on the correlation of weathering profile with flotation recovery. Once the weathering profile on PPM ore body have been discussed; then the discussion will focus on evaluating the flotation strategies that were aimed at improving the floatability of PPM weathered ore (Chapter 4.4). The chapter will then conclude with a section that explores the implications of these results for PGM mining operations.

5.1. EFFECTS OF ALTERATION ON THE PPM ORE

Figure 24 showed the density profile with depth in each lithology, and compared the weathering extent relative to one another. The data shows a subtle but clear increase in density with increasing depth. This may be related to the fact that alteration of the parent rock or mineral inevitably result in a lighter density. The extent of weathering in each rock type can be deduced from the slope and the scatter of the data points (see Figure 24). The weathering of the primary silicates results in secondary silicates such as talc, chlorite and serpentine. These secondary silicate rocks were found to be present in PPM ore closer to the surface, as shown by Q-XRD analysis (Table 12). The extent of weathering varied according to the lithology, where pyroxenite and orthopyroxene type rocks proved to be more susceptible compared to plagioclase type rocks, such as anorthosite (compare Figure 24 B with other lithologies). This difference could be related to the way in which the basic silicate, SiO_4, tetrahedra of each rock type are combined and linked together (Klein and Hurlbut, 1993). Also, the type of cations within the silicate structure plays a role: Iron and magnesium are more mobile, and therefore such rocks get affected by alteration easily (Cawthorn and Lewis, 2009). The greatest density variation with depth was noticed for those lithologies which were rich in magnesium and iron silicates (olivine, orthopyroxene); namely the Merensky reef hanging wall pyroxenite, Upper Pseudo reef pegmatoidal pyroxenite and Lower Pseudo reef olivine pyroxenite.

The alterations were not only limited to silicate minerals, as SEM studies of the tails indicates (Figure 29). The base metal oxide observed in the tailings confirmed that alteration of PGM bearing minerals was most likely responsible for the poor recovery of PGEs. The absence of chalcopyrite in the PPM concentrate, and the finding of this mineral in the tailings, was also an indication of the presence of passivating layer around the sulphide mineral that prevented chalcopyrite to float.

5.2. Correlation of PGE Recovery with Depth

5.2.1. Weathering Profile

The results presented in section 4.2 show that the metallurgical performance of the ore improves with increasing depth. Section 4.1 presented the results of in situ rock density versus spatial mining depth, and showed the rock density improved with increasing depth.

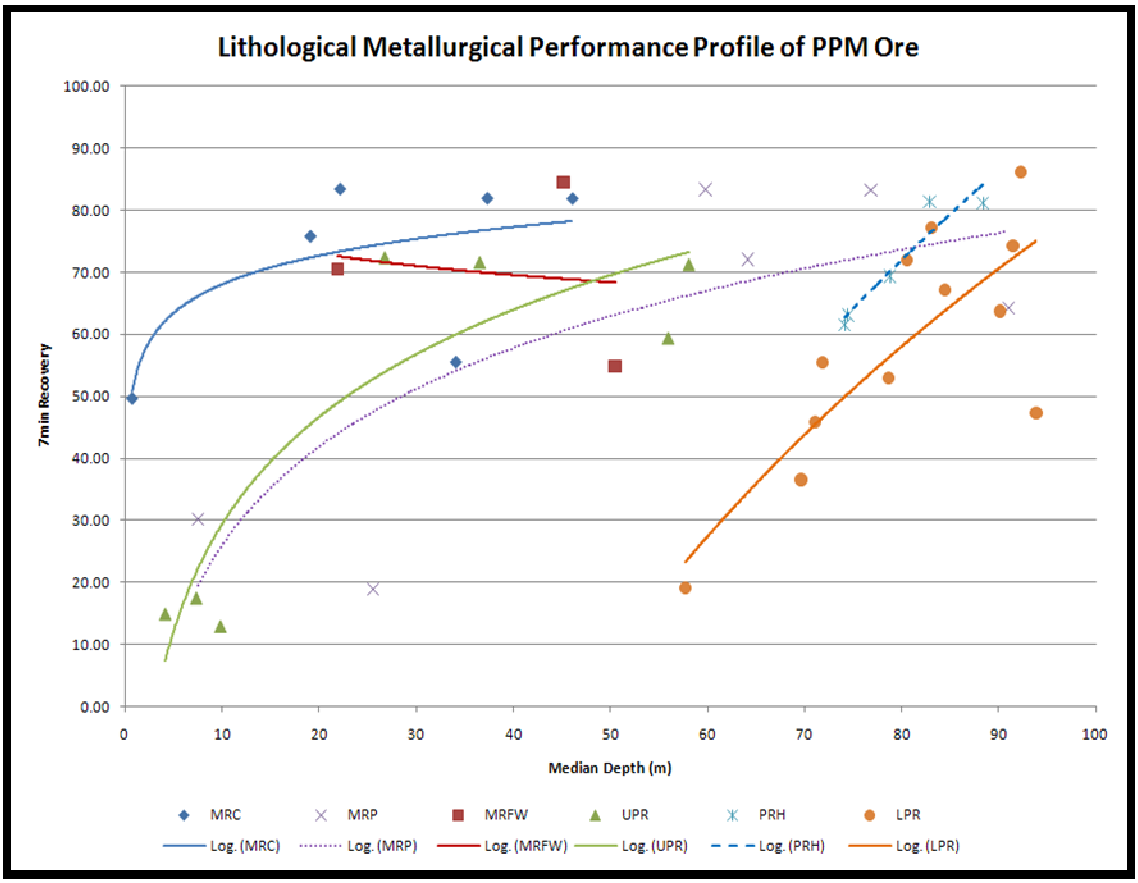

FIGURE 52: LITHOLOGICAL METALLURGICAL PERFORMANCE PROFILE BASED ON EXPLORATION DIAMOND DRILL CORE SAMPLES COMMISSIONED BY (HOLOHAN, 2009)

Since metallurgical test work presented in section 3.1.2 was based on percussion drilling samples, it was not possible to determine the weathering profile with respect to specific lithology. However, this work concurred with similar work previously commissioned by (Holohan, 2009) on diamond drill core samples, which also showed improved metallurgical performance with increasing depth (Figure 52). There is an exception with Merensky Footwall (Figure 52) that seems to have remained unaffected by weathering. The results from in situ density measurements (Figure 24 b) also showed that anorthosite (Merensky Footwall) competently maintained its density irrespective of the depth. The Lower pseudo and harzburgite seem to be most susceptible to weathering as seen by the steep increase in metallurgical performance toward the deep end of the ore body (Figure 52). However, the density measurements results indicated that the most friable is the upper pseudo reef which showed more erratic density (Figure 24 c).

Figure 52 also seems to support the observations made in section 4.2 (Figure 25, Figure 26, Figure 27, and Figure 28) where the in situ metallurgical performance profile was shown to increase with increasing depth. There is some work in the literature (Bartlett, 1998) that also shows that oxidation of the ore body diminishes with increasing depth. There might be some variation in terms of metallurgical performance resulting from lithological variation, but weathering seems to have significant impact on metallurgical performance.

5.2.2. MINERALOGY

The mineralogical work done indicated that the material from near the surface had significant amounts of weathered material, such as talc, enstatite, base metal oxides and chlorites. It was surprising to find no chalcopyrite in the final concentrate as measured by XRD. This was unexpected, since silicate ore normally contains chalcopyrite as a major PGM value mineral. However, a significant amount of chalcopyrite was detected in the plant tailings. There has been some report in literature that chalcopyrite does show some ambiguous behaviour; depending on the ore type (Bulatovic, 2007). It has been reported that chalcopyrite from porphyry copper ores floats usually with high recovery on any thiol collector. But the flotation of chalcopyrite from massive ore is heavily depended on collector type, the pH, the

modifier or depressant used. The literature (Bulatovic, 2007) further stated that chalcopyrite floatability can also become inhibited in the presence of pyrrhotite. Considering all these dynamics of chalcopyrite flotation, perhaps the type of ore at PPM and substantial amount of pyrrhotite in the ore can explain the peculiar observation of seemingly high amounts of chalcopyrite in the tailings as opposed to almost nothing in the final concentrate.

Pyrrhotite was detected as the most abundant sulphide mineral in the final Merensky concentrate based on XRD quantification (Table 12). The concentrate also contained a significant amount of iron oxides and chrome particles. However, the pyrrhotite that was detected in the final tails was fully liberated and the size range was about 25 micron. Although 25 micron is on the lower range for flotation, it should be floatable given sufficient residence time (Bryson, 2004).

Pentlandite particles were also detected, but the Ni content was close to 38 wt%, approximating violarite. Violarite is a form of mineral alteration and it is a slow floater. Most of the pentlandite detected in the final concentrate was occluded in enstatite. It is likely that these particles reported to the final concentrate due to the flotation of enstatite and not pentlandite. Although flotation of enstatite is not welcomed, the fact that it occluded most of pentlandite would make it difficult to discourage its flotation. This is probably one of the few cases where weathering caused gangue minerals to float, and because the gangue mineral occluded the targeted mineral, its flotation assisted the flotation of payable metals. However, this observation warrants an investigation into a fine milling to liberate occluded PGM bearing minerals, since most of the locked sulphides were found locked in enstatite.

The MLA revealed that the PGM bearing minerals found in the tailings were predominantly comprised of PGE-sulphides, with lesser amounts of PGE-alloys. There was also a significant amount of PGE tellurides. Some of the flotation performance was lost due to poor liberation of particle below 20 microns. However, a significant proportion (55.4 %) of the PGMs in the tailings was associated with liberated BMS (Table 13). And also, the PGMs in 20-40 µm size range were mostly liberated (72%,

by wt) (Figure 32), yet they were found in the tailings. The particle size range of 20-40 µm is known to float considerably well (Bryson, 2004).

Although a base metal sulphide search was not done on the MLA sample, it is possible that most of these base metal sulphides were chalcopyrite, violarite and pyrrhotite as seen from SEM work.

There were other issues highlighted by both the MLA and XRD/SEM work, the point of interest to this thesis was the fact that PGM bearing mineral alteration appeared to be responsible for poor metallurgical performance. It is likely that weathered gangue minerals competed for reagents and bubble attachment. The weathered gangue mineral such as talc, are naturally hydrophobic and so they float relatively easy (Martinovic et al., 2005). The XRD results (Table 12), showed that enstatite was the second most predominant gangue mineral found in the ore concentrate. Enstatite is similar to talc, because to some extent, it also floats naturally. Although enstatite is not naturally hydrophobic, it tends to float using two mechanisms: surface coating with talc, and activation by flotation reagents. The amount of hydrophobic gangue mineral in weathered ore competes with payable minerals for these flotation reagents.

Notwithstanding the presence of problematic altered gangue minerals, the presence of problematic PGM species was also noticed; namely PGE alloys and tellurides (See Appendix 6). The study by Shackleton et al. (2007) on the surface characteristics of Pt-Pd tellurides showed that the flotation performance of the Pt-Pd tellurides was more readily affected by oxidation. This may account for the presence of 10.1 % maslovite (Pt-Pd telluride) within the tailings samples. Furthermore, the PGE alloys (23.1% ferroplatinum, 16.0 % plumbopalladinite) are known to be problematic to flotation ((Penberthy et al., 2000), (Vermaak et al., 2007) and (Cabri, 2002)), and other PGM producers make use of magnetic separation to recover these minerals. There was no surface coatings of the PGM bearing minerals noted either on the SEM ore MLA analysis, suggesting that if there was any an oxidation coating or rims on the PGM minerals, they were sub-micron scale and needed to be studied at higher resolutions than is done in a standard SEM or MLA analysis. Indeed Jasieniak (2009)

and Jasieniak et. al. (2010) observed surface coating on these minerals using ToF-SIMS and XPS analysis techniques. However, there was some evidence of alteration of the BMS on the PPM silicate reef ore, in terms of an association with magnetite (observed in the microscopy investigations in this study and by Duarte et al. (2004)). There was also the presence of magnetic pyrrhotite, which is known to readily oxidise, and shows poor flotation performance (Becker, 2009). The presence of pyrite and altered pentlandite (violarite) as well as millerite also indicated the occurrence of weathering ((Duarte et al., 2004) and (Grobler, 2010)).

As mentioned earlier, research has shown that sulphide minerals such as pyrite or pyrrhotite, when exposed to moderate or high oxidizing potentials they eminently response poorly to flotation (Mendiratta, 2000). The iron-oxidation product that normally forms on the surface of weathered sulphide minerals renders the surface hydrophilic, thereby reducing its flotation performance.

The sulphide mineral surface is influenced by defects, size and reactivity, which tends to increase with impurities such as iron, therefore the sulphide mineral surface preparation for activation and the degree of pre-oxidation on the surface, does affect the available surface area for adsorption of flotation reagents. The literature review has also shown that oxidised iron-containing sulphide minerals, iron gets oxidised to form oxyhydroxides on the surface leaving the underlying surface sulphur rich ((Newell et al., 2006), (Vaughan et al., 1997)). This sulphur rich underlying surface was described by Buckley et al. (1985) as “metal deficient” or polysulphides. It was shown in (Newell et al., 2006) work that flotation recovery rapidly decreased with increasing oxidation. It has been reported that the gangue minerals even float preferentially over the sulphide mineral oxides (Lee et al., 2009).

5.3. STRATEGIES TO IMPROVE PGE FLOTATION PERFORMANCE

5.3.1. PRE-LEACH

There is an indication that pre-leaching can improve flotation recoveries by over 20% (Figure 35). In order to understand how pre-leaching enhances the flotation recovery of altered or weathered ores, it is important to understand the role of surface chemistry in flotation (Figure 15). In most cases, the oxidised sulphide minerals are

surrounded by a surface layer of ferric oxide/hydroxides that inhibits collector adsorption (Boulton, 2002). Pre-leaching aims to remove the oxide layer on the PGM bearing mineral surface and consequently expose a fresh sulphide surface underneath allowing effective collector adsorption. Excess acid addition during the pre-leach however, seems to have an additional pacifying effect resulting in poorer flotation recovery (Figure 34). Excess acid addition most likely causes digestion of the sulphide mineral surface beyond the oxide layer causing the freshly polished mineral surface to re-oxidise ((Luszczkiewicz and Chmielewski, 2008), (Arlauckas et al., 2004), (Mphela, 2010) and (Linter and Burstein, 1999)).

Although acid leaching showed improved recovery, the grade-recovery curve (Figure 35) showed poor grade which implied poor selectivity. There is no apparent reasons from the test work to explain the poorer selectivity. However, the answer likely lies with particle size distribution. With acid leaching, the particles size distribution was reduced as acid digest particle surface in accordance with shrinking core model ((England et al., 1999), (Cai et al., 2005) and (Mphela, 2010)). The reduced particle size would increase the surface area making easy for any particle to be entrained. It is also possible that the acid preferentially corroded the sulphide mineral along the grain boundary, detaching PGE minerals from the sulphide minerals. It has been previously noted that the PPM PGM particles are mostly in the sub-microns (particle size less than 2 microns) making them too small for optimal flotation (Mintek, 2004b).

5.3.2. HYDROXAMATES

The results presented in this study, section 4.4.2 (Figure 36, Figure 37, Figure 38 and Figure 39) showed that the hydroxamate co-collector improved recovery by approximately 10%. This means that it aided the recovery of the more oxidised particles that could not be recovered by xanthate alone. Hydroxamates are classified as chelating collectors that are largely used as oxide collectors and are known to form complexes with almost all metals (Assis et al., 1996). There is however, little agreement in the literature on the mechanism by which the hydroxamate induces hydrophobicity. Recent vibrational spectroscopy and X-ray photoelectron spectroscopy (XPS) studies have shown the existence of copper n-

octanohydroxamate layer on copper oxide and copper carbonate hydroxide (Hope et al., 2010). Some believe it is the adsorption density that determines the mineral-hydroxamate complex stability (Lee et al., 2009).

The performance of hydroxamates has been linked to the carbon-chain length. Longer carbon chain ($>C_9$) hydroxamate appear to show reduced flotation performance. N-octyl hydroxamate collectors (AM28) has been used successfully to recover the oxide sulphide mineral component in mixed copper sulphide/oxide blends without reducing the recovery of the sulphide minerals (Lee et al., 2009). There have been other studies that have shown that AM28 had a strong affinity for iron as well, and was used to float goethite and hematite ((Fuerstenau et al., 1970) and (Fuerstenau et al., 1968)). The PGE at PPM are associated to both iron minerals and copper mineral, and AM28 would be suited for this type of ore.

It has been argued in the literature that the selectivity of sulphide mineral flotation with hydroxamates depends on the balance between at least two characteristics: sulphide mineral solubility and the stability constant of the complex hydroxamate/lattice cation (Assis et al., 1996). This view also was in agreement with the study of Fuerstenau et al. (1970) which showed better recovery and selectivity were achieved at longer conditioning times and higher reagent dosage. The reagent dosage screening tests that were done for this study also showed increasing recovery with increasing dosage (see Appendix 7.3)

Although most literature suggest hydroxamate based collectors should not be used on fine material, the finer grind (90% passing 75 microns) in Figure 36 shows that AM28 was still able to improve the recoveries. In terms of selectivity, AM28 seemed to drop somewhat compared to the control case (Figure 37). In view of the fact that AM28 has been reported to have strong affinity towards iron and copper ((Fuerstenau et al., 1968), (Fuerstenau et al., 1970), (Hope et al., 2010), (Lee et al., 2009) and (Assis et al., 1996)), it is possible that the recovery dropped because of the increased surface area which required even more reagent.

5.3.3. THIONOCARBAMATES

The commercial supplier (Beijing Tecrich Development Co., Ltd) of thionocarbamates (TC) claimed that these reagents have a strong rational molecular structure, with the moderate positive coordinate bond intensity and reverse coordinate that help them to bond with BMS (Huang, 2010). Beijing Tecrich Development Corporation claimed that TC reagents have shown stronger collection power, better selectivity and less dosage requirements on copper ores. These attributes were accredited to the modification of thionocarbamates by adding a bond they termed "dXY -ð*" in the molecule. In comparison with traditional reagents, TC-series were claimed to be more suitable to the flotation of Cu-Zn,Pb-Zn, Cu-Pb-Zn, Cu-S, Zn-S, Au and Ag ores as well as the recovery of associated precious metals, Au, Ag, Pt, Pd, Mo . Although there were three thionocarbamates based reagents tested (TC1000, TC3000, and TC6000), the results presented in section 4.4.3 suggests that only two of these reagents, TC1000 and TC6000, need to be considered further. TC3000 showed almost no metallurgical response with the ore tested. The reason for this is not known; potentially this was caused by the interaction between the thionocarbamate molecule and the molecule of the secondary xanthate molecule included. On the other hand, TC1000 and TC6000 showed some improvements especially in terms of selectivity (Figure 40, Figure 41, and Figure 43). TC1000 was ~100% modified thionocarbamates while TC6000 also contained xanthogen formate.

The literature has indicated that thionocarbamate collectors could be used to improve the separation of copper activated sphalerite from pyrite or separation of chalcopyrite from pyrite. Thionocarbamate was seen as copper specific collector (Boulton, 2002). Although thionocarbamates have been used as xanthate replacement, no literature was found where thionocarbamates are used in tandem with xanthates. One of the early thionocarbamate that was patented was a dialkyl thionocarbamate collector containing 0-isopropyl-N-ethyl thionocarbamate (IPETC) as the major component. This collector proved to be selective for copper sulfide flotation, particularly against gangue iron sulphides (Fairthorne, 1996).

TC1000 appeared to have improved selectivity (Figure 41) with marginal improvement on recovery. Since TC1000 contained only thionocarbamates, it is

possible the selectivity was improved by preferential collection of copper sulphide mineral over pyrite, in line with the argument advanced by Boulton (2002) and Fairthorne (1996). However, this does not explain the role of xanthate which was also present at the time, unless thionocarbamates also discourages activity of sulphide mineral gangues such as pyrite.

TC6000 on the other hand seemed to have preferred to improve recovery over selectivity (Figure 41). Even so, the selectivity was marginally affected. Perhaps what made TC6000 to advance recovery compared to TC1000 was the presence of xanthogen formate molecules. One would image that xanthogen readily forms dixanthogen, a molecule that is accredited to pyrite flotation (He, 2006). Perhaps the improved recovery was also due to an increased amount of xanthogen that readily floated more of iron sulphide minerals.

Unlike hydroxamate, thionocarbamates are not known to be oxide collectors. The marginal improvement in recovery was probably due to improved collection of copper sulphides as opposed to oxide collection. One interesting point would be to investigate the effect of copper activation prior to thionocarbamates collection.

5.3.4. Fatty Acids

The results presented in Figure 45 and Figure 47 shows both the metallurgical recovery curve and grade-recovery curve of the two fatty acids (TC2000 and BC364) investigated relative to the normal reagent suite. This study was confined only to metallurgical performance; hence no attempt was made to investigate the flotation mechanism. The high recovery of TC2000 and even BC364 was accompanied by high mass pull, as seen on Figure 48. Because of high mass pull associated with high recovery, it is possible that both the recovery and the mass pull were largely influenced by the stability of the froth, which fatty acids are known to induce. Fatty acid also have the -OH group that frothers typically have and this makes them self-frothing. Experience has shown that excessive froth tends to reduce selectivity by allowing entrainment as oppose to true flotation.

Although there was a clear low selectivity on these fatty acids (Figure 47), over 80% of the PGMs were still recovered. Based on the tests done in this study, it not

possible to determine if the PGM's were recovered by entrainment. However, it is possible that the fatty acids managed to activate PGM bearing minerals and a host of other non-PGM bearing minerals, coupled with entrainment that was caused by a rather more stable froth bed.

5.4. Implications For Mineral Processing

The mineral processing implications that will be discuss in this section only covers the evaluated treatment strategies, but does not includes the implications in so far as selective mining of altered ore is concerned.

5.4.1. Use of Pre-Leaching prior to flotation

The recovery curves shown in Figure 35 suggest that pre-leaching may be a viable option at PPM because of improved recovery with the same selectivity. However, in order to utilise this strategy; the mine would require specialised reactor tanks and cells that are able to withstand the acidic conditions. Most flotation plants are built from carbon steel material without any rubber lining that could protect equipment from acid corrosion. A further neutralisation process of the pre-treated material with a base reagent such as caustic soda to raise the pH would also be required. The additional costs, associated with these add-ons, together with the additional capital costs could probably discourage the mines from the onset. Although, most PGE mining operations experience some difficulties with oxidised ore, but majority of these ores are sulphides. The amounts of oxidised ore that are encountered are probably not in sufficient quantities to warrant contraction of the plant with exotic material, such as stainless steel.

The use of sulphuric acid may not have been an ideal solution for PGM bearing mineral surface etching, because of its severe corrosive and oxidising properties, and investigation of other forms of acids for flotation pre-leaching may be necessary. Perhaps carbon dioxide can provide a milder form of acid etching. As discussed in literature review section 2.3.2, carbon dioxide was shown to have depassivation effect on oxidised pyrrhotite surface. Mphela (2010) showed that carbon dioxide restores the polarity resistance to values similar to polished pyrrhotite surface. This may suggest that carbon dioxide dissociates into carbonic acid which may be

digesting hydroxyl groups on the mineral surface. For most plant sulphuric acid pre-leach may not be practical but carbon dioxide may offer similar benefits as sulphuric acid but at milder form and easier in terms of handling.

Perhaps carbon dioxide can offer an opportunity. As discussed in the literature review section 2.3.2, carbon dioxide was shown to have depassivation effect on oxidised pyrrhotite surface. Mphela (2010) showed that carbon dioxide restores the polarity resistance to values similar to a polished pyrrhotite surface. This may suggest that carbon dioxide dissociates into carbonic acid which may be digesting hydroxyl groups on the mineral surface. For most plant sulphuric acid pre-leach may not be practical but carbon dioxide may offer similar benefits as sulphuric acid pre-leaching.

The acid consumption with sulphuric acid was probably not only for sulphide mineral oxide layer digestion, but the presence of other acid consuming mineral such as carbonates and dolomites made use of the acid as well. It is not easy to determine acid demand for any particular ore before hand, but trial and error method can be utilised to quantify the acid demand for a particular ore.

5.4.2. Use of Co-Collectors

The use of co-collectors offers another opportunity for PGM operations. In most base metal operation, collector selection is informed by the need to suppress gangue sulphide minerals like pyrite and pyrrhotite. However, in PGM mineral processing plants, the flotation of iron mineral is desirable, as these iron mineral also contain PGEs. Unlike the major infrastructural changes that would be required to implement acid pre-leaching at flotation plants, the addition of co-collectors would probably only require the consideration of sufficient residence time.

Hydroxamate Co-Collectors

The results from this study have shown the potential impact which the hydroxymate co-collector offers in terms of improved recovery on altered or oxidised PGM ores. These reagents are already used industrially during the processing of copper oxide ores and are attractive due to their affinity towards both copper and iron minerals. In the PGM context, the PGEs are known to be associated with several base metal

sulphide minerals (e.g. tetraferroplatinum [PtFe] and tulameenite [Pt_2CuFe]) and so by association, this may result in improved PGE recovery. However, further mineralogical analyses would be needed to ensure that the hydroxymate collectors do not cause increased pyrite recovery, where there is known to be little PGE association (Dare and Barnes, 2010). A further consideration associated with the use of the hydroxamate co-collectors is that, the success of hydroxamate may be related to conditioning time (section 5.3.2). It appears to require long conditioning time which suggests poor kinetics related to sulphide mineral solubility ((Pradip, 1987), (Pradip and Fuerstenau, 1984), (Assis et al., 1996) and (Fuerstenau et al., 1970)).

THIONOCARBAMATES

Thionocarbamates do seem to have a place in PGM flotation plants. However, their application is not necessarily to target oxidised ore. But because of their strong affinity towards copper sulphide ores, these reagents will most likely improve selectivity and therefore increase concentrate grades. In the case of PPM ore where there has been some indication that chalcopyrite remained largely in the tailings, thionocarbamates could be used as a co-collector.

FATTY ACIDS

Although the use of the fatty acid co-collectors has shown significant improvements (TC2000 and BC364, see Figure 51) in terms of PGE recovery, the poor selectivity exhibited is not in their favour. Low selectivity with large mass pull, results in low concentrate grade which is not sealable. The amount of mass pull (almost 50% see appendix 7.5) will not be acceptable due to high reagent consumption and limited cleaners capacity. The results shown in Figure 51 and Figure 52 indicate that a combination of the fatty acids with the thionocarbamates show some promise and should be investigated further.

6. CHAPTER SIX: CONCLUSIONS AND RECOMMENDATIONS

Based on the observations of the results presented in chapter 4 and the discussion presented in chapter 5, the following conclusions and recommendations are made.

6.1. CONCLUSIONS

The motivation for the work presented in this thesis emanated from the nature of the poor metallurgical performance obtained during the flotation process at the PPM plant. At PPM, the ore body outcrops within the project property, which is ideal for open pit mining. However, it soon became clear that the ore extracted from near the surface showed poor flotation performance with erratic recoveries (typically less than 35%; Figure 14).

The aim of the thesis was to address the following three key questions:

1. How does the PPM ore body changes with depth?
2. Can the loss of PGE recovery be correlated with depth and why?
3. How can flotation performance of altered PPM ore be improved?

The first key question was addressed using density profiling of in situ material from the PPM mine property, where a small, yet clear decrease in density occurred with decreasing depth. The decrease in density was attributed to the formation of secondary silicate minerals such as talc, chlorite and serpentine (Table 12). The extent of weathering varied according to the lithology, where rocks rich in the Mg-Fe silicates (e.g. pyroxenite) proved to be more susceptible to alteration compared to plagioclase type rocks like anorthosite (see Figure 24 B).

The second key question was addressed by a series of flotation recovery profile tests in conjunction with various mineralogical analyses. The results showed poor recovery from ore derived near surface that gradually increased as the transition to fresh ore occurred at ~40 m depth across the mine property (Figure 25, Figure 26, Figure 27, and Figure 28). The results showed a strong correlation between depth and the recovery.

Mineralogical investigation of the flotation feed, tailings and concentrate of the material mined near the surface showed a significant amount of fully liberated PGMs (54.3%) that failed to float. Also, the PGMs in the particles size range of 20-40 µm (mostly liberated

(72%, by wt), (Figure 32) were found in the tailings. The tailings also contained PGM alloys and tellurides which are known to be susceptible to oxidation. There was about 10.1% of maslovite, 23.1% of ferroplatinum, and 16.0 % plumbopalladinite (Table 22, Appendix 6). Although there were no surface coatings noted on the PGMs by SEM and MLA analysis, it is possible that any oxidation coatings or rims on the PGM particles could have been in the sub-micron scale that needed to be studied at higher resolutions. However, there was some evidence of oxidation of the BMS in the form of copper oxide and zinc oxide noticed through SEM investigation (Figure 29). The presence of violarite and millerite was another indication for alteration of BMS.

In order to address the third key question, selected flotation strategies were evaluated. Acid pre-leaching with sulphuric acid showed positive signs in terms of recovery (20% improvement, Figure 35 D), but the selectivity was not considered satisfactory (see grade recovery curve Figure 35 B). The acid is thought to digest the oxidised layer on the PGM bearing mineral surface, thereby exposing a fresh mineral surface for collector-mineral interactions to take place unimpeded. However, the acid may have activated gangue minerals as well, which resulted in low selectivity. The need for additional reagents (sulphuric acid, neutralising reagents) over and above normal flotation reagents, and the need to modify the plant infrastructure such that it can withstand the corrosive conditions is likely to discourage the implementation of this strategy on a full scale. Carbon dioxide, apart from assisting non-oxidative leaching by restricting oxygen absorption into the slurry, it can also provide a milder form of acid etching (see section 2.3.2), by dissociating into carbonic acid which has a de-passivating effect on oxidised sulphide mineral surface.

The use of co-collectors, on the other hand, does not require infrastructural changes and the only consideration is the necessary residence time to allow for sufficient collector adsorption during conditioning. Co-collectors are considered even more attractive due to their ability to recover material that would otherwise not be collected by traditional xanthate collectors without affecting the collecting ability of the xanthate. In terms of the co-collectors evaluated, the hydroxamate based collector showed the best metallurgical performance (15% improvement in recovery and good grades, Figure 38). The success of the hydroxamates is borne out of their affinity towards copper and iron

minerals. Considering that PPM ore contains appreciable amount of PGMs and PGM alloys, e.g. ferroplatinum, associated with these minerals (Figure 6), the hydroxamate collector opens new opportunities. In this context it should be noted that the conditioning time used in this study for the hydroxamate may not have been optimal, and extended conditioning times could in fact result in further recovery improvements.

The thionocarbamate co-collectors were found to improve selectivity but with marginal improvement on recovery (Figure 43). The reason for this was attributed to their affinity towards copper as opposed to iron minerals. PGMs at PPM are found mostly associated with iron minerals. The use of thionocarbamates can however, be used to target the poor chalcopyrite recoveries that was noted in the PPM ore.

The fatty acid co-collectors on the other hand showed the greatest improvements in recovery (~30%), confirming their affinity toward oxidised minerals. However, the selectivity was very poor and with high mass recoveries (~50%). It was unclear whether this reagent showed improved recoveries due to its ability to target the more oxidised minerals or due to its natural frothability that acted as a strong froth stabiliser, thereby decreasing concentrate grade by entrainment. The use of fatty acids in combination with thionocarbamates appeared to have noticeable improvement on both selectivity and recovery. However, the improvements noticed were still not as much as the improvements obtained from the use of hydroxamate based co-collector.

The study has hence shown that the ore at PPM is largely oxidised near the surface and material mined near-surface should be expected to show poor metallurgical performance. However, as mining depth increases, the recoveries will improve because the ore will slowly transitions towards fresh sulphides. Beyond the depth of 40 m below surface, the recoveries should be expected to approach the maximum obtainable recoveries. This is because both, the flotation performance profiling and density profiling, showed that the PPM ore was largely fresh below 40 m. Understanding the effect of alteration on the geology and mineralogy of the ore can assist in better understanding the mechanisms controlling flotation performance. The results from the flotation strategies evaluation show the existence of the possibility to improve flotation performance of PPM oxidised ore. The flotation performance improvement can be

achieved by either polishing the oxidised surface layer of the PGM bearing mineral with acid, or by using some form of a co-collector that has a strong affinity toward base metal ions present in the altered or oxidised targeted mineral.

6.2. RECOMMENDATIONS

Based on the findings and conclusions of this thesis, the following recommendations are made:

- Further investigation into PPM ore mineralogy in order to gain an understanding of the gangue mineralogy with respect to the effects of weathering. The question that should probably be answered is whether alteration has caused the formation of phyllosilicates minerals that are known to be rheologically complex and whether weathering has also caused the formation of more naturally floatable gangue.

- The work that was conducted in this study could not positively identify the presence of surface coating, in the form of oxide layer or other passivating layers. It is therefore recommended to conduct further mineralogical investigations to determine the nature of weathered valuable mineral surfaces. Perhaps weathered PGM bearing mineral surface can be studied with other techniques such as ToF-SIMS, and XPS.

- Pyrrhotite mineral has been shown to be a significant BMS mineral at PPM but it has not been established to what extend does pyrrhotite host the PGE minerals. It is therefore recommended that a study be conducted to quantify relative PGM association with pyrrhotite as well as other BMS. Furthermore, the compositional variation of pyrrhotite on the ore body in terms of magnetic and non-magnetic phases of pyrrhotite will need to be investigated.

- Since this study was limited to evaluating flotation strategies that could possibly improve the metallurgical performance of weathered ore, the results obtained from hydroxamate based collector will require further investigation. In particular, more attention will be required on the conditioning time and dosage rate. Also a clearer understanding on adsorption mechanism and the type of PGM bearing particle gets targeted by hydroxamate.

- Although the results obtained from acid pre-leach were promising, the need for additional reagents (both sulphuric acid, and neutralising reagents) over and above normal flotation reagents, and infrastructural adjustments required to withstand the corrosive conditions, would make adoption of this technology difficult. However, it is recommended that carbon dioxide be investigated as a form of milder acid that can be used to polish oxidised PGM bearing mineral surface.

- The other technique which was not considered in this study but has previously yielded positive results is sulphidisation. It is therefore recommended that this technique be investigated for PPM weathered ore. Sulphidisation, if applied correctly, has been shown to successfully re-activate oxidised sulphide minerals surface.

REFERENCES

1. Adam, K., Natarajan, K. A. and Iwasaki, I. (1984) Grinding Media wear and its effect on the flotation of sulphide minerals. *International Journal of Mineral Processing* **12,** 39-54.

2. Ansari, A. and Pawlik, M. (2007) Floatability of chalcopyrite and molybdenite in the presence of lignosulfonates. Part I. Adsorption studies. *Minerals Engineering* **20,** 608.

3. Arlauckas, S. M., Hurowitz, J. A., Tosca, N. J. and McLennan, S. M. (2004) Iron oxide weathering in sulphuric acid: Implications for Mars. *Lunar and Planetary Science* **XXXV,** 1868.

4. Armitage, P. E. B., McDonald, I., Edward, J. S. and Manby, G. M. (2002) Platinum group element mineralisation in the Platreef and calc-silicate footwall at Sandsloot, Potgietersrus District, South Africa. *Transactions of the Institute of Mining and Metallurgy* **111,** B36-B45.

5. Assis, S. M., Montenegro, L. C. M. and Peres, A. E. C. (1996) Utilisation of hydroxamate in minerals froth flotation. *Minerals Engineering* **9,** 103-114.

6. Ballhaus, C. and Ryan, C. G. (1995) Platinum-group elements in the Merensky reef. I. PGE in solid solution in base metal sulfides and the down-temperature equilibration history of Merensky ores. *Contribution to Mineralogy and Petrology* **122,** 241-251.

7. Baltrusaitis, J., Schuttlefield, J. D., Zeitler, E., Jensen, J. and Grassian, V. H. (2007) Surface reaction of carbon dioxide at the adsorbed water oxide interface. *The Journal of Physical Chemistry C* **111,** 14870-14880.

8. Baltrusaitis, J., Schuttlefield, J. D., Zeitler, E. and Grassian, V. H. (2010) Carbon dioxide adsorption on oxide nanoparticles, pp. 1-43.

9. Baltrusaitis, J. and Grassian, V. H. (2005) Surface reactions of carbon dioxide at the adsorbed water-iron interface. *The Journal of Physical Chemistry B* **109,** 12227-12230.

10. Bartlett, R. W. (1998) Solution Mining. In *Leaching and Fluid Recovery of Materials*, Gorden and Breach Science Publishers.

11. Becker, M. (2009) The mineralogy and crystallography of pyrrhotite from selected nickel and PGE ore deposit and its effect on flotation performance. In *Department of Materials Science and Metallurgical Engineering*-239, Thesis, University of Pretoria, Pretoria.

12. Becker, M., Harris, P. J., Wiese, J. G. and Bradshaw, D. J. (2006) The use of quantitative mineralogical data to interpret the behaviour of gangue minerals in the flotation of Merensky reef ore. In MEI Automated Mineralogy, MeI, Brisbane.

13. Belzile, N., Chen, Y., Cai, M. and Li, Y. (2004) A review of pyrrhotite oxidation. *Journal of Geochemical Exploration* **84,** 65-76.

14. Boulton, A. B. (2002) Improving sulphide mineral flotation selectivity against iron sulphide gangue. In *Ian Wark Research Institute*, University of South Australia.

15. Bradshaw, D. J., Cruywagen, J. J. and O'connor, C. T. (1995) Thermochemical measurements of the surface reaction of sodium cyclohexyl-dithionocarbamate, potassium n-butyl xanthate and a thiol mixture with pyrite. *Minerals Engineering* **8,** 1175-1184.

16. Brough, C. (2008) An investigation into the process mineralogy of merensky reef at northam platinum limited. In *Chemical Engineering*, University of Cape Town, Cape Town.

17. Bryson, M. A. W. (2004) Mineralogical control of minerals processing circuit design. *The Journal of The Southern African Institute of Mining and Metallurgy***,** 307-310.

18. Buckley, A. N. (1987) The oxidation of cobaltite. *Australian Journal of Chemistry* **40,** 231-239.

19. Buckley, A. N., Hamilton, I. C. and Woods, R. (1985) Investitgation of the surface oxidation of sulphide minerals by linear potential sweep voltammetry and X-ray photoelectron spectroscopy. In *In: Forssberg, K.S.E. (Ed.), Flotation of Sulfide Minerals*, pp. 41-60, Elsevier, Amsterdam.

20. Buckley, A. N. and Woods, R. (1985) An X-ray photoelectron spectroscopic study of oxidised pyrrhotite surface. *I. Exposure to air. Applied Surface Science 2***,** 280-287.

21. Bulatovic, S. M. (2007) Handbook of flotation reagents. In *Flotation of Sulphide Ores, Vol. 1*, (ed. S. M. Bulatovic)-443, Elsevier, Oxford.

22. Cabri, L. J. (2002) The platinum-group minerals. In *The Geology, Geochemistry, Mineralogy and Mineral Beneficiation of Platinum-Group Elements, Vol. 54*, (ed. L. J. Cabri), pp. 13-129, CIM.

23. Cai, M., Dang, Z., Chen, Y. and Belzile, N. (2005) The passivation of pyrrhotite by surface coating. *Chemosphere***,** 569-667.

24. Cawthorn, R., Christopher, A. L., Schouwstra, R. P. and Mellowship, P. (2002) Relationship between PGE and PGM in the Bushveld. *The Canadian Mineralogist* **40,** 311-328.

25. Cawthorn, R. G. and Lewis, A. D. (2009) Origin of Anorthosite and Magnetite layers in the bushveld complex, contrained by major element composition of plagioclase. *Journal of Petrology* **50,** 1607-1637.

26. Chanturiya, V., Makarov, V., Forsling, W., Makarov, D., Vasil'eva, T., Trofimenko, T. and Kuznetsov, V. (2004) The effect of crystallochemical peculiarities of nickel sulphide minerals on flotation of copper-nickel ore. *International Journal of Mineral Processing* **74,** 289-301.

27. Chesworth, W. (2008) Encyclopedia of soil science, pp. 363 - 369-809, Springer, New York.

28. Chetty, D., Gryffenberg, L., Lekgetho, T. B. and Molebale, I. J. (2009) Automated SEM study of PGM distribution across a UG2 flotation concentrate bank: implications for understanding PGM floatability. *The Journal of The Southern African Institute of Mining and Metallurgy* **109,** 587-593.

29. Cornell, R. M. and Schwertmann, U. (2003) The iron oxides: structure, properties, reactions, occurrences, and uses, pp. 201 - 221-665, Wiley-VCH, Weinheim.

30. Crossling, K. and Mupakati, T. (2009a) Geological Modelling, (ed. B. Platinum), Boynton Investments (Pty) Ltd., Centurion.

31. Crossling, K. and Mupakati, T. (2009b) Tushenkomst 135JP Optimised Pit, Boynton Investments (Pty) Ltd., Centurion.

32. Dare, S. A. S. and Barnes, S.-J. (2010) Platinum-Group Element (PGE)-Bearing Pyrites in Pyrrhotite-Rich Sulfides from McCreedy and Creighton Ni-Cu-PGE Sulfide Deposits, Sudbury, Canada. In *11th International Platinum Symposium*, International Platinum Symposium, Sudbury.

33. Davidson, M. S. (2009) An investigation of copper recovery from a sulphide oxide ore with a mixed collector system. In *Department of Mining Engineering*-195, Queen's University, Kingston.

34. Derbyshire, J. (2009) Plant Commissioning, (ed. M. Ramonotsi), PPM, Pilanersberg.

35. Diakonov, I. I., Schott, J., Martin, F., Harrichourry, J. and Escalier, J. (1999) Iron(III) solubility and speciation in aqueous solutions. Experimental study and modelling: Part 1. Hematite solubility from 60 to 300°C in NaOH–NaCl solutions and thermodynamic properties of Fe(OH)42(aq). *Geochimica et Cosmochimica Acta* **63,** 2247-2261.

36. Dowling, E. C. J., Klimpel, R. R. and Aplan, F. F. (1985) Model discrimination in the flotation of base metal sulphide ores - circuitry and reagent variations. *Minerals Metallurgical Processing***,** 87-101.

37. Duarte, J. C., Duarte, V. H. and Clark, W. (2004) Optical microscopy and XRD of two Merensky borehole cores from Tuschenkomst and the determination of the PGM mode of occurrence in the two milled flotation feed samples, pp. 1-17, Mintek, Randburg.

38. England, K. E. R., Charnock, J. M., Pattrick, R. A. D. and Vaughan, D. J. (1999) Surface oxidation studies of chalcopyrite and pyrite by glacing-angle x-ray absorption spectroscopy (REFLEXAFS). *Mineralogical Magazine* **63,** 559-566.

39. Fairthorne, G. A. (1996) The interaction of thionocarbamate and thiourea collectors with sulphide mineral surface. In *Applied Science in Chemical Technology*-337, University of South Australia.

40. Fandrich, R., Gu, Y., Burrows, D. and Moeller, K. (2007) Modern SEM-based mineral liberation analysis. *International Journal of Mineral Processing* **84,** 310-320.

41. Feitknecht, W. and Schindler, P. (1963) Solubility Constants of Metal Oxides, Metal Hydroxides and Metal Hydroxide Salts in Aqueous Solution. In *International Union of Pure and Applied Chemistry*, pp. v-69, Butterworths, London.

42. Fornasiero, D., Li, F., Ralston, J. and Smart, R. S. (1994) Oxidation of galena surface I. *X-ray photoelectron spectroscopic and dissolution kinetics studies. Journal of Colloid Interface Science* **164,** 333-344.

43. Fuerstenau, M. C. (1982) Chemistry of collectors in solution. In *Principles of Flotation*, (ed. R. P. King), pp. 1-16, SAIMM, Johannesburg.

44. Fuerstenau, M. C. , Harper, R. W. and Miller, J. D. (1970) Minerals Beneficiation - Hydroxamate vs. Fatty Acid Flotation of Iron Oxide. *AIME Transactions*.

45. Fuerstenau, M. C. , Miller, J. D. and Gutierrez, G. (1968) Minerals Beneficiation - Selective Flotation of Iron Oxide. *AIME Transactions*.

46. Fuerstenau, M. C., Lopez-Valdivieso, A. and Fuerstenau, D. W. (1988) Role of hydrolyzed cations in the natural hydrophobicity of talc. *International Journal of Mineral Processing* **23,** 161-170.

47. Fuerstenau, M. C., Miller, J. D. and Kuhn, M. C. (1985) Chemistry of flotation. *AIME*.

48. Gay, L. S. (2004) A liberation model comminution based on probability theory. *Mineral Engineering Journal* **17,** 325-534.

49. Gerson, A. R. and Jasieniak, M. (2008) The effects of surface oxidation on the Cu activation of pentlandite and pyrrhotite. In Proceeding of the XXIV International Mineral Processing Congress, (eds. W. D. Guo, S. C. Yao, W. F. Liang, Z. L. Cheng and H. Long), pp. 1054-1063, Science Press Beijing, Beijing.

50. Gerson, A. R., Lange, A. G., Prince, K. . E. and Smart, R. S. (1999) The mechanism of copper activation of sphalerite. Applied Surface Science 137, 207-223.

51. Glembotskii, V. A., Klassen, V. I. and Plaksin, I. N. (1972) Flotation. In *Primary Sources*, New York.

52. Grobler, W. A. (2010) Scanning Electron Microscope study of UG2 and Merensky Production samples from Pilanesburg Planitum, Betachem, Pretoria.

53. Gu, G., Sun, X., Li, J. and Hu, Y. (2010) Influences of collector DLZ on chalcopyrite and pyrite flotation . *Journal of Central South University of Technology* **17,** 285-288.

54. Guilbert, J. M. and Park, C. F. (1986) The geology of ore deposits-985, Freeman, W. H., New York.

55. Guo, H. and Yen, W.-T. (2003) Pulp potential and floatability of chalcopyrite. *Minerals Engineering* **16,** 247-256.

56. Gupta, A. and Yan, D. S. (2006) Introduction to Mineral Processing Design and Operations, pp. v-dccviii, Perth.

57. Buckenham, M. H.; Mackenzie, J. M. W. (1962) Fatty acids as flotation reagents for calcite. *AIME Transactions* **223,** 450-454.

58. Hayward, G. A. (2006) Density data for resource estimation on Tuschenkomst, Boynton Investments (Pty) Ltd., Centurion.

59. He, S. (2006) Depression of pyrite in flotation of copper ores. In *Ian Wark Research Institute*-260, University of South Australia.

60. Holwell, D. A., Mcdonald, I. and Armitage, P. E. B. (2006) Platinum-group mineral assemblages in the Platreef at the Sandsloot Mine, northern Bushveld Complex, South Africa. *Mineralogical Magazine* **70,** 83-101.

61. Hope, G. A., Woods, R., Parker, G. K., Buckley, A. N. and McLean, J. (2010) A vibrational spectroscopy and XPS investigation of the interactionof hydroxamate reagents on copper oxide minerals. *Minerals Engineering* **23,** 952-959.

62. Hosseini, H. S. (2008) Physicochemical studies of oxide zinc mineral flotation. In *Department of chemical engineerig and geoscience*-62, Lulea University of Technology, Lulea.

63. Huang, A. (2010) The Latest Patent Technique in the TC1000 and its application in the Flotation of Base Metal Sulfide Ores, (ed. J. Derbyshire), Boynton Investments (Pty) Ltd., Centurion.

64. Hughes, T. (2005) AM2 – a hydroxamate flotation collector reagent for oxides and oxidised mineral systems. *Australian Journal of Mining***,** 58-59.

65. Hukki, R. T. and Vartiainen, O. (1953) An investigation of the collecting effect of fatty acids in tall oil on oxide, particularly on Ilmenite. *AIME Transactions* **196,** 818.

66. Jang, J., Dempsey, B. A. and Burgos, W. D. (2007) Solubility of Hematite Revisited: Effects of hydration. *Environmental Science and Technology* **41,** 7303-7308.

67. Jasieniak, M. and Smart, R. S. (2009) Collectorless flotation of pyroxene in Merensky ore: Residual layer identification using statistical ToF-SIMS analysis. International Journal of Mineral Processing 92, 169-176.

68. Jasieniak, M. and Smart, R. S. (2010) Surface chemical mechanisms of inadvertent recovery of chromite in UG2 ore flotation: Residual layer identification using statistical ToF-SIMS analysis. International Journal of Mineral Processing 94, 72-82.

69. Jin, R., Ye, Y. and Miller, J. D. (1988) The hydrophobic charecter of pretreated coal surface.

70. Jones, C. F., LeCount, S., Smart, R. S. and White, T. (1992) Compositional and structural alteration of pyrrhotite surfaces in solution: XPS and XRD studies. *Applied Surface Science* **55,** 65-85.

71. Kawatra, S. K. and Eisele, T. C. (1992) Recovery of pyrite in coal flotation: Entrainment or hydrophobicity. *Minerals Metallurgical Processing* **9,** 57-61.

72. Kelsall, D. F. (1961) Application of probability in assessment of flotation systems. *Bulletin of the Institute of Mining and Metallurgy* **70,** 191-191.

73. Kinloch, E. D. and Peyerl, W. (1990) Platinum-group minerals in various rock type of the Merenskey Reef: Genetic implications. *Economic Geology 85***,** 537-555.

74. Klassen, V. I. and Mokrousov, V. A. (1963) An introduction to the theory of flotation, Butterworths, London.

75. Klein, C. and Hurlbut, C. S. (1993) Manual of Mineralogy. In *21st Edition*, (ed. J. D. Dana), pp. 654 - 667-681, John Wiley & Sons, INC., New York.

76. Klimpel, R. R. (1980) Selection of chemical reagent for flotation.

77. Klimpel, R. R. (1995) The Influence of Frother Structure on Industrial Coal Flotation. In *High-Efficiency Coal Preparation*, (ed. S. Kawatra), pp. 141-151, Society for Mining, Metallurgy and Exploration Co, Littleton CO.

78. Lamya, R. M. (2007) A fundamental evaluation of the atmospheric pre-leach section of the nickel-copper matte treatment process-213, University of Stellenbosch, Stellenbosch.

79. Lastra, R. (2007) Seven practical application cases of liberation analysis. *International Journal of Mineral Processing* **84,** 337-347.

80. Lee, K., Archibald, D., McLean, J. and Reuter, M. A. (2009) Flotation of mixed copper oxide and sulphide minerals with xanthate and hydroxamate collectors. *Minerals Engineering* **22,** 395-401.

81. Legrand, D. L., Bancroft, G. M. and Nesbitt, H. W. (2005a) Oxidation of pentlandite and pyrrhotite surfaces at pH 9.3: Part 2. *Effect of xanthates and dissolved oxygen. American Mineralogist* **90,** 1055-1061.

82. Legrand, D. L., Bancroft, G. M. and Nesbitt, H. W. (2005b) Oxidation/alteration of pentlandite and pyrrhotite surfaces at pH 9.3: Part 1. *Assignment of XPS spectra and chemical trends. American Mineralogist* **90,** 1042-1054.

83. Leterme, P., Gayot, A., Bizi, M. and Flament, M. P. (2004) Influence of the morphogranulometry and hydrophobicity of talc on its antisticking power in the production of tablets. *International Journal of Pharmacy* **289,** 109-115.

84. Liddell, K. S. (2009) 25 Years of UG2 Concentrators. In *Mintek 75 - A Celebration of Technology Conference*, Mintek, Randburg.

85. Lindsay, N. M. (1988) The processing and recovery of the Platinum-group elements. In *The processing and recovery of the Platinum-group elements*, University of Witwatersrand, Johannesburg.

86. Linter, B. R. and Burstein, G. T. (1999) Reaction of pipeline steels in carbon dioxide. *Corrosion Science* **41,** 117-139.

87. Liu, G., Zhong, H., Dai, T. and Xia, L. (2008) Investigation of the effect of N-substituents on performance of thionocarbamates as selective collectors for copper sulfides by ab initio calculations. *Minerals Engineering* **21,** 1050-1054.

88. Lundgaard, K. L., Tegner, G., Kruger, F. J. and Wilson, R. (2006) Trapped intercumulus liquids in the Main Zone of the eastern Bushveld Complex, South Africa. *Contribution to Mineralogy and Petrology* **151,** 352-369.

89. Luszczkiewicz, A. and Chmielewski, T. (2008) Acid treatment of copper sulphide middlings and rougher concentrates in the flotation circuit of carbonate ores. *International Journal of Mineral Processing* **88,** 45-52.

90. Martinovic, J., Bradshaw, D. J. and Harris, P. J. (2005) *The Journal of The Southern African Institute of Mining and Metallurgy* **105,** 349-355.

91. Mendiratta, N. K. (2000) Kinetics studies of sulphide mineral oxidation and xanthate adsorption. In *Materials Engineering and Science*-162, Virginia Polytechnic Institute and State University, Virginia.

92. Metso, M. (2006) Basic in Mineral Processing, Metso Minerals, Johannesburg.

93. Miller, J. D., Jin, R., Ye, Y. and Sadowski, Z. (1987) Carbon dioxide for fine coal flotation. *Colloids and Surface* **8,** 137.

94. Miller, J. D. and Misra, T. A. (1987) Coal cleaning by gaseous carbon dioxide conditioning and froth flotation.

95. Mintek, M. (2004a) Optical microscopy and XRD of two Merensky borehole cores from Tuschenkomst and the determination of the PGM mode of occurrence in the two milled flotation feed samples, Mintek, Randburg.

96. Mintek, M. (2004b) The determination of the PGM mode of occurrence in the Tuschenkomst oxidised Silicate Reef and Tuschenkomst fresh UG2 rougher tailings and Tuschenkomst fresh UG2 secondary cleaner tails, pp. 1-13, Mintek, Randburg.

97. Molengraaff, G. A. F. (1904) Geology of the Transvaal , Esson and Perkin, Johannesburg.

98. Mphela, N. (2010) Fundamental studies of the electrochemical and flotation behaviour of pyrrhotite. In *Department of Materials Science and Metallurgical Engineering*-208, University of Pretoria, Pretoria.

99. Mycroft, J. R., Nesbitt, H. W. and Pratt, A. R. (1995) X-ray photoelectron and Auger electron spectroscopy of air-oxidized pyrrhotite:Distribution of oxidized species with depth. *Geochimica et Cosmochimica Acta* **59,** 721-733.

100. Newell, A. J. H., Bradshaw, D. J. and Harris, P. J. (2006) The effect of heavy oxidation upon flotation and potential remedies for Merensky type sulfides. *Mineral Engineering Journal* **19,** 675-686.

101. Nicholson, R. V. and Scharer, J. M. (1994) Laboratory studies of pyrrhotite oxidation kinetics. In *Environmental Geochemistry of Sulphide Oxidation*, (ed. C. Alpers, Blowes, D.W.), pp. 14-30, ACS Symposium Series, Washington, DC.

102. Palmer, D. A., Benezeth, P. and Wesolowski, D. J. (2004) Solubility of Nickel Oxide and Hydration in Water. In *14th International Conference on the Properties of Water and Steam, Vol. 14*, pp. 264-269, IAPWS, Kyoto.

103. Palmer, D. A. and Benezeth, P. (2004) Solubility of Copper Oxides in water and Steam. In *14th International Conference on the Properties of Water and Steam, Vol. 14*, pp. 491-496, IAPWS, Kyoto.

104. Pearse, M. J. (2005) An overview of the use of chemical reagents in mineral processing. *Minerals Engineering* **18,** 139-149.

105. Penberthy, C. J., Oosthuyzen, E. J. and Markle, R. K. (2000) The recovery of platinum-group elements from UG-2 chromitite, Bushveld Complex - a mineralogical perspective. *Mineral and Petrology* **68,** 213-222.

106. Penberthy, C. J. and Merkle, R. K. W. (1999) Lateral variations in the platinum-group element content and mineralogy of the UG2 ChromititeL ayer,B ushveldC omplex. *South African Journal of Geology* **102,** 240-250.

107. Phetla, T. P. and Muzenda, E. (2010) A Multistage Sulphidisation Flotation Procedure for a low Grade Malachite Copper Ore. *World Academy of Science* **69,** 255-261.

108. Pradip, P. (1987) Surface chemistry and application of alkyl hydrodamate collectors in mineral flotation. *Transactions of the Indian Institute of Metals* **40,** 287.

109. Pradip, P. and Fuerstenau, D. W. (1984) Mineral flotation with hydroxamate collectors. In *Reagents in the Minerals Industry*, (eds. M. J. Jones and R. Oblatt), pp. 161-168, Institution of Mining and Metallurgy, London.

110. Pratt, A. R., Muir, I. J. and Nesbitt, H. W. (1994) X-ray photoelectron and Auger electron spectroscopic studies of pyrrhotite and mechanism of air oxidation. *Geochimica et Cosmochimica Acta ,58***,** 827-841.

111. Prendergast, M. D. (1988) The geology and economic potential of the PGE-rich Main sulphide Zone of the Great Dyke, Zimbabwe. *Geoplatinum* **87,** 281-302.

112. Quast, K. (2006) Flotation of hematite using C6–C18 saturated fatty acids. *Minerals Engineering* **19,** 582-597.

113. Quast, K. B. (2000) A review of Hematite flotation using 12-Carbon chain collectors. *Minerals Engineering* **13,** 1361-1376.

114. Ramachandra, R. S. (2004) Surface Chemistry for Froth Flotation-744.

115. Randolph, N. G. (1993) Precious Metals. *Pure and Applied Chemistry* **65,** 2411-2416.

116. Rao, S. R. (2004) Surface chemistry of Froth Flotation. In *Reagent and Mechanism, Vol. 2*, (ed. J. Leja), Kluwer Academic/Plenum Publishers, New York.

117. Reuters, M. (2010) 2010. US Platinum ETF seen as precursor for significant investment buying. In *PLATINUM GROUP METALS, Vol. 2010*, (ed. L. Williams), Mineweb, London.

118. Richardson, S. and Vaughan, D. J. (1989) Surface alteration of pentlandite and spectroscopic evidence for secondary violarite formation. *Mineralogical Magazine* **53,** 213-222.

119. Rumball, J. A. and Richmond, G. D. (1996) Measurement of oxidation in a base metal flotation circuit by selective leaching with EDTA. *International Journal of Mineral Processing* **48,** 1-20.

120. Runge, K. C., Franzidis, J. P. and Manlapig, E. V. (2003) A study of the flotation characteristics of different mineralogical classes in different streams of an industrial circuit. In *XXII International Mineral Processing Congress*, (ed. D. Bradshaw, Lorenzen, L.), pp. 962-972, Document Transformantion Technologies, Cape Town.

121. Scott, W. B. (1921) An introduction to Geology, The Macmillan Company, Princeton.

122. Selfe, G. R. (2006) Density of Tuschenkomst critical zone lithologies as measrued by geophysical logs, GRS Consulting, Johannesburg.

123. Shackleton, N. J., Malysiak, V. and O'connor, C. T. (2007) Surface characteristics and flotation behaviour of platinu and palladium tellurite. *Minerals Engineering* **20,** 1232-1245.

124. Sheridan, M. S., Nagaraj, D. R., Fornasiero, D. and Ralston, J. (2002) The use of a factorial experimental design to study collector properties of N-allyl-O-alkyl thionocarbamate collectorin the flotation of a copper ore. *Minerals Engineering* **15,** 333-340.

125. Smart, R. S. (1991) Surface layers in base metal sulphide flotation. *Mineral Engineering Journal* **4,** 891-909.

126. Smart, R. S., Amarantidis, J., Skinner, W., Prestige, C. A., LaVanier, L. and Grano, S. (1998) Surface Analytical studies of oxidation and collector adsorption in sulphide mineral flotation. *Scanning Microscopy* **12,** 553-583.

127. Smith, D. S. and Basson, I. J. (2003) Normal reef subfacies of the Merensky reef at northam platinum mine, Zwartklip facies, Western Bushveld Complex, South Africa. *The Canadian Mineralogist* **42,** 243-260.

128. Smith, S. (2010) PGM ANALYSIS OF LOW GRADE FEED AND TAILINGS SAMPLES. In *Pilanesberg Platinum Mines*, pp. 1-15, ALS Laboratory Group, Johannesburg.

129. Stumpfl, E. F. and Clark, A. M. (1965) Mineralogical notes. *The American Mineralogist* **50,** 1068-1074.

130. Holohan, T. (2009) Analysis of Metallurgical Data on Bankable Feasibility Study, Boynton Investments (Pty) Ltd., Centurion.

131. Tromans, D. (2008) Mineral Communition:. *Mineral Engineering Journal* **21,** 613-620.

132. van Oss, C. J. (2008) The properties of water and their role in colloidal and biological systems, pp. 177-224, Academic Press, Amsterdam.

133. Vaughan, D. J., Becker, U. and Wright, K. (1997) Sulphide mineral surfaces: theory and experiment. *International Journal of Mineral Processing* **51,** 1-14.

134. Vermaak, C. F. and Hendriks, L. P. (1976) A review of the mineralogy of the Merensky Reef, with specific reference to new data on the precious metal mineralogy. *Economic Geology* **71,** 1244-1269.

135. Vermaak, M. K. G., Pistorious, P. C. and Venter, J. A. (2007) Fundamental electrochemical and Raman spectroscopic investigations of the flotation behaviour of PtAs2. *Minerals Engineering* **20,** 1153-1158.

136. Viljoen, M. J. (1999) The nature and origin of the Merensky Reef of the western Bushveld Complex based on geological facies and geophysical data. *South African Journal of Geology* **102,** 221-239.

137. Viljoen, M. J. and W., S. L. (1998) Platinum-group metals. In *Mineral Resources of South Africa, Vol. 16*, (eds. M. G. C. Wilson and C. R. Anhaeusser), Council for Geoscience, Pretoria.

138. Waldeck, H. (2007) Pilanesberg PGM Project - BFS Report. In *Bankable Feasibility Study*, Boynton Investments (Pty) Ltd., Centurion.

139. Whelan, W. and Brown, D. J. (1956) Particle-bubble attachment in froth flotation. *Bulletin of the Institute of Mining and Metallurgy* **XX,** 181-192.

140. Xiao, Z. and Laplante, A. R. (2004) Characterizing and recovering the platinum group minerals–a review. *Minerals Engineering* **17,** 961-979.

141. Yoon, R. H. and Basilio, C. I. (1993) Adsorption of thiol collectors on sulphide minerals and precious metals - a new perspective. In *Proceedings of the XVIII International Mineral Processing Congress*, pp. 611, International Mineral Processing Congress, Sydney.

142. Zachwieja, J. B., McCarron, J. J., Walker, G. W. and Buckley, A. N. (1989) Correlation between the surface compostion and collectorless flotation of chalcopyrite. *Journal of Colloid Interface Science* **132,** 462-468.

143. Zhu, W., Zhong, H., Hu, R., Liu, B., He, D., Song, X. and Deng, H. (2010) Platinum-group minerals and tellurides from the PGE-bearing Xinjie layered intrusion in the Emeishan Large Igneous Province, SW China. *Mineralogy and Petrology* **98,** 167-180.

APPENDICES

1. METALLURGICAL IN SITU SAMPLING PLAN

The RC pulp samples were composited according to the plan shown in Table 15. For instance, the first 5 rows in Table 15 show the number of samples for each lithology, composited to account for the first 5 m from surface (Bench 1). Within the first bench, there were 5 different flotation tests done to account for each class of grade; “blue (0.35 - 0.60g/t)”, “green (0.60 - 1.10g/t)”, “yellow (1.10- 1.60g/t)”, “red (1.60- 2.40g/t)”, and “pink (> 2.40g/t)”. It is important to note that the composite material for metallurgical test work were not stratifically arranged but were based on available RC pulp samples.

TABLE 15: THE PULP COMPOSITON PLAN FOR EACH METALLURGICAL TEST

Number of Samples in Each Bench Used											
Mine Region: RBS		MR	MRFW1	MRFW2	MRFW3	PRHZB	PRLR	PRUPR	# Comp	Composite Possible ?	Each Bench contained all the grade classes
0 - 5	Blue	5	14	0	0	11	4	1	35	YES	Bench 1
5 - 5	Green	6	22	0	0	6	9	2	45	YES	
5 - 5	Yellow	3	8	0	0	5	1	2	19	YES	
5 - 5	Red	4	8	0	0	5	3	3	23	YES	
5 - 5	Pink	5	11	0	0	15	6	4	41	YES	
0 - 10	Blue	8	19	0	0	8	1	8		YES	Bench 2
5 - 10	Green	11	14	0	0	11	8	7	51	YES	
5 - 10	Yellow	2	17	0	0	5	10	3	37	YES	
5 - 10	Red	3	14	0	0	7	17	6	47	YES	
5 - 10	Pink	9	30	0	0	19	12	12	82	YES	
10 - 15	Blue	10	27	0	0	13	6	8	64	YES	Bench 3
10 - 15	Green	8	22	0	0	14	11	5	60	YES	
10 - 15	Yellow	4	17	0	0	10	10	8	49	YES	
10 - 15	Red	8	23	0	0	9	12	6	58	YES	
10 - 15	Pink	9	30	0	0	8	17	19	83	YES	
15 - 20	Blue	16	26	0	0	8	4	16	70	YES	Bench 4
15 - 20	Green	14	18	0	0	6	18	10	66	YES	
15 - 20	Yellow	5	23	0	0	10	9	8	55	YES	
15 - 20	Red	8	18	0	0	13	16	10	65	YES	
15 - 20	Pink	5	38	0	0	13	19	17	92	YES	
20 - 25	Blue	4	14	0	0	14	10	6	48	YES	Bench 5
20 - 25	Green	16	24	0	0	27	19	14	100	YES	
20 - 25	Yellow	7	18	0	0	15	10	6	54	YES	
20 - 25	Red	6	23	0	0	17	14	8	68	YES	
20 - 25	Pink	12	33	0	0	30	16	25	116	YES	
25 - 30	Blue	8	13	0	0	16	13	7	57	YES	Bench 6
25 - 30	Green	5	18	0	0	38	25	9	93	YES	
25 - 30	Yellow	5	7	0	0	13	18	6	49	YES	
25 - 30	Red	3	8	0	0	20	25	16	72	YES	
25 - 30	Pink	17	31	0	0	57	33	45	183	YES	
30 - 35	Blue	0	5	0	0	7	8	5	25	YES	Bench 7
30 - 35	Green	2	9	0	0	14	14	5	44	YES	
30 - 35	Yellow	3	5	0	0	5	19	3	35	YES	
30 - 35	Red	1	2	0	0	8	21	8	40	YES	
30 - 35	Pink	3	14	0	0	23	32	18	90	YES	
35 - 40	Blue	0	1	0	0	2	3	0	6	NO	Bench 8
35 - 40	Green	1	5	0	0	3	5	1	15	NO	
35 - 40	Yellow	0	1	0	0	5	2	3	11	NO	
35 - 40	Red	1	2	0	0	6	3	1	13	NO	
35 - 40	Pink	1	9	0	0	16	8	6	40	YES	
40 - 45	Blue	0	2	0	0	1	2	0	5	NO	Bench 9
40 - 45	Green	0	3	0	0	1	1	0	5	NO	
40 - 45	Yellow	0	0	0	0	3	5	0	8	NO	
40 - 45	Red	1	0	0	0	3	1	1	6	NO	
40 - 45	Pink	0	1	0	0	2	2	0	5	NO	

2. PPM Process Water Analysis

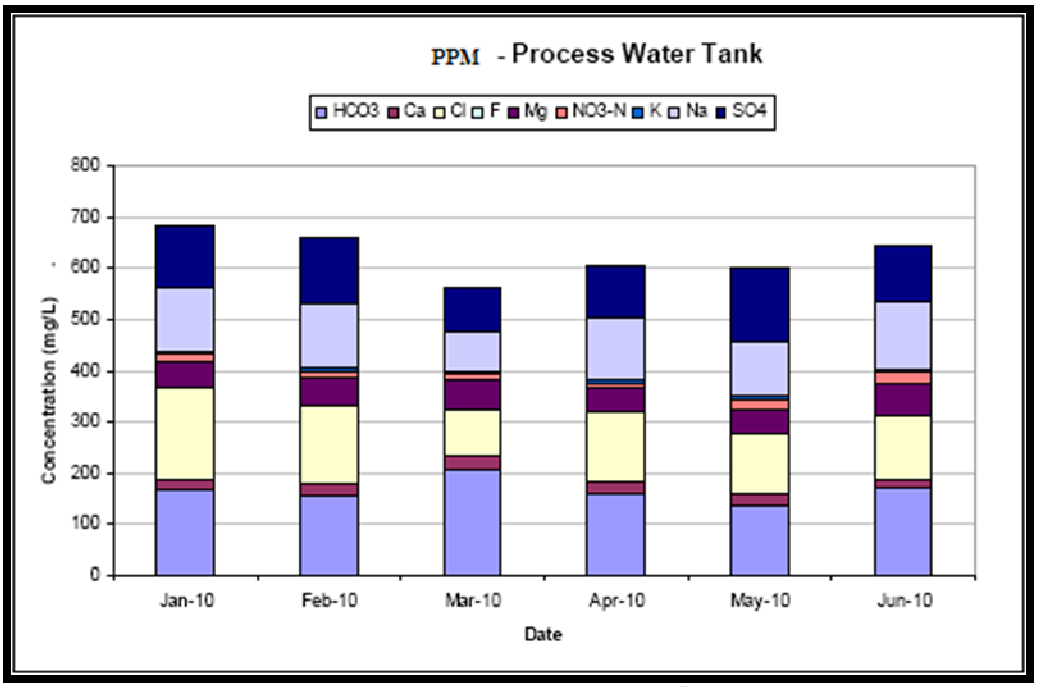

p

Figure 53: Comparative Chemical Analysis of PPM Process water

3. Assaying

The assaying method used was lead collection fire assay technique. The sample to be analysed was mixed in the flux comprising of varying amount lead oxide, soda ash, borax, silica, and the flour. For the first concentrate (the highest concentrate grade) and the second concentrate, about 15g of the sample was weight in triplicates depending of sample availability. The measured sample was mixed with R722 flux. For the third and forth concentrates about 20 – 25g of the sample was weighed also in triplicate. The tail and the head grade were also weighed in triplicate (80 – 100g each) and mixed with R0712 flux. The crucibles containing sample flux mixture were placed in the fusion furnace at 1150°C for about 1 hour. During this time the litharge was reduced by the flour to elemental lead which also collected all the PGMs contained in the sample. The gangue in the sample reacted chemically with the rest of the flux components to form a glassy slag. When fusion was complete, after 1 hour, the crucible pots were removed from the furnace and the melts inside were poured into a conical cast iron mould.

The lead formed a button at the bottom of the iron mould container and the contents were allowed to cool. This allowed the slag to separate from the lead button loaded with

whatever PGM's were present in the sample. The slag was separated from lead button by using deslugger machine which hammered the lead button into a small round ball. The deslugged lead button was then placed onto a pre-heated muffle cupels and heated in the muffle furnace at 1100°C. At this stage the cupellation process converts lead into lead oxide that tends to percolate into the cupel leaving a dore beat or PGM prills. This process also takes about 1 hour. The muffle cupels were then removed from the furnace and slowly cooled to room temperature in the fume cupboard.

The prills were then placed into the high temperature (HT) cupels and placed into the HT furnace at 1300°C. This process drives off residual lead and silver. The period of time for this process was 90 minutes. The time allowed in the HT furnace was enough to allow for the reading of three PGM elements and gold. The final prill was weighed and its mass was related to the aliquot of concentrates sample, tail sample or headgrade sample respectively. The readings were reported in grams per tons values.

4. Data Analysis

The assay result for all concentrates (RC1 to RC4, see Table 17) and the results of feed grade and the tailings were all collated to determine both the grade and PGM contained in each sample. The cumulative recovery curve was plotted against flotation time where each concentrate formed a data point on the curve against the time the froth was collected. The samples that floated positively were expected to form an increasingly diminishing cumulative recovery curve.

The grade of each concentrate was also calculated and used to plot the grade-recovery curve. The grade-recovery curve offers an opportunity to determine how amenable the material is to flotation cleaning. The curve is normally negatively sloped and the lower the gradient of the curve the harder it is to obtain high final concentrate grade from the material. The mass recovery at each concentrate was also calculated and the PGM recovery versus mass recover was plotted to determine the mass pull required for a particular cumulative grade required.

5.1. Data Analysis Illustration

By way of illustration, Table 16 below show the standard flotation conditions of the test work done on the "Pink (> 2.40g/t)" sample sourced from the UN region at the flinch (mining bench) of 35-40m below surface.

The metallurgical work done during PPM feasibility study had indicated that the use of copper sulphate as an activator was beneficial for Silicate Reef package. However, preliminary work done on this study did not show any significant improvement in so far as copper sulphate activation was concerned. As a result, copper sulphate activation was used initially during the in situ metallurgical profiling but never carried forward for subsequent work.

TABLE 16: GENERIC FLOTATION CONDITIONS

	Dosage	Cond. Time	Reagent
	(g/t)	(min)	Role
$CuSO_4$*	50	5	Activator
SIBX	100	2	Collector
AM28**	100	3	Co-collector
Sendep30	50	3	Depressant
Senfroth	50	0.5	Frother

*Activator was not used all the time only on metallurgical profiling tests.

**Co-collectors like AM28 were also only used when studying respective reagents.

Table 17 shows metallurgical test results with (Klimpel, 1980) and (Kelsall, 1961) model parameters. The fitting of the recovery versus time data was performed by applying the Klimpel and Kelsall Models to the recovery data. The Klimpel Model allows for a non-floatable species, and is of the form:

Equation 26:
$$R = R_u\left[1 - \frac{1 - exp(-k_{max}t)}{k_{max}t}\right]$$

Where R is the recovery, Ru is the ultimate recovery for the given species for an infinite flotation time, kmax is a constant and t is flotation time. The Kelsall Model characterises the mineral species into two rate constants, corresponding to slow and fast floating components. The model is of the form:

Equation 27:
$$R = \varphi_s[1 - exp(-k_s t)] + (1 - \varphi_s)[1 - exp(-k_f t)]$$

Where R is the recovery at time t, Φs is the mass fraction of the slow floating component, k_s and k_f are the rate constants for the slow and fast floating components respectively.

These equations were fitted to the measured recovery data using the Solver Routine in Microsoft Excel. The fitted parameters are shown in Table 17 where "RC pulp sampleID" shows the actual silicate RC samples used in this particular float test. The summary of results in Table 17 also shows the proportion of fast floating material Φf, which was calculated from 1-Φs.

TABLE 17: METALLURGICAL TEST WORK RESULTS FOR A SAMPLE –UN-MRP-PINK (> 2.40G/T)-3540

				Grade	Recovery		
Products	**Time (min)**	**Mass (g)**	**Mass (%)**	**3E+Au (g/t)**	**3E+Au (%)**		
RC1	1	28.09	1.48	10.40	4.27		
RC2	2	62.35	3.30	10.10	9.20		
RC3	4	90.22	4.77	7.20	9.49		
RC4	13	224.45	11.87	4.68	15.35		
RC Total		**405.11**	**21.42**	**6.47**	**38.31**		
RT		1486.51	78.58	2.84	61.69		
Head (calc.)		1891.62	100.00	3.62	100.00		
Head (meas.)				3.34			
		Mass Balance Variance		8%			
cumulative grades and recoveries					Measured	Klimpel	Kelsall
RC1	1	28.09	1.48	10.40	4.27	4.78	4.76
RC1,2	3	90.44	4.78	10.19	13.47	12.6	12.5
RC1,2,3	7	180.66	9.55	8.70	22.96	23.47	23.55
RC1,2,3,4	20	405.11	21.42	6.47	38.31	38.21	38.21
					Error^2	1.23	1.53
RC Pulp SampleID	***Mass***	***Assay***		Klimpel Model		Kelsall Model	
PPM008224	0.98	3.5	3.43	R_u	50.47	Φ_s	0.5772
PPM006131	1	3.74	3.74	k_{max}	0.20	k_s	0.0028
PPM007013	0.78	4.04	3.1512			k_f	0.1151
		11%	3.74				

The mass balance variance as also shown in Table 17 was obtained by reconciling the initial mass and head grade with the individual concentrate mass and grade recovered including tailings.

TABLE 18: ERROR PROPAGATION ON METALLURGICAL TEST WORK RESULTS FOR A SAMPLE –UN-MRP-PINK (> 2.40 g/t)-3540

Error Propagation				
		Grade	Recovery	
Mass (g)	Mass (%)	3E+Au (g/t)	3E+Au (%)	3E+Au
0.25	0.01	0.80	0.70	1.33
0.25	0.02	0.78	1.47	2.71
0.25	0.02	0.55	1.51	2.76
0.25	0.02	0.36	2.41	4.36
1.00	**0.07**	**0.54**	**6.10**	**11.16**
0.25	0.07	0.22	9.65	17.32
1.25	0.13	0.28	15.75	28.49

The flotation results were accepted if the mass balance variance is below 10%. The error is the sum of all errors cumulatively in the form of weighing error, errors associated with actual flotation test, and errors associated with assaying. In the case of "UN-MRP-PINK (> 2.40g/t)-3540" test result, the mass balance variance was 8% (see Table 17).

5.2. Kinetics Data

HYDROXAMATE KINETIC DATA

The kelsall model and Klimpel model was fitted on the recovery curve to obtain kinetic parameters of hydroxamate at the grind of 80% passing 75 microns and 90% passing 75 microns, and compared with the normal reagent suite.

TABLE 19: BENCH SCALE ROUGHER FLOTATION RATE MODELLING RESULTS FOR HYDROXAMATE BASE CO-COLLECTORS

Sample	Kelsall (Kelsall, 1961)				Klimpel (Dowling et al., 1985)	
	ϕ_f	ϕ_s	k_s	k_f	R_∞	k_{max}
80-NOAM	0.41	0.59	0.254	0.161	55.90	0.616
80-AM28	0.54	0.46	0.222	0.235	66.35	0.688
90-NOAM	0.47	0.53	0.187	0.168	58.11	0.501
90-AM28	0.55	0.45	0.070	0.255	63.87	0.586

The kinetic parameter shown in Table 19 above shows that hydroxamate based co-collector seems to increase the kinetic constant of material ground to 80% passing 75 microns. The kinetic constant of the material ground to 90% passing 75 microns dropped. The fraction of fast floating was increased from 41% to 54% (80% passing 75 microns). Although grinding finer seem to have negatively affected recovery (Figure 39),

where normal recovery dropped from 52.5% to 41.1%, Klimpel maximum recovery, R_∞ improved slightly and fraction of fast floating also increased from 41% to 47% (Table 19). By examining the Kelsall kinetic parameter of the slow floating fraction, it can be seen that grinding finer worsened the kinetic rate constant, k_s. And yet the Kelsall kinetic rate constant of fast floating particles seem to have generally improved from 0.16/min to over 0.24/min (Table 19). Also, the kinetic parameters in Table 19 show that grinding finer decreased the Klimpel maximum kinetic constant from around 0.6/min to around 0.5/min. However, addition of AM28 had a positive response towards Klimpel maximum kinetic constant. This was increased by about 0.85/min when AM28 was added, irrespective of the grind.

THIONOCARBAMATE KINETIC DATA

The kelsall model and Klimpel model was fitted on the recovery curve to obtain kinetic parameters for the three thionocarbamates used, and also compared with the normal reagent suite.

TABLE 20: BENCH SCALE ROUGHER FLOTATION RATE MODELLING RESULTS FOR THIONOCARBAMATE BASE CO-COLLECTORS

Sample	Kelsall (Kelsall, 1961)				Klimpel (Dowling et al., 1985)	
	ϕ_f	ϕ_s	k_s	k_f	R_∞	k_{max}
Normal	0.47	0.53	0.096	0.091	56.53	0.21
TC1000	0.46	0.54	0.063	0.144	54.29	0.32
TC3000	0.50	0.50	0.103	0.151	56.97	0.38
TC6000	0.49	0.51	0.135	0.142	59.97	0.41

According to the kinetic parameter shown in Table 20, thionocarbamate based co-collectors seem to have no significant effect on altering the fraction of both fast and slow floating particles. However, the Kelsall rate constant of slow floating particles was altered somewhat, TC1000 decreased the rate constant of slow floating while TC3000 and TC6000 increased the Kelsall rate constant by 7% and 40% respectively (Table 20).

In addition, kinetic parameters (Table 20) show that thionocarbamate based co-collectors had no significant effect on Klimpel maximum recovery, R_∞. But TC6000 increased the Klimpel maximum kinetic constant from 0.21/min to 0.41/min. This indicates an increase in the reagent selectivity.

FATTY ACIDS KINETIC DATA

The kelsall model and Klimpel model was fitted on the recovery curve to obtain kinetic parameters for the two fatty acids used, and as with the other tests, comparison with the normal reagent suite was made.

TABLE 21: BENCH SCALE ROUGHER FLOTATION RATE MODELLING RESULTS FOR FATTY ACIDS BASE CO-COLLECTORS

	Kelsall (Kelsall, 1961)				Klimpel (Dowling et al., 1985)	
Sample	ϕ_f	ϕ_s	k_s	k_f	R_∞	k_{max}
Normal	0.47	0.53	0.096	0.091	56.53	0.21
TC2000	0.91	0.09	0.596	0.121	100	0.32
BC-364	0.68	0.32	0.164	0.194	84.32	0.45

The kinetic parameters presented in Table 21 above show that the two fatty acids increased the fraction of the fast floating component significantly. BC364 seems to be slightly superior in terms of selectivity compared to TC2000.

6. Silicate PGM Association and Gran Size Distribution in the Feed and Tails

Table 22: PPM PGM Association in the Feed and Tailings (Smith, 2010)

Association	Silicate Feed	Silicate Tailings
Enclosed in Silicate	39.7	30.7
Attached to Silicate	28.9	33.7
*PGM/BMS/Gangue	0.5	1.1
Enclosed in BMS	0.0	0.0
Attached to BMS	8.9	22.1
**Grain boundary	17.0	9.8
Enclosed in Oxides	3.3	1.0
Attached to Oxides	1.7	1.6
Enclosed in Carbonates	0.0	0.0
Attached to Carbonates	0.0	0.0
Total	100.0	100.0

*PGM/BMS/Gangue – The PGM is associated with a BMS phase(s), which is locked within a gangue particle.

**Grain Boundary – refers to a PGM located between two gangue (non BMS) minerals

Figure 54: Relative PGM Abandance (% area)

Mineral	Silicate Feed	Silicate Tailings
Electrum	4.9	1.0
Ferroplatinum	15.1	23.1
Atokite	1.5	0.5
Plumbopalladinite	4.5	16.0
Sudburyite	4.4	2.2
Stumpflite	0.0	2.5
Cooperite	8.6	29.1
PtRhCuS	0.0	0.3
Kharaelakhite	0.5	0.0
Braggite	0.7	2.4
Vysoskite	5.7	0.0
Laurite	8.5	0.0
Sperrylite	6.8	11.6
Atheneite	0.4	0.0
Arsenopallandinite	26.9	0.9
Stillwaterite	1.9	0.1
Platarsite	0.4	0.0
PtPdSulphararsenide	0.4	0.1
Hollingworthite	0.0	0.0
Irarsite	1.4	0.0
Ruarsite	0.5	0.0
Temagamite	1.1	0.0
Maslovite	0.7	10.1
Moncheite	0.0	0.0
Kotulskite	5.1	0.2
Total	100.0	100.0

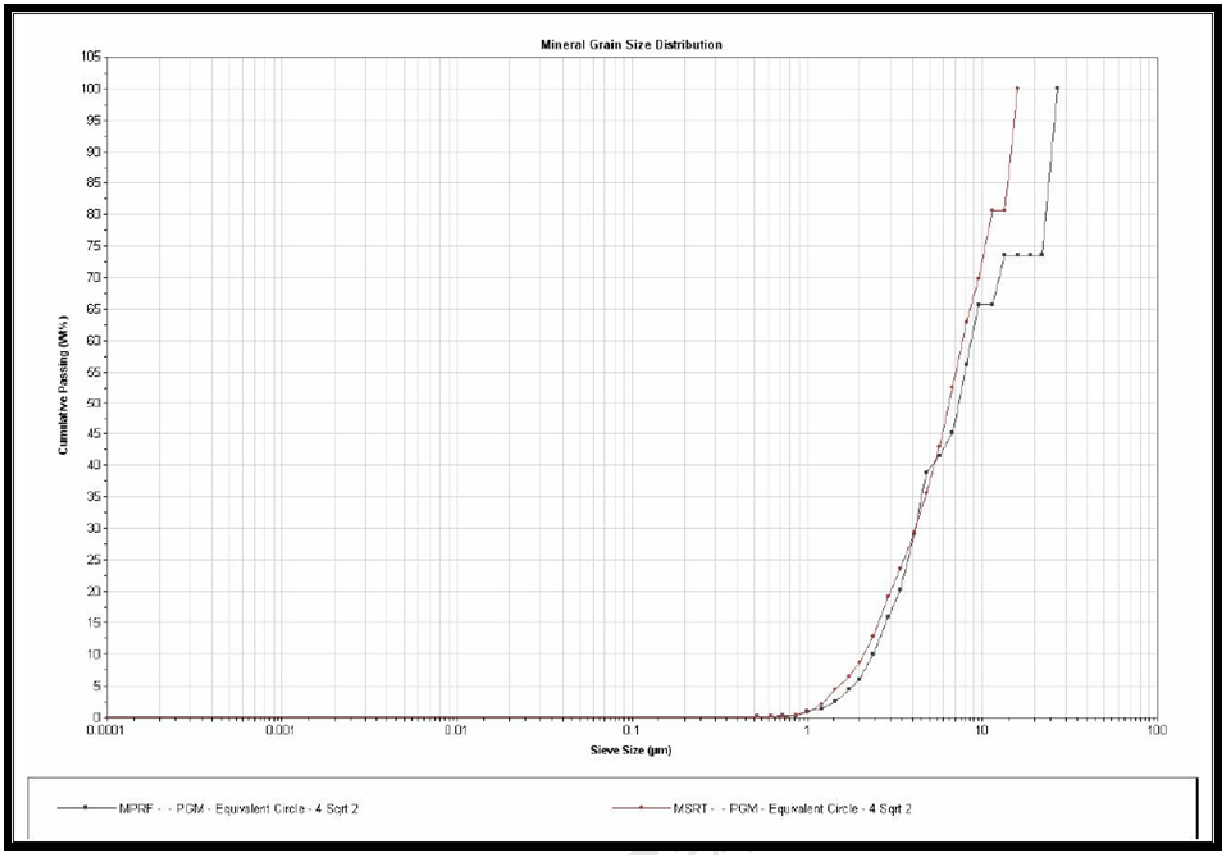

1cs

FIGURE 55: PPM GRAIN SIZE DISTRIBUTION FOR SILICATE FEED AND TAILINGS (SMITH, 2010)

7. Details Flotation Results

7.1. Effect % Slurry Solids on Floatation

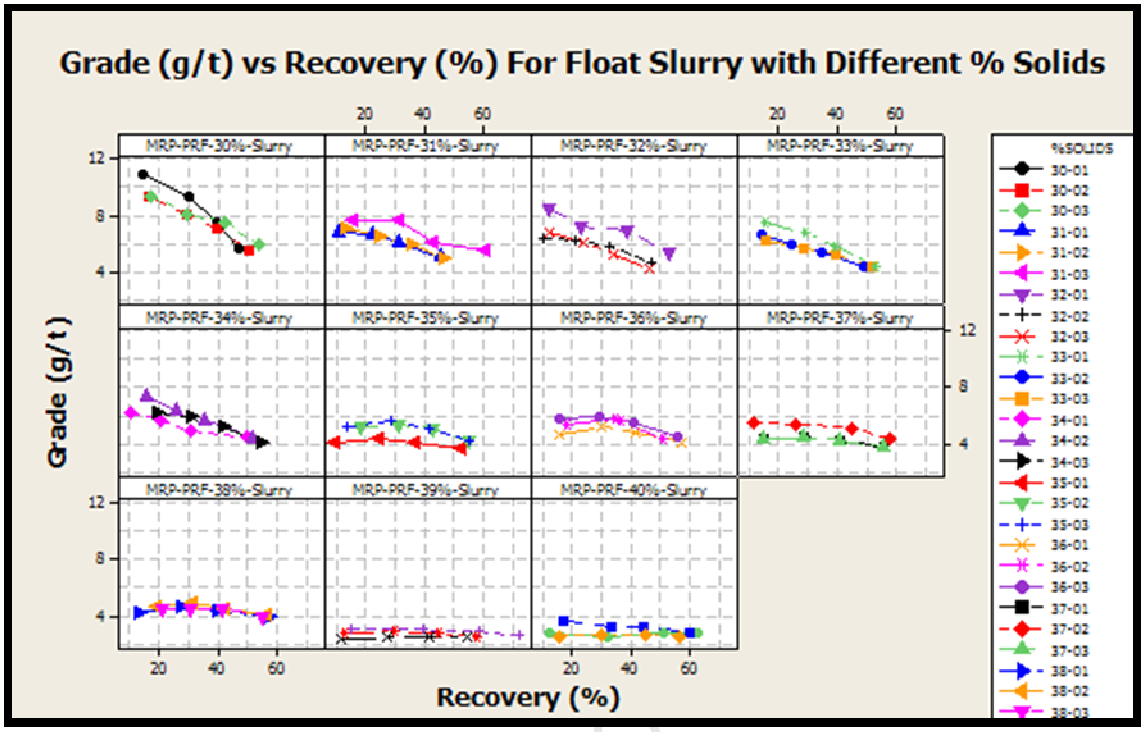

FIGURE 56: GRADE RECOVER CURVE SHOWING 30% SOLIDS PROVIDE LESS ENTRAIMENT AS DETERMINE BY THE GREATER GRADIENT CURVE COMPARED TO THE HIGHER % SOLIDS.

7.2. Acid Pre-Leach Results

TABLE 23: RESULTS OF ACID PRE-LEACH AT VARIOUS ACID DOSAGE (THE NUMBER AFTER HYPHEN ON SAMPLE_ID REPRESENTS A REPEAT)

SAMPLE_ID	Time (min)	Mass (g)	Mass (%)	Grade (g/t)	Recovery (%)
MRP-SRF-20ml-H2SO4-001	1	41.29	2.73	2.36	4.70
MRP-SRF-20ml-H2SO4-001	3	177.64	11.74	2.16	18.52
MRP-SRF-20ml-H2SO4-001	7	378.38	25.01	2.42	44.18
MRP-SRF-20ml-H2SO4-001	20	551.07	36.43	2.63	69.84
MRP-SRF-40ml-H2SO4-002	1	15.53	1.03	10.64	7.70
MRP-SRF-40ml-H2SO4-002	3	43.36	2.87	8.37	16.92
MRP-SRF-40ml-H2SO4-002	7	91.02	6.02	6.24	26.46
MRP-SRF-40ml-H2SO4-002	20	178.3	11.79	5.15	42.81
MRP-SRF-40ml-H2SO4-003	1	19.57	1.28	8.20	7.66
MRP-SRF-40ml-H2SO4-003	3	48.48	3.18	7.82	18.10
MRP-SRF-40ml-H2SO4-003	7	87.7	5.75	6.58	27.56
MRP-SRF-40ml-H2SO4-003	20	168.66	11.06	5.90	47.54
MRP-SRF-30ml-H2SO4-005	1	19.34	1.26	13.04	11.14

MRP-SRF-30ml-H2SO4-005	3	79.96	5.22	7.76	27.40
MRP-SRF-30ml-H2SO4-005	7	198.2	12.93	5.32	46.63
MRP-SRF-30ml-H2SO4-005	20	495.67	32.35	3.23	70.68
MRP-SRF-00ml-H2SO4-006	1	13.39	0.88	15.54	10.64
MRP-SRF-00ml-H2SO4-006	3	38.59	2.53	12.31	24.30
MRP-SRF-00ml-H2SO4-006	7	85.64	5.61	8.43	36.91
MRP-SRF-00ml-H2SO4-006	20	171.82	11.26	5.79	50.84
MRP-SRF-30ml-H2SO4-007	1	55.58	3.71	4.51	11.46
MRP-SRF-30ml-H2SO4-007	3	211.51	14.11	3.45	33.35
MRP-SRF-30ml-H2SO4-007	7	352.82	23.54	3.30	53.26
MRP-SRF-30ml-H2SO4-007	20	514.56	34.32	2.93	68.93

TABLE 24: FLOTATION RESULTS OF ACID PRE-LEACH (THE NUMBER AFTER HYPHEN ON SAMPLE_ID REPRESENTS A REPEAT)

Treatment	SAMPLE_ID	Time (min)	Mass (g)	Mass (%)	Grade (g/t)	Recovery (%)
NORMAL	NORMAL-01	1	20.14	1.32	6.49	8.57
NORMAL	NORMAL-01	3	58.60	3.84	4.69	18.02
NORMAL	NORMAL-01	7	130.62	8.56	3.69	31.57
NORMAL	NORMAL-01	20	247.59	16.22	2.70	43.83
NORMAL	NORMAL-02	1	31.35	2.05	5.37	9.98
NORMAL	NORMAL-02	3	78.16	5.12	4.68	21.70
NORMAL	NORMAL-02	7	149.16	9.78	3.59	31.72
NORMAL	NORMAL-02	20	254.44	16.67	2.93	44.20
NORMAL	NORMAL-04	1	36.35	2.36	3.39	9.61
NORMAL	NORMAL-04	3	96.96	6.29	2.84	21.46
NORMAL	NORMAL-04	7	175.12	11.37	2.51	34.20
NORMAL	NORMAL-04	20	286.15	18.58	2.07	46.23
NORMAL	NORMAL-06	1	23.76	1.55	5.19	9.79
NORMAL	NORMAL-06	3	49.49	3.22	4.47	17.56
NORMAL	NORMAL-06	7	100.60	6.55	3.38	27.02
NORMAL	NORMAL-06	20	212.09	13.81	2.69	45.35
PRE-LEACH	FH2SO4-02	1	29.44	1.95	2.86	6.41
PRE-LEACH	FH2SO4-02	3	119.65	7.91	2.20	20.00
PRE-LEACH	FH2SO4-02	7	253.50	16.75	1.84	38.59
PRE-LEACH	FH2SO4-02	20	669.87	44.27	1.34	68.55
PRE-LEACH	FH2SO4-03	1	84.44	5.56	1.39	9.80
PRE-LEACH	FH2SO4-03	3	181.35	11.94	1.35	20.49
PRE-LEACH	FH2SO4-03	7	273.20	17.99	1.36	40.92
PRE-LEACH	FH2SO4-03	20	466.63	30.73	1.51	68.71
PRE-LEACH	FH2SO4-04	1	55.76	3.65	2.84	12.67
PRE-LEACH	FH2SO4-04	3	137.22	8.99	2.29	25.19
PRE-LEACH	FH2SO4-04	7	270.30	17.70	1.99	43.07
PRE-LEACH	FH2SO4-04	20	417.01	27.31	1.83	70.92
PRE-LEACH	FH2SO4-05	1	55.58	3.71	4.51	11.46

PRE-LEACH	FH2SO4-05	3	211.51	14.11	3.45	33.35
PRE-LEACH	FH2SO4-05	7	352.82	23.54	3.30	53.26
PRE-LEACH	FH2SO4-05	20	514.56	34.32	2.93	68.93

7.3. RESULTS OF HYDROXAMATE BASED CO-COLLECTOR

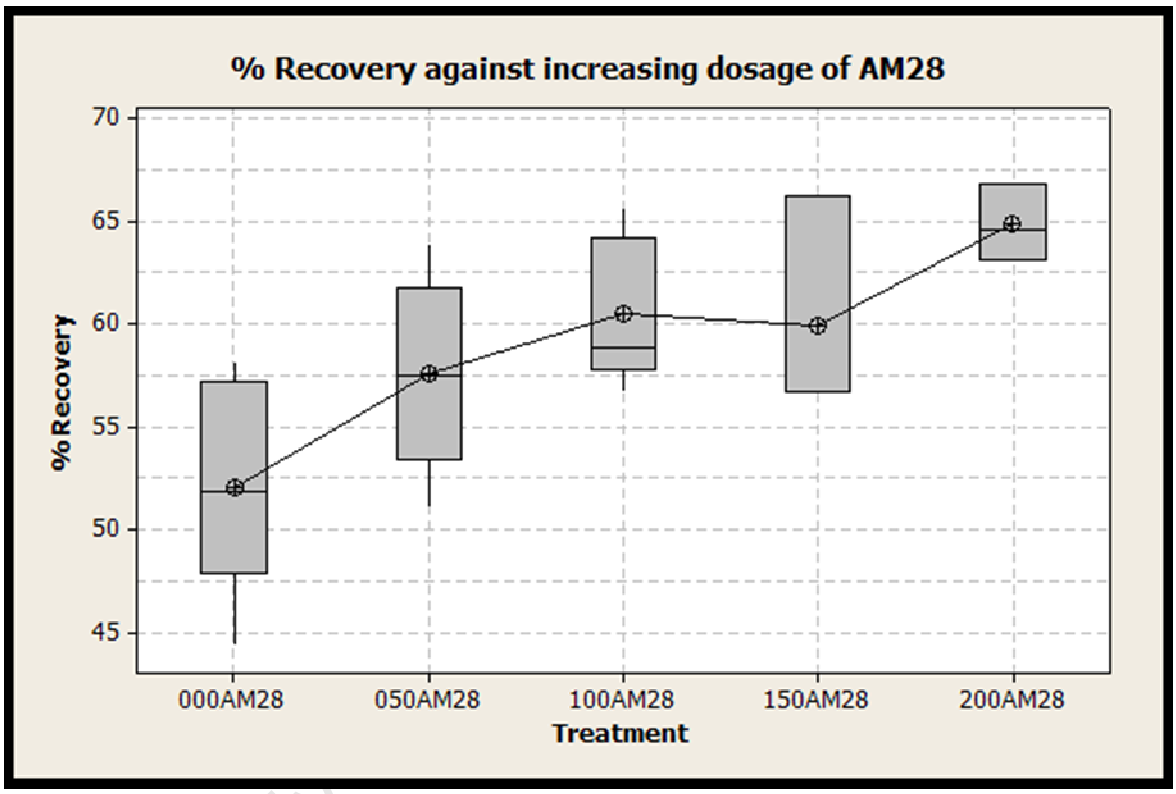

FIGURE 57: THE EFFECT OF INCREASING AM28 DOSAGE FROM 50 G/T TO 200 G/T. INCREASING AM28 DOSAGE ALSO SHOWS AN INCREASE IN RECOVERY.

The main effect plot on recovery as shown in Figure 58 above makes it clear that the use of AM28 as co-collector has more impact on metallurgical performance compared to simple grind variation.

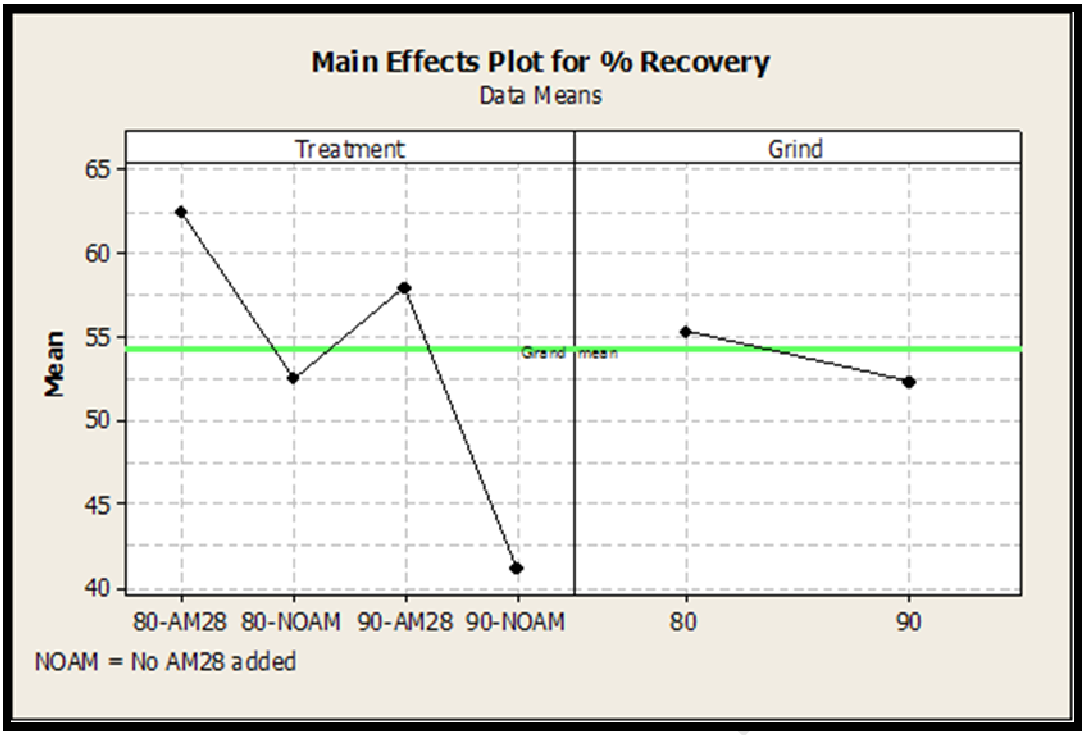

FIGURE 58: MAIN EFFECT PLOT ON THE RECOVERY WITH RESPECT TO AM28 TREATMENT AND GRIND

TABLE 25: FLOATION RESULTS OF MATERIAL TREATED WITH OR WITHOUT AM28 AT 80 AND 90% GRIND OF -75 MICRONS

Treatment	SAMPLE_ID	Time (min)	Mass (g)	Mass (%)	Grade (g/t)	Recovery (%)
90-AM28	MRP-SRF-100-90-AM28-002	1	55.07	3.64	4.69	13.32
90-AM28	MRP-SRF-100-90-AM28-002	3	167.42	11.05	3.97	34.24
90-AM28	MRP-SRF-100-90-AM28-002	7	312.49	20.63	3.29	52.95
90-AM28	MRP-SRF-100-90-AM28-002	20	405.7	26.78	2.78	58.24
90-AM28	MRP-SRF-100-90-AM28-003	1	51.15	3.33	7.15	17.64
90-AM28	MRP-SRF-100-90-AM28-003	3	130.4	8.49	5.50	34.61
90-AM28	MRP-SRF-100-90-AM28-003	7	228.53	14.88	4.35	47.96
90-AM28	MRP-SRF-100-90-AM28-003	20	332.96	21.68	3.77	60.55
90-AM28	MRP-SRF-100-90-AM28-004	1	55.83	3.67	6.13	18.76
90-AM28	MRP-SRF-100-90-AM28-004	3	136.1	8.95	4.89	36.48
90-AM28	MRP-SRF-100-90-AM28-004	7	245.19	16.13	3.69	49.64
90-AM28	MRP-SRF-100-90-AM28-004	20	355.39	23.37	2.91	56.58
90-NOAM	MRP-SRF-100-90-NOAM-001	1	24.91	1.64	5.93	8.05
90-NOAM	MRP-SRF-100-90-NOAM-001	3	58.39	3.86	5.05	16.06
90-NOAM	MRP-SRF-100-90-NOAM-001	7	115.34	7.62	4.25	26.71
90-NOAM	MRP-SRF-100-90-NOAM-001	20	208.94	13.80	3.53	40.23
90-NOAM	MRP-SRF-100-90-NOAM-002	1	33.46	2.20	5.50	10.00
90-NOAM	MRP-SRF-100-90-NOAM-002	3	80.22	5.28	4.18	18.21
90-NOAM	MRP-SRF-100-90-NOAM-002	7	148.57	9.79	3.73	30.13
90-NOAM	MRP-SRF-100-90-NOAM-002	20	252.79	16.65	3.08	42.25

80-NOAM	MRP-SRF-100-80-NOAM-003	1	37.93	2.52	5.01	10.50
80-NOAM	MRP-SRF-100-80-NOAM-003	3	92.04	6.10	5.58	28.41
80-NOAM	MRP-SRF-100-80-NOAM-003	7	168.29	11.16	4.67	43.42
80-NOAM	MRP-SRF-100-80-NOAM-003	20	266.81	17.70	3.39	49.93
80-AM28	MRP-SRF-100-80-AM28-201	1	42.79	2.84	10.10	21.47
80-AM28	MRP-SRF-100-80-AM28-201	3	104.53	6.93	7.07	36.72
80-AM28	MRP-SRF-100-80-AM28-201	7	175.88	11.66	5.78	50.55
80-AM28	MRP-SRF-100-80-AM28-201	20	269.38	17.86	4.62	61.84
80-AM28	MRP-SRF-100-80-AM28-202	1	38.74	2.57	10.70	20.55
80-AM28	MRP-SRF-100-80-AM28-202	3	102.13	6.77	7.44	37.64
80-AM28	MRP-SRF-100-80-AM28-202	7	179.62	11.91	5.83	51.89
80-AM28	MRP-SRF-100-80-AM28-202	20	261.75	17.36	4.76	61.71
80-AM28	MRP-SRF-100-80-AM28-204	1	37.18	2.43	8.93	18.33
80-AM28	MRP-SRF-100-80-AM28-204	3	92.44	6.04	7.44	37.94
80-AM28	MRP-SRF-100-80-AM28-204	7	162.38	10.61	5.77	51.77
80-AM28	MRP-SRF-100-80-AM28-204	20	272.33	17.80	4.25	63.90
80-NOAM	MRP-SRF-100-80-NOAM-203	1	25.22	1.66	13.32	16.30
80-NOAM	MRP-SRF-100-80-NOAM-203	3	59.33	3.90	11.01	31.71
80-NOAM	MRP-SRF-100-80-NOAM-203	7	110.42	7.26	8.22	44.05
80-NOAM	MRP-SRF-100-80-NOAM-203	20	192.85	12.69	6.01	56.21
80-NOAM	MRP-SRF-100-80-NOAM-204	1	27.22	1.79	14.84	19.54
80-NOAM	MRP-SRF-100-80-NOAM-204	3	66.68	4.38	10.82	34.91
80-NOAM	MRP-SRF-100-80-NOAM-204	7	126.14	8.29	7.31	44.63
80-NOAM	MRP-SRF-100-80-NOAM-204	20	220.43	14.48	5.30	56.54

7.4. RESULTS OF THIONOCARBAMATE BASED CO-COLLECTOR

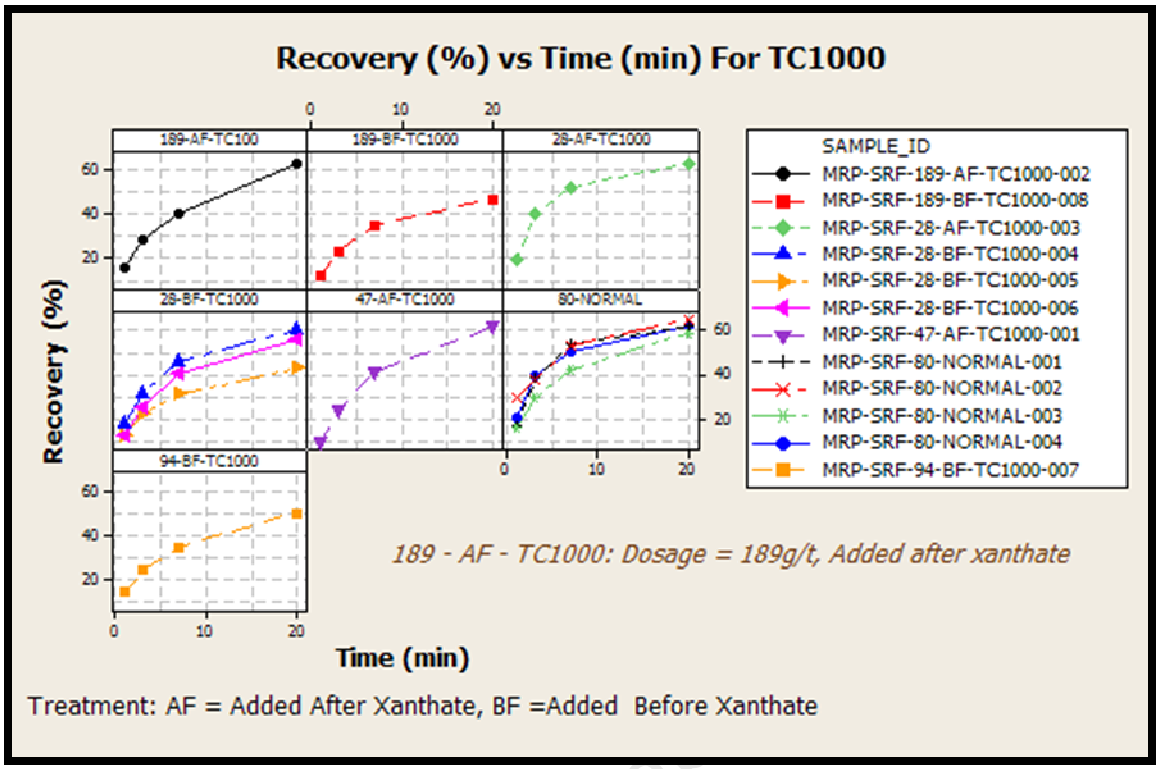

FIGURE 59: THIONOCARBAMATE DOSAGE SCREENING RESULTS SHOWN THE BEST RESULTS WERE ACHIEVED WHEN THE REAGENT IS ADDED AFTER XANTHATE ADDITION AND ALTHOUGH HIGHER DOSAGE RATE WAS ADDED; 28 g/t STILL GAVE SIMILAR OUTCOME IN TERMS OF OVERALL RECOVERY.

TABLE 26: FLOTATION RESULTS OF MATERIAL TREATED WITH VARIOUS THIONOCARBAMATE REAGENTS COMPARED TO NORMAL REAGENT SUITE.

Treatment	SAMPLE_ID	Time (min)	Mass (g)	Mass (%)	Grade (g/t)	Recovery (%)
NORMAL	NORMAL-01	1	20.14	1.32	6.49	8.57
NORMAL	NORMAL-01	3	58.6	3.84	4.69	18.02
NORMAL	NORMAL-01	7	130.62	8.56	3.69	31.57
NORMAL	NORMAL-01	20	247.59	16.22	2.70	43.83
NORMAL	NORMAL-02	1	31.35	2.05	5.37	9.98
NORMAL	NORMAL-02	3	78.16	5.12	4.68	21.70
NORMAL	NORMAL-02	7	149.16	9.78	3.59	31.72
NORMAL	NORMAL-02	20	254.44	16.67	2.93	44.20
NORMAL	NORMAL-04	1	36.35	2.36	3.39	9.61
NORMAL	NORMAL-04	3	96.96	6.29	2.84	21.46
NORMAL	NORMAL-04	7	175.12	11.37	2.51	34.20
NORMAL	NORMAL-04	20	286.15	18.58	2.07	46.23
TC1000	TC1000-01	1	22.7	1.49	4.59	8.32
TC1000	TC1000-01	3	57.99	3.81	4.06	18.80
TC1000	TC1000-01	7	121.62	7.99	3.21	31.14

TC1000	TC1000-01	20	239.51	15.73	2.28	43.66
TC3000	TC3000-01	1	29.11	1.91	4.04	6.70
TC3000	TC3000-01	3	77.1	5.06	3.81	16.72
TC3000	TC3000-01	7	151.89	9.96	3.32	28.73
TC3000	TC3000-01	20	264.65	17.36	2.78	41.90
TC6000	TC6000-01	1	22.85	1.50	6.56	9.96
TC6000	TC6000-01	3	58.74	3.85	5.36	20.93
TC6000	TC6000-01	7	119.19	7.81	4.37	34.59
TC6000	TC6000-01	20	235.76	15.46	3.32	52.02
TC1000	TC1000-02	1	18.94	1.24	6.28	9.90
TC1000	TC1000-02	3	55.72	3.65	4.46	20.70
TC1000	TC1000-02	7	109.79	7.19	3.47	31.68
TC1000	TC1000-02	20	216.35	14.16	2.71	48.70
TC3000	TC3000-02	1	27.66	1.81	5.73	9.55
TC3000	TC3000-02	3	73.6	4.83	4.98	22.10
TC3000	TC3000-02	7	133.45	8.75	3.97	31.94
TC3000	TC3000-02	20	241.65	15.85	3.04	44.34
TC6000	TC6000-02	1	23.16	1.52	7.04	11.37
TC6000	TC6000-02	3	60.63	3.98	5.71	24.16
TC6000	TC6000-02	7	117.29	7.70	4.32	35.34
TC6000	TC6000-02	20	214.22	14.06	3.33	49.75
TC1000	TC1000-03	1	19.24	1.26	5.93	9.12
TC1000	TC1000-03	3	49.04	3.20	5.06	19.84
TC1000	TC1000-03	7	101.13	6.60	4.03	32.57
TC1000	TC1000-03	20	189.63	12.38	3.06	46.37
TC3000	TC3000-03	1	27.92	1.84	4.08	9.65
TC3000	TC3000-03	3	70.01	4.62	3.26	19.32
TC3000	TC3000-03	7	130.36	8.60	2.70	29.80
TC3000	TC3000-03	20	231.06	15.24	2.27	44.48
TC6000	TC6000-03	1	36.17	2.37	5.67	15.46
TC6000	TC6000-03	3	79.33	5.21	4.59	27.47
TC6000	TC6000-03	7	145.84	9.57	3.52	38.75
TC6000	TC6000-03	20	261.16	17.14	2.81	55.27

7.5. FATTY ACIDS

TABLE 27: FLOTATION RESULTS OF MATERIAL TREATED WITH BC364 AND TC2000 COMPARED TO NORMAL REAGENT SUITE

Treatment	SAMPLE_ID	Time (min)	Mass (g)	Mass (%)	Grade (g/t)	Recovery (%)
BC~364	BC~364-09	1	90.28	5.94	2.02	10.64
BC~364	BC~364-09	3	220.36	14.49	1.88	24.23
BC~364	BC~364-09	7	466.42	30.67	1.55	42.32
BC~364	BC~364-09	20	797.77	52.46	1.43	66.68
BC~364	BC~364-10	1	64.28	4.22	4.40	15.83

BC~364	BC~364-10	3	175.08	11.50	3.70	36.29
BC~364	BC~364-10	7	271.88	17.86	3.39	51.52
BC~364	BC~364-10	20	393.93	25.88	2.93	64.63
BC~364	BC~364-11	1	46.74	3.09	3.13	8.89
BC~364	BC~364-11	3	171.88	11.38	2.69	28.13
BC~364	BC~364-11	7	297.18	19.67	2.73	49.22
BC~364	BC~364-11	20	454.46	30.08	2.34	64.70
BC~364	BC~364-12	1	61.17	4.02	2.69	10.64
BC~364	BC~364-12	3	169.22	11.13	2.25	24.62
BC~364	BC~364-12	7	368.96	24.27	1.68	40.12
BC~364	BC~364-12	20	540.86	35.58	1.88	65.80
BC~364	BC~364-01	1	115.92	7.63	1.89	18.95
BC~364	BC~364-01	3	266.88	17.56	1.57	36.31
BC~364	BC~364-01	7	420.45	27.67	1.47	53.31
BC~364	BC~364-01	20	606.31	39.90	1.46	76.30
BC~364	BC~364-03	1	87.69	5.65	1.82	13.69
BC~364	BC~364-03	3	190.14	12.25	1.52	24.77
BC~364	BC~364-03	7	454.52	29.28	1.41	54.94
BC~364	BC~364-03	20	601.46	38.74	1.32	68.18
BC~364	BC~364-04	1	82.18	5.39	2.50	12.67
BC~364	BC~364-04	3	254.64	16.71	2.28	35.74
BC~364	BC~364-04	7	480.3	31.52	2.09	61.90
BC~364	BC~364-04	20	575.97	37.79	2.08	73.70
BC~364	BC~364-05	1	82.06	5.43	3.96	26.20
BC~364	BC~364-05	3	168.82	11.16	2.93	39.90
BC~364	BC~364-05	7	260.7	17.24	2.87	60.27
BC~364	BC~364-05	20	356.91	23.60	2.47	71.13
NORMAL	NORMAL-01	1	20.14	1.32	6.49	8.57
NORMAL	NORMAL-01	3	58.6	3.84	4.69	18.02
NORMAL	NORMAL-01	7	130.62	8.56	3.69	31.57
NORMAL	NORMAL-01	20	247.59	16.22	2.70	43.83
NORMAL	NORMAL-02	1	31.35	2.05	5.37	9.98
NORMAL	NORMAL-02	3	78.16	5.12	4.68	21.70
NORMAL	NORMAL-02	7	149.16	9.78	3.59	31.72
NORMAL	NORMAL-02	20	254.44	16.67	2.93	44.20
NORMAL	NORMAL-04	1	36.35	2.36	3.39	9.61
NORMAL	NORMAL-04	3	96.96	6.29	2.84	21.46
NORMAL	NORMAL-04	7	175.12	11.37	2.51	34.20
NORMAL	NORMAL-04	20	286.15	18.58	2.07	46.23
BC~364	BC~364-06	1	82.06	5.43	3.96	29.84
BC~364	BC~364-06	3	168.82	11.16	2.93	45.45
BC~364	BC~364-06	7	260.7	17.24	2.34	56.08
BC~364	BC~364-06	20	356.91	23.60	2.05	67.12
BC~364	BC~364-07	1	49.26	3.20	4.40	16.72
BC~364	BC~364-07	3	115.57	7.51	4.19	37.40

BC~364	BC~364-07	7	184.63	12.00	3.85	54.83
BC~364	BC~364-07	20	275.9	17.94	3.65	77.60
TC2000	TC2000-01	1	88.33	5.82	2.00	14.60
TC2000	TC2000-01	3	181.57	11.97	1.82	27.32
TC2000	TC2000-01	7	378.75	24.97	1.57	49.15
TC2000	TC2000-01	20	936.54	61.74	1.09	84.65
TC2000	TC2000-02	1	78.58	5.14	2.18	10.77
TC2000	TC2000-02	3	152.97	10.01	2.53	24.28
TC2000	TC2000-02	7	397.47	26.00	2.18	54.56
TC2000	TC2000-02	20	932.43	61.00	1.42	83.14
TC2000	TC2000-03	1	96.18	6.34	2.75	16.56
TC2000	TC2000-03	3	219.23	14.44	2.45	33.67
TC2000	TC2000-03	7	494.42	32.57	1.77	54.69
TC2000	TC2000-03	20	879.12	57.91	1.52	83.60
NORMAL	NORMAL-06	1	23.76	1.55	5.19	9.79
NORMAL	NORMAL-06	3	49.49	3.22	4.47	17.56
NORMAL	NORMAL-06	7	100.6	6.55	3.38	27.02
NORMAL	NORMAL-06	20	212.09	13.81	2.69	45.35

7.6. COMBINED FLOAT RESULTS

TABLE 28: FLOTATION RESULTS FOR ALL COLLECTORS EVALUATED INCLUDING THE ACID PRE-LEACH RESULTS COMPARED TO NORMAL REAGENT SUITE

Treatment	SAMPLE_ID	Time (min)	Mass (g)	Mass (%)	Grade (g/t)	Recovery (%)
NORMAL	NORMAL-01	1	20.14	1.32	6.49	8.57
NORMAL	NORMAL-01	3	58.6	3.84	4.69	18.02
NORMAL	NORMAL-01	7	130.62	8.56	3.69	31.57
NORMAL	NORMAL-01	20	247.59	16.22	2.70	43.83
NORMAL	NORMAL-02	1	31.35	2.05	5.37	9.98
NORMAL	NORMAL-02	3	78.16	5.12	4.68	21.70
NORMAL	NORMAL-02	7	149.16	9.78	3.59	31.72
NORMAL	NORMAL-02	20	254.44	16.67	2.93	44.20
NORMAL	NORMAL-04	1	36.35	2.36	3.39	9.61
NORMAL	NORMAL-04	3	96.96	6.29	2.84	21.46
NORMAL	NORMAL-04	7	175.12	11.37	2.51	34.20
NORMAL	NORMAL-04	20	286.15	18.58	2.07	46.23
FATC10	FATC10-01	1	31.04	2.03	4.97	9.34
FATC10	FATC10-01	3	88.91	5.83	4.50	24.24
FATC10	FATC10-01	7	155.83	10.21	4.05	38.23
FATC10	FATC10-01	20	264.11	17.31	3.34	53.38
FATC10	FATC10-02	1	34.17	2.24	5.73	13.20
FATC10	FATC10-02	3	94.23	6.18	4.07	25.87
FATC10	FATC10-02	7	169.5	11.11	3.48	39.77
FATC10	FATC10-02	20	280.14	18.36	2.90	54.68

TC1000	TC1000-01	1	22.7	1.49	4.59	8.32
TC1000	TC1000-01	3	57.99	3.81	4.06	18.80
TC1000	TC1000-01	7	121.62	7.99	3.21	31.14
TC1000	TC1000-01	20	239.51	15.73	2.28	43.66
TC3000	TC3000-01	1	29.11	1.91	4.04	6.70
TC3000	TC3000-01	3	77.1	5.06	3.81	16.72
TC3000	TC3000-01	7	151.89	9.96	3.32	28.73
TC3000	TC3000-01	20	264.65	17.36	2.78	41.90
TC6000	TC6000-01	1	22.85	1.50	6.56	9.96
TC6000	TC6000-01	3	58.74	3.85	5.36	20.93
TC6000	TC6000-01	7	119.19	7.81	4.37	34.59
TC6000	TC6000-01	20	235.76	15.46	3.32	52.02
TC1000	TC1000-02	1	18.94	1.24	6.28	9.90
TC1000	TC1000-02	3	55.72	3.65	4.46	20.70
TC1000	TC1000-02	7	109.79	7.19	3.47	31.68
TC1000	TC1000-02	20	216.35	14.16	2.71	48.70
TC3000	TC3000-02	1	27.66	1.81	5.73	9.55
TC3000	TC3000-02	3	73.6	4.83	4.98	22.10
TC3000	TC3000-02	7	133.45	8.75	3.97	31.94
TC3000	TC3000-02	20	241.65	15.85	3.04	44.34
TC6000	TC6000-02	1	23.16	1.52	7.04	11.37
TC6000	TC6000-02	3	60.63	3.98	5.71	24.16
TC6000	TC6000-02	7	117.29	7.70	4.32	35.34
TC6000	TC6000-02	20	214.22	14.06	3.33	49.75
TC1000	TC1000-03	1	19.24	1.26	5.93	9.12
TC1000	TC1000-03	3	49.04	3.20	5.06	19.84
TC1000	TC1000-03	7	101.13	6.60	4.03	32.57
TC1000	TC1000-03	20	189.63	12.38	3.06	46.37
TC3000	TC3000-03	1	27.92	1.84	4.08	9.65
TC3000	TC3000-03	3	70.01	4.62	3.26	19.32
TC3000	TC3000-03	7	130.36	8.60	2.70	29.80
TC3000	TC3000-03	20	231.06	15.24	2.27	44.48
TC6000	TC6000-03	1	36.17	2.37	5.67	15.46
TC6000	TC6000-03	3	79.33	5.21	4.59	27.47
TC6000	TC6000-03	7	145.84	9.57	3.52	38.75
TC6000	TC6000-03	20	261.16	17.14	2.81	55.27
FATC60	FATC60-01	1	52.68	3.46	2.89	10.97
FATC60	FATC60-01	3	163.38	10.74	2.17	25.58
FATC60	FATC60-01	7	333.02	21.88	1.96	46.98
FATC60	FATC60-01	20	666.72	43.81	1.48	61.03
FATC60	FATC60-03	1	43.55	2.86	3.63	13.74
FATC60	FATC60-03	3	126.47	8.32	3.05	33.57
FATC60	FATC60-03	7	209.5	13.78	2.78	50.67
FATC60	FATC60-03	20	317.73	20.89	2.22	61.31
FATC60	FATC60-04	1	36.54	2.40	3.85	11.34

FATC60	FATC60-04	3	98.86	6.48	3.28	26.11
FATC60	FATC60-04	7	169.73	11.13	3.02	41.31
FATC60	FATC60-04	20	272.24	17.85	2.62	57.59
NORMAL	NORMAL-06	1	23.76	1.55	5.19	9.79
NORMAL	NORMAL-06	3	49.49	3.22	4.47	17.56
NORMAL	NORMAL-06	7	100.6	6.55	3.38	27.02
NORMAL	NORMAL-06	20	212.09	13.81	2.69	45.35
PRE-LEACH	PRE-LEACH-02	1	29.44	1.95	2.86	6.41
PRE-LEACH	PRE-LEACH-02	3	119.65	7.91	2.20	20.00
PRE-LEACH	PRE-LEACH-02	7	253.5	16.75	1.84	42.59
PRE-LEACH	PRE-LEACH-02	20	669.87	44.27	1.34	68.55
PRE-LEACH	PRE-LEACH-03	1	84.44	5.56	1.39	9.80
PRE-LEACH	PRE-LEACH-03	3	181.35	11.94	1.35	20.49
PRE-LEACH	PRE-LEACH-03	7	273.2	17.99	1.36	40.92
PRE-LEACH	PRE-LEACH-03	20	466.63	30.73	1.51	58.71
PRE-LEACH	PRE-LEACH-04	1	55.76	3.65	2.84	12.67
PRE-LEACH	PRE-LEACH-04	3	137.22	8.99	2.29	25.19
PRE-LEACH	PRE-LEACH-04	7	270.3	17.70	1.99	43.07
PRE-LEACH	PRE-LEACH-04	20	417.01	27.31	1.83	60.92
80-AM28	80-AM28-01	1	42.79	2.84	10.10	21.47
80-AM28	80-AM28-01	3	104.53	6.93	7.07	36.72
80-AM28	80-AM28-01	7	175.88	11.66	5.78	50.55
80-AM28	80-AM28-01	20	269.38	17.86	4.62	61.84
80-AM28	80-AM28-02	1	38.74	2.57	10.70	20.55
80-AM28	80-AM28-02	3	102.13	6.77	7.44	37.64
80-AM28	80-AM28-02	7	179.62	11.91	5.83	51.89
80-AM28	80-AM28-02	20	261.75	17.36	4.76	61.71
80-AM28	80-AM28-04	1	37.18	2.43	8.93	18.33
80-AM28	80-AM28-04	3	92.44	6.04	7.44	37.94
80-AM28	80-AM28-04	7	162.38	10.61	5.77	51.77
80-AM28	80-AM28-04	20	272.33	17.80	4.25	63.90